This is to certify that the

dissertation entitled

A MICROMECHANICS-BASED
INDEPENDENT MODE FAILURE CRITERION
FOR FIBER-REINFORCED COMPOSITES
presented by

Yong-Bae Cho

has been accepted towards fulfillment
of the requirements for

Master's degree in Mechanics

Ronald C. Averill
Major professor

Date 11/14/94

A MICROMECHANICS-BASED INDEPENDENT MODE FAILURE CRITERION FOR FIBER-REINFORCED COMPOSITES

By

Yong-Bae Cho

A THESIS

Submitted to
Michigan State University
in partial fulfillment of the requirements
for the degree of

MASTER OF SCIENCE

Department of Material Science and Mechanics

1994

ABSTRACT

A MICROMECHANICS-BASED INDEPENDENT MODE FAILURE CRITERION FOR FIBER-REINFORCED COMPOSITES

By

Yong-Bae Cho

Failure criteria for composite materials have been developed based on a micromechanics elasticity solution for continuous fiber reinforced composites. The criteria can be cast in several forms, including composite and independent mode polynomial forms. Composite failure is predicted when stress or strain states in any of the constituents due to a lamina (composite) load exceed a critical level as predicted by a properly chosen failure criterion for each constituent. Thus, unidirectional strengths as well as strengths under multi-axial loading of the lamina are determined. Failure envelopes can be fit to a Tsai-Wu type lamina failure theory by using the predicted unidirectional strengths and nonlinear regression to determine the interaction terms. It is also possible to cast the failure model in a simple mathematical form with separate criteria for each mode of failure as a function of the macro (composite) stress state. The current model includes the option to extract average "in-situ" constituent strength properties using unidirectional composite strength data, thus indirectly accounting for the variations in geometry, stiffness, and strength in composite material system.

To My Parents

ACKNOWLEDGMENT

I wish to express my deepest thanks to my advisor Dr. R. C. Averill for his kind guidance and assistance throughout this study. His academic excellence and good personality have provided a constant source of encouragement.

I also wish to express my appreciation to Dr. I.M. Jasiuk and Dr. D. Liu for serving on my graduate committee.

Finally, I would like to thank my family for their loving support.

TABLE OF CONTENTS

LIST OF TABLES

LIST OF FIGURES

CHAPTER I
INTRODUCTION

1.1 Motivation

Composite materials have been used for centuries, and a lot of natural composites exist in nature. According to history, ancient Mongolians used animal tendons, wood and silk to make laminated bows in B.C. 7. Since the 1920's, glass fiber reinforced resin has been used, but its application was confined due to low stiffness of the glass fiber. It was not until the 1960's that the concept of composite materials was established and research on composite materials began [1]. Since the early 1960's, the space and aeronautics industries' increasing demand on high performance materials that are stiffer, stronger, and lighter has led to development of composite materials by combining different materials in order to obtain specific characteristics and properties. In the 1970's, advanced fibers of extremely high modulus, for example, Boron, Aramid and SiC fibers, were developed. They have been used as a reinforcing agent in the form of either fiber, whisker or particulate to reinforce the polymer (resin), metal and ceramic matrices. The fiber reinforced composite materials have been more prevalent than any other form of composite, because the fibrous form of a material is generally much stronger and stiffer than any other form. In the composite materials where fibers are adopted as a reinforcing agent, there is typically no reinforcement in the transverse fiber direction. This problem can be resolved by stacking layers (lamination) with different orientations.

In general, composite materials have properties which can not be achieved by any of the constituents acting alone. They have better properties in stiffness, insulation, strength, weight, damping, corrosion resistance and thermal expansion than the conventional monolithic materials, and are able to meet design requirements with great advantage in aerospace structures, aircraft, automobiles, sporting goods, marine structures and many others [3]. On the other hand, the properties depend on many factors, like processing conditions, the form of reinforcing agent, fiber volume fraction, fiber distribution, interface bonding stress, void content, etc. [5].

Advanced fiber reinforced composites have outstanding strength-to-weight properties and often have been used in strength-critical applications where the stiffness and strength of the materials are the critical factors to be considered. Therefore, for the purpose of designing composite structures efficiently, it is very important that we can predict the strength of a composite material under the various loading conditions in service. The use of a failure criterion for a composite material enables us to predict the strength under combined stresses. Thus the efficient design of structures can be performed on the basis of the predicted strengths.

A composite material is composed of matrix, interphase and fiber, and the performance is achieved by binding the constituents. The fracture of composite materials results from four possible major reasons: (i) fiber fracture, (ii) matrix cracking, (iii) fiber/matrix interface debonding, and (iv) fiber buckling or kinking. These modes of failure don't occur simultaneously in all constituents but initiate as micro-cracks at the constituent level, and unite or propagate as external loading (for example, force, heat and moisture) is increased. Therefore, the strength of a composite material depends on the strength properties of the constituents as well as their interactions. Generally, the existence of mul-

tiple failure modes complicates the assessment of the strength compared with isotropic material.

To estimate the strength of composite materials, there are two different approaches for failure or damage prediction - a phenomenological (macromechanics) approach which tries to correlate experimental observations mathematically but does not necessarily explain the mechanism of failure, and a mechanistic (micromechanics) approach where micromechanical stresses in each constituent are used. Composite materials are anisotropic and heterogeneous, so the mean stress at macro level is different from the actual stress in the constituents. In the phenomenological analyses, the properties of all the constituents are homogenized into an equivalent substance so that each lamina can be assumed to be homogeneous and orthotropic. Then prediction of failure or damage is accomplished by adopting a proper phenomenological failure criterion. The phenomenological failure criteria are empirical in nature, and are basically an attempt to express the yield or failure envelopes of a material in stress or strain space. Most of the phenomenological criteria are able to predict only the failure load, but not to differentiate among the modes of failure. Therefore, it would be more realistic and accurate to analyze stress and check the damage in every point at the constituent level. However, it has been shown from the ultimate failure experiments of carbon-epoxy laminates that if a composite is laminated with plies, a ply criterion can be presumably used for all laminates [6]. Thus, it is desirable to establish a failure criterion at a lamina level.

In the present study, failure loads and modes are predicted by the evaluation of the stress/strain states in each constituent using a micromechanical elasticity solution and employing the phenomenological failure criteria in each constituent in order to evaluate damage at the micromechanical level. In this way, the failure envelope for each constitu-

ent is represented in the stress or strain space. By superimposing failure envelopes of the constituents and identifying their intersection, a failure envelope of a lamina is attained. If the constituent strength properties are known, the strength of a lamina can be determined by detecting the critical stress or strain states at the constituent level. Inversely, using the experimentally measured unidirectional strengths of a lamina as in the solution, the strengths of each constituent can be "backed out" by identifying the maximum stress in a constituent. The resulting failure model thus requires less experimental strength data than those models currently available, yet provides predictions of both the failure load and mechanism.

1.2 Literature Review of Failure Criterion

As composite materials were introduced in structural members, a number of failure criteria for composites were proposed from the late 1960's to predict their uniaxial and multiaxial strengths. Rowlands [7] reviewed the phenomenological failure criteria in 1985, and Nahas [8] surveyed the failure theories for laminated composites in 1986. According to Nahas's investigation, there exist at least 30 failure criteria, which can be classified into four categories - the limit criteria, the interaction criteria, the tensor polynomial criteria and the direct laminate criteria. Because failure of composites is complicated by the existence of several mechanisms, including fiber fracture and micro-buckling, fiber/matrix interface debonding, matrix cavitation and crack propagation, most of the available failure criteria can predict the occurrence of failure but do not describe the failure mode. Such criteria can thus be regarded as phenomenological in nature [15].

Azzi and Tsai [9] developed a failure criterion by applying Hill's [10] failure criterion

for anisotropic materials to transversely isotropic materials in a plane stress state. Using the stress transformation law, they proved that the failure criterion is applicable to the most general case of a unidirectional composite subjected to a combined state of stress. The theoretical predictions were in good agreement with the experimental results.

Hoffman [11] developed a failure criterion that was modified from the Hill's failure criterion for anisotropic materials by adding some linear terms to account for the different tension and compression strengths. Only uniaxial tensile and compressive tests on variously oriented specimens were performed to verify the theory.

Tsai and Wu [12] proposed a failure criterion in the form of a scalar function of two strength tensors on the assumption that there exists a failure surface in the stress space in the scalar form. The linear terms in it take into account the difference in strengths due to positive and negative stresses and the quadratic terms define an ellipsoid in stress space. It also accounts for interactions between stress components as independent material properties. The strength components can be transformed to the other axes by the tensor transformation law.

Wu and Schueblein [13] proposed three basic approaches to establish a third order failure criterion for laminates and discussed the merit and shortcoming of each method. The basic approaches are: (1) The determination of laminate failure from lamina failure criterion, (2) Direct experimental determination of the laminate failure surface and (3) Hybrid approach using a lamina failure criterion to guide testing of the laminate. Among the approaches, the hybrid approach utilizing a quadratic polynomial type failure criterion for lamina and classical laminated plate theory was adopted to develop their theory. Then the third order failure criterion for laminate was obtained in terms of laminate loads. This approach can provide the necessary critical experiments with the consequence of minimiz-

ing experimental permutation and maximizing the reliability of laminate failure.

Tennyson, et. al. [14] developed the cubic tensor polynomial failure criterion to predict failure stress more accurately, since the failure surface may not be ellipsoidal in shape. They showed how to evaluate the strength parameters in plane stress state. The strength parameters F_i and F_{ijk} were determined by a hybrid method which utilized a biaxial strength test and four constraint equations derived by establishing the cubic strength equation and its discriminant. The results of an extensive series of tests showed that the quadratic polynomial failure criterion is too conservative and the cubic polynomial failure criterion is quite accurate.

Jiang and Tennyson [15] developed a new approach to overcome the problem that the failure surface based on a cubic tensor polynomial failure criterion is not always closed. To ensure that the failure criterion yields a locally closed failure surface, the inherent conditions in the cubic criterion were derived. The least square method with Lagrange multipliers to incorporate the derived conditions was utilized to evaluate the least-squares best fit curve to the available data of biaxial load tests. The quadratic and cubic interaction strength parameters were obtained. They showed Tennyson's cubic theory without constraints significantly overestimates the failure stress in the compression-compression quadrant. Failure tests undertaken using a laminated tube agreed well with results of the new criterion.

Yeh and Kim [16] proposed a failure criterion based on the Yeh-Stratton criterion [17] for isotropic material. It is similar to Mohr's criterion and is applicable for both ductile and brittle materials. The criterion is composed of the first order terms of normal stresses, the second order terms of shear stresses, and the interaction term. The unique feature of the theory is the ability of its format to accommodate the different values of the coefficient

of interaction term by types of stress and types of materials. The predictions of the failure by this theory were in good agreement with the experiments.

Wu [18] discussed the resolution of strength tensors and proposed the methods for the critical determination of interaction terms in the Tsai-Wu failure criterion. It was found out that the variation in the interaction component F_{12} is dependent on both the magnitude of the biaxial strength and the magnitude of the ratio of the stress components. He also mentioned the optimal experiments and optimal biaxial stress ratio to provide good resolution of F_{12}.

Considering the influence of the interaction term on the shape of Tsai-Wu's failure envelope, which can vary from an ellipse to parallel lines, and to hyperbola depending on the value of the interaction term, Tsai and Hahn proposed a new method to obtain interaction terms [19]. The interaction terms are obtained by assuming that the Tsai-Wu's failure criteria is a generalization of the Von Mises criterion. They investigated the values of interaction term, F_{12}, for several material, and showed Tsai-Wu failure theory using the proposed interaction term is in good agreement with the experimental result.

Wu and Stachurski [21] suggested a different approach to derive the interaction term, F_{12}, in the Tsai-Wu failure theory. They considered that the value of F_{12} is related to the rotation of the failure ellipse from the major strength axis, and proposed a way to determine F_{12} different from the one proposed by Tsai and Hahn [19]. It was demonstrated that F_{12} proposed by them offered good prediction of failure for thermoplastic and paper materials, while F_{12} proposed by Tsai and Hahn gave good failure predictions for fiber reinforced composites.

Hashin [22] developed a three dimensional failure criterion of unidirectional fiber composites in terms of quadratic stress polynomials by considering that unidirectional

fiber composites are transversely isotropic and the applied average stress state should be invariant about the fiber axis. The criterion is composed of four distinct failure modes - tensile and compressive modes of fiber and matrix. The theory was compared with the experiment results of off-axis specimen for a plane stress state, and gave reasonable strength predictions.

In order to make the classical lamination theory fit to a fully three dimensional lamination theory, Christensen [23] showed that the terms corresponding to out-of-plane strains in stiffness matrix are independent of fiber orientation by introducing two restrictions, and all the terms can be represented by three engineering properties. In connection with this work, considering stress-strain relations, he developed a failure criterion which reduces into direct fiber failure mode and fiber/matrix interaction failure mode, and involves four parameters to be determined from experiments.

Zhu, et. al. [24] proposed a statistical tensile failure theory for unidirectional fiber composites. Assuming that the strength of a fiber is a statistical quantity and that the fibers around a broken fiber are subjected to local stress concentrations, they obtained the axial strength of composites by correlating the number of broken fibers to the tensile stress. The experimental results were in good agreement with the theory, however this theory is confined to predicting the axial strength of unidirectional fiber composites.

Neale and Labossiere [25] developed a parametric failure criterion for lamina under plane stress, considering that since the ultimate strength for any stress combination be finite, the failure surface must be closed and must be symmetrical with respect to the plane $\tau_{12} = 0$. The failure surface is represented by the spherical coordinates, and the angles and length from the origin to the failure surface are determined by the stress state. They showed that this failure theory can encompass Tsai-Wu's quadratic tensor polynomial and

Tennyson's cubic tensor polynomial failure criteria. They demonstrated that the parametric failure envelope describes the failure data as efficiently as the quadratic and cubic failure criteria and less parameters were required.

Feng [26] developed a failure criterion as a function of strain energy invariants for unidirectional fiber-reinforced composites based on the transversely isotropic properties and the strain invariants of finite elasticity. It was assumed that failure occurs when the strain energy density reaches its maximum value. The distortional energy, the dilatational energy and the differential between compressive and tensile strengths are the governing quantities in the criterion. The criterion can be simplified into the fiber and matrix modes, and can be derived into one for infinitesimal strain elasticity.

Hart-Smith [33, 34] pointed out the reason why it is incorrect to adopt the polynomial type interaction failure theories whenever the failure mode of a composite changes with the state of stress. He suggested that separate envelopes for every possible failure mode should be obtained first, and then should be superimposed, not interacted.

Wakashima et. al. [27] derived micromechanically a failure criterion for unidirectional composites composed of ductile matrix and plastically nondeformable inclusions. Assuming that the matrix material obeys the Levy - Von Mises flow rule and the matrix plastic strains are uniform, and using the potential energy function and Lagrange multipliers method, they obtained a failure criterion which is formally identical with Tsai-Wu's phenomenological failure criterion. Adopting the modified Eshelby's theory on the transformation and inhomogeniety problems of an ellipsoidal inclusion, they obtained the strength parameters from the potential energy function. The numerical results were not compared with the experimental results.

The strengths of unidirectional composites were predicted and the effects of thermal

residual stress on the strength was investigated by Ishikawa [28], utilizing the micromechanical elasticity solution and assuming that the composites see failure if the stress level of one of the constituents reaches the failure criterion for the constituent. It was observed that the thermal residual stresses do not have a primary effect on the composite strength if the interface normal strength is large, and the failure prediction by Tsai - Wu criterion with the minimum interaction coefficient F_{12} is fit to that by maximum principal stress criterion in the matrix. The thermal residual stress was verified by means of photoelasticity.

Dvorak and Bahei-El-Din [29] studied the elastic-plastic behavior of composites in terms of constituent properties, their volume fractions and mutual constraints between phases by assuming the model that each of the cylindrical fibers has a vanishingly small diameter and that the fibers occupy a finite volume fraction of the composite. By virtue of the assumption, it was found that the local stress and strain fields are uniform, so the microstructure of the composite was not explicitly accounted for. Elastic moduli, yield conditions, and hardening rules are derived.

Realizing that the strength of composites depends on that of each constituent, Skudra [30] developed a failure criterion to determine the polymer matrix composite strength on the basis of the existing states of stress or strains in the constituent. After establishing the strength criteria for each constituent by understanding the characteristics of material properties and how the constituents behave in a composite, he derived the suitable failure criteria for each mode of failure for a unidirectional lamina. For matrix, since the ultimate strain is not constant but depends on the loading duration, the energy criterion which assumes that matrix fails with time if the work of stresses reaches an ultimate value was chosen as the failure criterion. For fiber, it was assumed that the fiber fails if the strain in the fiber is equal to or greater than the strain at the starting point of the avalanche fracture

of fibers (as predicted by statistical theory), and that the fibers are in a uniaxial state of stress. For interface, the failure models were divided into two types - the abrupt transfer model and the model of diffusion interlayer, and the failure criterion was derived separately. The micromechanical stress analysis of the matrix was performed by taking a representative volume element of the repeating cell. With the failure criterion of each constituent and mechanical stresses, the failure theory for lamina was obtained. Then, using the lamina failure criterion and lamination theory, the failure criteria for laminates was derived.

A micromechanical failure criterion for unidirectional composites was suggested by Aboudi [31]. It was assumed that failure of the composite occurs when one of the micro-stresses reaches a micro-failure criterion, and that plane stress state loading is acting on the composites. Maximum stress failure criterion was adopted for fiber and matrix. If material strengths of constituents were not available, they were obtained from the micro-mechnical model by checking the maximum stress in the constituent when the strength of the composite was applied as a load. It was ascertained that the strength of matrix in composites is larger than that of matrix material in bulk due to the constraint effect.

By means of homogenization of material properties and definition of a failure domain, a strength criterion for unidirectional and multidirectional fiber composites was derived by Landriani and Taliercio [32]. The periodic unit cell of composite was used, and homogenized into an equivalent homogeneous medium. The strength domain of the homogenized medium was defined first, and then the real strength domain was obtained by considering the contribution of failure of each constituent. Some unavailable strengths of each constituent were obtained from composite strength by making some reasonable assumption about the behavior of the constituent material, and the obtained constituent strengths were

used in order to check the reliability of the theoretical model.

1.3 The Present Study

Based on a review of available failure models for fiber-reinforced composite materials, it was concluded that there is still a need for a failure criterion that is accurate, predicts both failure loads and mechanisms, is easy to use, and requires limited experimental data, The objective of the current study is to develop and assess a new model that attempts to combine many useful aspects of other failure models and criteria into one that meets these requirements. This model is based on a micromechnical model, though the final mathematical form is cast in the form of convenient phenomenological models.

In Chapter 2, the micromechanics model used will be described briefly. Chapter 3-5 will discuss various aspects of the failure model. Numerical results will be presented in Chapter 6, and Chapter 7 contains conclusions and recommendations for further study.

CHAPTER II
MICROMECHANICAL ELASTICITY ANALYSIS

2.1 Introduction

In this chapter, the analytical model for micromechanical elasticity analysis will be reviewed briefly [35]. The constitutive relations will be set up first, and then the governing equation for the model will be derived by writing the equilibrium equations in terms of displacements. Considering the boundary conditions, the solution of the equations for several loading cases will be discussed. Then the method of calculating effective composite properties will be established.

2.2 Analytical Model and Mathematical Formulation

Since the fiber distribution in composites becomes more regular as the fiber volume fraction increases, it is usually assumed that the fiber packing is uniform, even though fibers are irregularly distributed throughout the cross-section. The frequently adopted fiber distributions are the square and hexagonal arrays which can be regarded as special cases of the diamond arrays (see Figure 1).

The fundamental assumptions of the analytical model are made as follows:

a) The fibers have infinite length and a uniform circular cross-section along the length of the fiber.

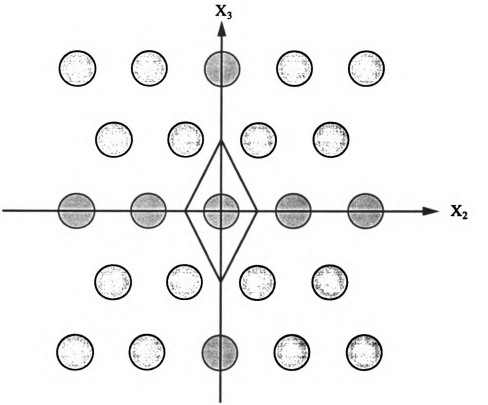

Figure 1. Cross section of a fiber reinforced composite material with fibers packed in a diamond array

b) The fibers are continuous, straight, perfectly aligned with the X_1-axis, and arranged in a periodic diamond array.

c) Fiber coatings or interfaces are represented by concentric circular cylinders around the fiber, and are perfectly bonded with the other constituents (fiber and matrix).

d) All materials are homogeneous and linearly elastic.

e) The outermost constituent (matrix) is transversely isotropic, and the other phases (fiber and interfaces) are cylindrically orthotropic.

f) Mechanical loads are applied at infinity, and do not vary along the X_1 -direction.

Based on the assumptions a) - d), it is secured that many planes of geometric symmetry exist in the composite material. If the region of interest is sufficiently far away from the point of load application or geometric constraint, each fiber and its encompassing phases in that region will see the same deformation due to the applied loads. Therefore, only a single fiber and its surrounding constituents need to be analyzed. Thus, the behavior of the lamina can be investigated by considering only a small region, or a unit cell (representative volume element, (RVE)) (See Figure 2).

Since the overall composite properties are dominated by the properties of each constituent, it is of crucial importance to establish realistic constitutive relationships for each material in any micromechanical model. Therefore, in the present model, all stiffness properties are functions of temperature and moisture content. On the other hand, the coefficients of thermal expansion depend only on temperature and the coefficients of expansion due to moisture content depend only on the current moisture level.

The cylindrical coordinates shown Figure 2 are chosen to get the analytical solution, therefore x, θ, r are utilized as subscripts. In this notation, the constitutive equations for a material with cylindrically-orthotropic properties take the form:

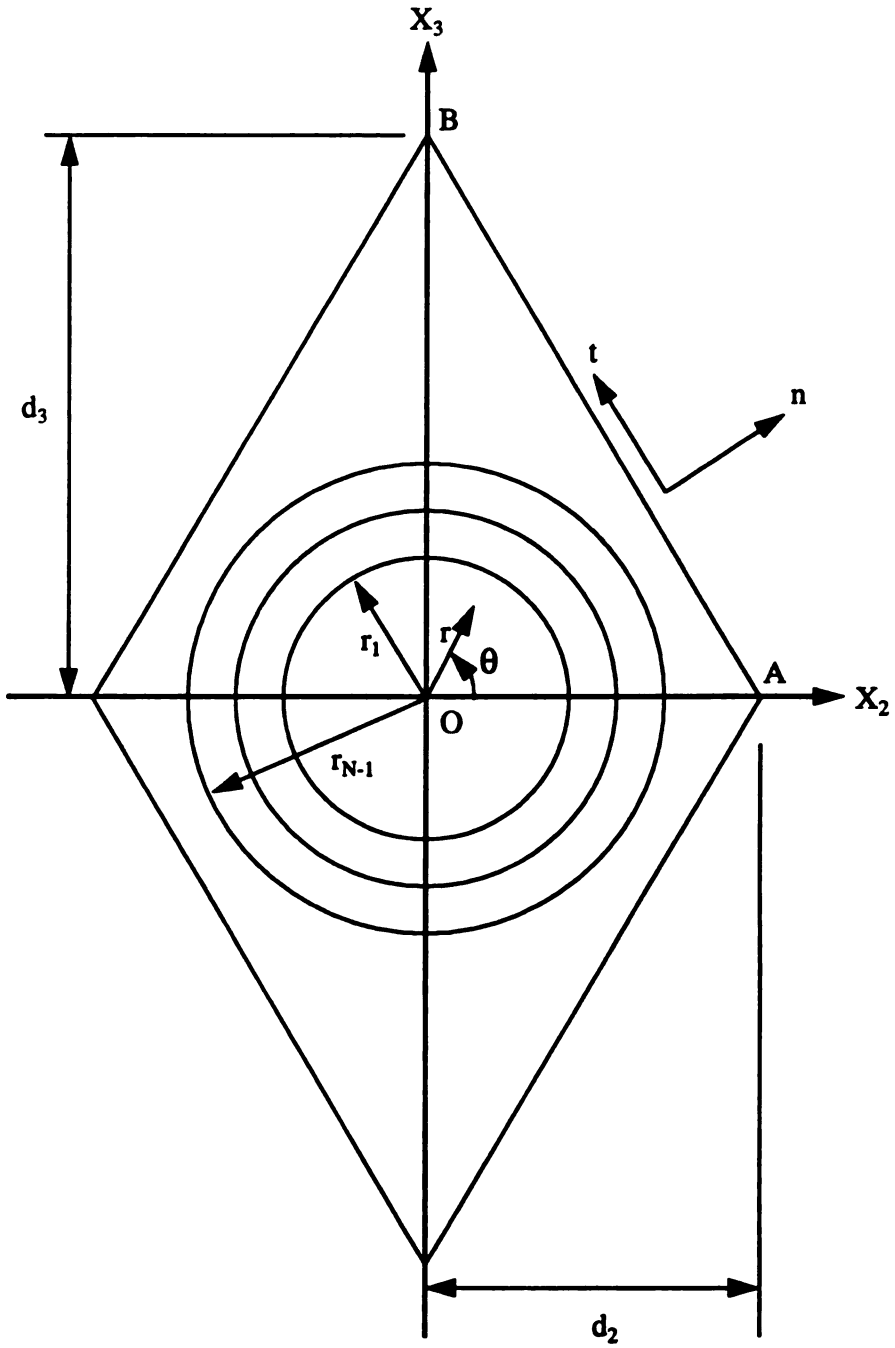

Figure 2. Diamond RVE used in the micromechanical model

$$\begin{Bmatrix} \sigma_x^{(n)} \\ \sigma_\theta^{(n)} \\ \sigma_r^{(n)} \end{Bmatrix} = \begin{bmatrix} C_{11}^{(n)} & C_{12}^{(n)} & C_{13}^{(n)} \\ C_{12}^{(n)} & C_{22}^{(n)} & C_{23}^{(n)} \\ C_{13}^{(n)} & C_{23}^{(n)} & C_{33}^{(n)} \end{bmatrix} \begin{Bmatrix} \varepsilon_x^{(n)} - \Phi_x^{(n)}(T) - \Psi_x^{(n)}(M) \\ \varepsilon_\theta^{(n)} - \Phi_\theta^{(n)}(T) - \Psi_\theta^{(n)}(M) \\ \varepsilon_r^{(n)} - \Phi_r^{(n)}(T) - \Psi_r^{(n)}(M) \end{Bmatrix} \tag{2.2.1}$$

$$\tau_{\theta r}^{(n)} = C_{44}^{(n)} \gamma_{\theta r}^{(n)}, \quad \tau_{xr}^{(n)} = C_{55}^{(n)} \gamma_{xr}^{(n)}, \quad \tau_{x\theta}^{(n)} = C_{66}^{(n)} \gamma_{x\theta}^{(n)}$$

where the superscript (n) ranges from 1 to N, and N is the number of constituents in the composite system. In Eq. (2.2.1),

$$\Phi_i(T) = \int_{T_0}^{T_1} \alpha_i(T)\, dT, \quad (i = x, \theta, r) \tag{2.2.2}$$

is the thermal strain, T_0 and T_1 are the reference (stress free) and final (current) temperatures respectively, and α_i is the coefficient of thermal expansion in the i^{th} -direction. Similarly,

$$\Psi_i(M) = \int_{M_0}^{M_1} \beta_i(M)\, dM, \quad (i = x, \theta, r) \tag{2.2.3}$$

is the strain due to moisture, M_0 and M_1 are the reference (stress free) and final(current) moisture levels respectively, and $\beta_i(M)$ is the coefficient of expansion in the i^{th} -direction due to moisture permeation.

For transversely isotropic materials, the material stiffness coefficients $C_{ij}(T, M)$ have the following relationships:

$$C_{22}^{(n)} = C_{33}^{(n)}, \quad C_{12}^{(n)} = C_{13}^{(n)}, \quad C_{44}^{(n)} = \frac{C_{22}^{(n)} - C_{23}^{(n)}}{2}, \quad C_{55}^{(n)} = C_{66}^{(n)} \tag{2.2.4}$$

The assumptions (a - c, f) ensure that the strains are in a state of generalized plane strain, therefore the displacements take the form:

$$\begin{aligned} u_x^{(n)}(x,\theta,r) &= u^{(n)}(\theta,r) + x\hat{\varepsilon}_x \\ u_\theta^{(n)}(x,\theta,r) &= v^{(n)}(\theta,r) \\ u_r^{(n)}(x,\theta,r) &= w^{(n)}(\theta,r) \end{aligned} \tag{2.2.5}$$

where $\hat{\varepsilon}_x$ is the uniform strain in the lamina in the fiber direction (along X_1 axis). The strain - displacement relations are as follows:

$$\begin{aligned} \varepsilon_x^{(n)} &= \hat{\varepsilon}_x & \gamma_{\theta r}^{(n)} &= \frac{\partial v}{\partial r}^{(n)} - \frac{v^{(n)}}{r} + \frac{1}{r}\frac{\partial w}{\partial \theta}^{(n)} \\ \varepsilon_\theta^{(n)} &= \frac{1}{r}\frac{\partial v}{\partial \theta}^{(n)} + \frac{w^{(n)}}{r} & \gamma_{xr}^{(n)} &= \frac{\partial u}{\partial r}^{(n)} \\ \varepsilon_r^{(n)} &= \frac{\partial w}{\partial r}^{(n)} & \gamma_{x\theta}^{(n)} &= \frac{1}{r}\frac{\partial u}{\partial \theta}^{(n)} \end{aligned} \tag{2.2.6}$$

The equilibrium equations in cylindrical coordinates for generalized plane stress are given as:

$$\begin{aligned} \frac{1}{r}\frac{\partial \tau_{x\theta}^{(n)}}{\partial \theta} + \frac{\partial \tau_{\theta r}^{(n)}}{\partial r} + \frac{\tau_{\theta r}^{(n)}}{r} &= 0 \\ \frac{1}{r}\frac{\partial \sigma_\theta^{(n)}}{\partial \theta} + \frac{\partial \tau_{\theta r}^{(n)}}{\partial r} + \frac{2\tau_{\theta r}^{(n)}}{r} &= 0 \\ \frac{1}{r}\frac{\partial \tau_{\theta r}^{(n)}}{\partial \theta} + \frac{\partial \sigma_r^{(n)}}{\partial r} + \frac{\sigma_r^{(n)} - \sigma_\theta^{(n)}}{r} &= 0 \end{aligned} \tag{2.2.7}$$

The governing equations in terms of displacements are obtained by substituting Eq. (2.2.1) and Eqs. (2.2.5) - (2.2.6) into Eq. (2.2.7):

$$C_{55}^{(n)}\left(r^2\frac{\partial^2 u}{\partial r^2}^{(n)} + r\frac{\partial u}{\partial r}^{(n)}\right) + C_{66}^{(n)}\left(\frac{\partial^2 u}{\partial \theta^2}^{(n)}\right) = 0$$

$$C_{12}^{(n)} r\left(\frac{\partial \hat{\varepsilon}_x}{\partial \theta} - \frac{\partial \Phi_x^{(n)}}{\partial \theta} - \frac{\partial \Psi_x^{(n)}}{\partial \theta}\right) + C_{23}^{(n)} r\left(\frac{\partial^2 w^{(n)}}{\partial r \partial \theta} - \frac{\partial \Phi_r^{(n)}}{\partial \theta} - \frac{\partial \Psi_r^{(n)}}{\partial \theta}\right)$$
$$+ C_{22}^{(n)}\left(\frac{\partial^2 v^{(n)}}{\partial \theta^2} + \frac{\partial w^{(n)}}{\partial \theta} - r\frac{\partial \Phi_\theta^{(n)}}{\partial \theta} - r\frac{\partial \Psi_\theta^{(n)}}{\partial \theta}\right)$$
$$+ C_{44}^{(n)}\left(r^2\frac{\partial^2 v^{(n)}}{\partial r^2} + r\frac{\partial v^{(n)}}{\partial r} - v^{(n)} + r\frac{\partial^2 w^{(n)}}{\partial r \partial \theta} + \frac{\partial w^{(n)}}{\partial \theta}\right) = 0$$

$$C_{12}^{(n)} r\left(-\hat{\varepsilon}_x + \Phi_x^{(n)} + \Psi_x^{(n)}\right) + C_{22}^{(n)}\left(-\frac{\partial v^{(n)}}{\partial \theta} - w^{(n)} + r\Phi_x^{(n)} + r\Psi_x^{(n)}\right) \qquad (2.2.8)$$
$$+ C_{13}^{(n)} r\left(\hat{\varepsilon}_x - \Phi_x^{(n)} - \Psi_x^{(n)} + r\frac{\partial \hat{\varepsilon}_x}{\partial r} - r\frac{\partial \Phi_x^{(n)}}{\partial r} - r\frac{\partial \Psi_x^{(n)}}{\partial r}\right)$$
$$+ C_{23}^{(n)} r\left(\frac{\partial^2 v^{(n)}}{\partial r \partial \theta} - \Phi_\theta^{(n)} - \Psi_\theta^{(n)} + \Phi_r^{(n)} + \Psi_r^{(n)} - r\frac{\partial \Phi_\theta^{(n)}}{\partial r} - r\frac{\partial \Psi_\theta^{(n)}}{\partial r}\right)$$
$$+ C_{33}^{(n)} r\left(r\frac{\partial^2 w^{(n)}}{\partial r^2} + \frac{\partial w^{(n)}}{\partial r} - \Phi_r^{(n)} - \Psi_r^{(n)} - r\frac{\partial \Phi_r^{(n)}}{\partial r} - r\frac{\partial \Psi_r^{(n)}}{\partial r}\right)$$
$$+ C_{44}^{(n)}\left(r\frac{\partial^2 v^{(n)}}{\partial r \partial \theta} - \frac{\partial v^{(n)}}{\partial \theta} + \frac{\partial^2 w^{(n)}}{\partial \theta^2}\right) = 0$$

In the Eqs. (2.2.8), the first one governs the deformation due to longitudinal shear, and the latter two govern the behavior due to normal, transverse shear, and hygrothermal loading. The first one is decoupled from the other ones. Moreover, considering the number of planes of geometric symmetry in the fiber geometry, the solution to the last two of Eq. (2.2.8) can be divided into a symmetric part (due to normal and hygrothermal loads) and an antisymmetric part (due to transverse shear loads). The solution to the first equation may be separated into a response due to shear in the X_1 - X_2 plane and a response due to shear in the X_1 - X_3 plane.

2.3 Solution for Symmetric Loading

The solution to the last two of Eq. (2.2.8) for deformations due to applied normal strains $(\varepsilon_1 = \hat{\varepsilon}_1, \varepsilon_2 = \hat{\varepsilon}_2, \varepsilon_3 = \hat{\varepsilon}_3)$ and hygrothermal loads $(\Delta M, \Delta T)$ are:

$$\begin{aligned} v^{(n)}(\theta, r) &= \sum_{i=1}^{\infty} v_i^{(n)}(r)\sin(2i\theta) \\ w^{(n)}(\theta, r) &= \sum_{i=1}^{\infty} w_i^{(n)}(r)\cos(2i\theta) \end{aligned} \tag{2.3.1}$$

and:

$$\begin{aligned} &\Phi_x^{(n)}(\theta, r) = \sum_{i=0}^{\infty} \Phi_{x_i}^{(n)}(r)\cos(2i\theta), \quad \Psi_x^{(n)}(\theta, r) = \sum_{i=0}^{\infty} \Psi_{x_i}^{(n)}(r)\cos(2i\theta) \\ &\Phi_\theta^{(n)}(\theta, r) = \sum_{i=0}^{\infty} \Phi_{\theta_i}^{(n)}(r)\cos(2i\theta), \quad \Psi_\theta^{(n)}(\theta, r) = \sum_{i=0}^{\infty} \Psi_{\theta_i}^{(n)}(r)\cos(2i\theta) \\ &\Phi_r^{(n)}(\theta, r) = \sum_{i=0}^{\infty} \Phi_{r_i}^{(n)}(r)\cos(2i\theta), \quad \Psi_r^{(n)}(\theta, r) = \sum_{i=0}^{\infty} \Psi_{r_i}^{(n)}(r)\cos(2i\theta) \\ &\hat{\varepsilon}_x(\theta, r) = \sum_{i=0}^{\infty} \hat{\varepsilon}_{x_i}(r)\cos(2i\theta) \end{aligned} \tag{2.3.2}$$

The following equations are obtained by substituting Eq. (2.3.1) and Eq. (2.3.2) into the last two of Eq. (2.2.8).

$$\begin{aligned} \sum_{i=0}^{\infty} \sin(2i\theta) \Bigg\{ & C_{22}^{(n)}\left(-4i^2 v_i^{(n)} - 2i w_i^{(n)}\right) + C_{23}^{(n)}\left(-2ir\frac{dw_i^{(n)}}{dr}\right) \\ & + C_{44}^{(n)}\left(r^2\frac{d^2 v_i^{(n)}}{dr^2} + r\frac{dv_i^{(n)}}{dr} - v_i^{(n)} - 2ir\frac{dw_i^{(n)}}{dr} - 2iw_i^{(n)}\right)\Bigg\} = 0 \end{aligned} \tag{2.3.3}$$

$$\sum_{i=0}^{\infty} \cos(2i\theta) \left\{ C_{22}^{(n)} \left(-2iv_i^{(n)} - w_i^{(n)} \right) + C_{33}^{(n)} \left(r^2 \frac{d^2 w_i^{(n)}}{dr^2} + r \frac{dw_i^{(n)}}{dr} \right) \right. \tag{2.3.4}$$

$$+ C_{23}^{(n)} \left(2ir \frac{dv_i^{(n)}}{dr} \right) + C_{44}^{(n)} \left(2ir \frac{dv_i^{(n)}}{dr} - 2iv_i^{(n)} - 4i^2 w_i^{(n)} \right)$$

$$+ r \left(C_{12}^{(n)} - C_{13}^{(n)} \right) \left(-\hat{\varepsilon}_{x_i} + \Phi_{x_i}^{(n)} + \Psi_{x_i}^{(n)} \right) + r \left(C_{22}^{(n)} - C_{33}^{(n)} \right)$$

$$\left. \bullet \left(\Phi_{\theta_i}^{(n)} + \Psi_{\theta_i}^{(n)} \right) + r \left(C_{23}^{(n)} - C_{33}^{(n)} \right) \left(\Phi_{r_i}^{(n)} + \Psi_{r_i}^{(n)} \right) \right\} = 0$$

When $i = 0$, Eq. (2.3.3) vanishes, and the solution to Eq. (2.3.4) for orthotropic materials can be obtained as follows:

$$w_0^{(n)} = B_{01}^{(n)} r^{\lambda_{01}^{(n)}} + B_{02}^{(n)} r^{\lambda_{02}^{(n)}} + H^{(n)} r \tag{2.3.5}$$

where $B_{01}^{(n)}$ and $B_{02}^{(n)}$ are constants, $\lambda_{01}^{(n)} = \sqrt{C_{22}^{(n)} / C_{33}^{(n)}}$, $\lambda_{02}^{(n)} = -\sqrt{C_{22}^{(n)} / C_{33}^{(n)}}$, and

$$H^{(n)} = \left\{ \frac{1}{C_{33}^{(n)} - C_{22}^{(n)}} \left(C_{13}^{(n)} - C_{12}^{(n)} \right) \left(-\hat{\varepsilon}_{x_0} + \Phi_{x_0}^{(n)} + \Psi_{x_0}^{(n)} \right) \right. \tag{2.3.6}$$

$$\left. + \left(C_{23}^{(n)} - C_{22}^{(n)} \right) \left(\Phi_{\theta_0}^{(n)} + \Psi_{\theta_0}^{(n)} \right) + \left(C_{33}^{(n)} - C_{22}^{(n)} \right) \left(\Phi_{r_0}^{(n)} + \Psi_{r_0}^{(n)} \right) \right\}$$

For transversely isotropic or isotropic materials: $H^{(n)} = 0$, $\lambda_{01}^{(n)} = 1$, $\lambda_{02}^{(n)} = -1$.

When $i > 0$, the solution to Eqs. (2.3.3) and (2.3.4) is written in the form:

$$v_i^{(n)} = \sum_{j=1}^{4} A_{ij}^{(n)} r^{\lambda_{ij}^{(n)}} \tag{2.3.7}$$

$$w_i^{(n)} = \sum_{j=1}^{4} B_{ij}^{(n)} r^{\lambda_{ij}^{(n)}}$$

where $A_{ij}^{(n)}$ and $B_{ij}^{(n)}$ are constants and $\lambda_{ij}^{(n)}$ are the eigenvalues of the solution. By substitution of Eq. (2.3.7) into Eqs. (2.3.3) and (2.3.4), the solution can be written as:

$$\begin{aligned} v^{(n)}(\theta, r) &= \sum_{i=1}^{\infty}\sum_{j=1}^{4} \xi_{ij}^{(n)} B_{ij}^{(n)} r^{\lambda_{ij}^{(n)}} \sin(2i\theta) \\ w^{(n)}(\theta, r) &= B_{01}^{(n)} r^{\lambda_{01}^{(n)}} + B_{02}^{(n)} r^{\lambda_{02}^{(n)}} + H^{(n)} r + \sum_{i=1}^{\infty}\sum_{j=1}^{4} B_{ij}^{(n)} r^{\lambda_{ij}^{(n)}} \cos(2i\theta) \end{aligned} \tag{2.3.8}$$

where:

$$\xi_{ij}^{(n)} = \frac{C_{22}^{(n)} - \left(\lambda_{ij}^{(n)}\right)^2 C_{33}^{(n)} + 4i^2 C_{44}^{(n)}}{2i\lambda_{ij}^{(n)}\left(C_{23}^{(n)} + C_{44}^{(n)}\right) - 2i\left(C_{22}^{(n)} + C_{44}^{(n)}\right)} \tag{2.3.9}$$

$$\begin{aligned} \lambda_{i1}^{(n)} &= +\sqrt{-\frac{b_i^{(n)}}{2a_i^{(n)}} + \frac{1}{2a_i^{(n)}}\sqrt{\left(b_i^{(n)}\right)^2 - 4a_i^{(n)} c_i^{(n)}}} \\ \lambda_{i2}^{(n)} &= +\sqrt{-\frac{b_i^{(n)}}{2a_i^{(n)}} - \frac{1}{2a_i^{(n)}}\sqrt{\left(b_i^{(n)}\right)^2 - 4a_i^{(n)} c_i^{(n)}}} \\ \lambda_{i3}^{(n)} &= -\sqrt{-\frac{b_i^{(n)}}{2a_i^{(n)}} + \frac{1}{2a_i^{(n)}}\sqrt{\left(b_i^{(n)}\right)^2 - 4a_i^{(n)} c_i^{(n)}}} \\ \lambda_{i4}^{(n)} &= -\sqrt{-\frac{b_i^{(n)}}{2a_i^{(n)}} - \frac{1}{2a_i^{(n)}}\sqrt{\left(b_i^{(n)}\right)^2 - 4a_i^{(n)} c_i^{(n)}}} \end{aligned} \tag{2.3.10}$$

$$\begin{aligned} a_i^{(n)} &= C_{33}^{(n)} C_{44}^{(n)} \\ b_i^{(n)} &= -4i^2 C_{22}^{(n)} C_{33}^{(n)} - C_{22}^{(n)} C_{44}^{(n)} - C_{33}^{(n)} C_{44}^{(n)} + 4i^2\left(C_{23}^{(n)}\right)^2 \\ &\quad + 8i^2 C_{23}^{(n)} C_{44}^{(n)} \\ c_i^{(n)} &= C_{22}^{(n)} C_{44}^{(n)}\left(4i^2 - 1\right)^2 \end{aligned} \tag{2.3.11}$$

$B_{ij}^{(n)}$ are the unknown coefficients to be determined as follows.

To eliminate displacement and stress singularity in fiber, some coefficient should be set to zero. That is:

$$B_{02}^{(1)} = B_{i3}^{(1)} = B_{i4}^{(1)} = 0$$

At each constituent interface r_n, displacements and normal stress components must be continuous:

$$\begin{aligned} v^{(n)}(\theta, r_n) &= v^{(n+1)}(\theta, r_n) \\ w^{(n)}(\theta, r_n) &= w^{(n+1)}(\theta, r_n) \\ \sigma_r^{(n)}(\theta, r_n) &= \sigma_r^{(n+1)}(\theta, r_n) \\ \tau_{\theta r}^{(n)}(\theta, r_n) &= \tau_{\theta r}^{(n+1)}(\theta, r_n) \end{aligned} \tag{2.3.12}$$

In the diamond array, the outer boundary conditions of a cell are determined, when a cell is deformed, by assuming that [36, 37, 38]:

1. a cell must retain the symmetry with respect to both axes (two fold symmetry),

2. the deformed shape must remain typical of all the other cells,

3. the repeating adjacent cells are congruent.

In addition, the displacements and stresses must be continuous across the repeating cell boundaries, so the following conditions are obtained:

$$\begin{aligned} (u_2)_P + (u_2)_{P''} &= \hat{\varepsilon}_2 d_2 \\ (u_3)_P + (u_3)_{P''} &= \hat{\varepsilon}_3 d_3 \\ (\sigma_n)_P &= (\sigma_n)_{P''} \\ (\tau_{nt})_P &= (\tau_{nt})_{P''} \end{aligned} \tag{2.3.13}$$

where $(\sigma_n)_P$ and $(\tau_{nt})_P$ are the normal and shearing stresses at the boundary AB, and the $\hat{\varepsilon}_2$ and $\hat{\varepsilon}_3$ are the applied strains in the X_2 and X_3 directions, respectively. The points P and P″ are located on boundary AB as shown in Figure 3, and the locations are defined as follows:

If the point P has the polar coordinates (r_P, θ_P), then due to the two fold symmetry and congruency of the adjacent repeating cells, the coordinate of point P″ will be:

$$\begin{aligned} r_{P''} &= \sqrt{(d_2 - r_P\cos\theta_P)^2 + (d_3 - r_P\sin\theta_P)^2} \\ \theta_{P''} &= \operatorname{atan}\left(\frac{d_3 - r_P\sin\theta_P}{d_2 - r_P\cos\theta_P}\right) \end{aligned} \tag{2.3.14}$$

2.4 Solution for Transverse Shear Loading

Since the last two of Eqs. (2.2.8) are also the governing equations for the deformations caused by applied transverse shearing strain (γ_{23}), and the solution procedure is the same as the aforementioned symmetric loading, only the final form of solution will be given here. The solution can be written as follows:

$$\begin{aligned} v^{(n)}(\theta, r) &= D_{01}^{(n)} r + D_{02}^{(n)} \frac{1}{r} + \sum_{i=1}^{\infty}\sum_{j=1}^{4} \xi_{ij}^{(n)} D_{ij}^{(n)} r^{\lambda_{ij}^{(n)}} \cos(2i\theta) \\ w^{(n)}(\theta, r) &= \sum_{i=1}^{\infty}\sum_{j=1}^{4} \xi_{ij}^{(n)} D_{ij}^{(n)} r^{\lambda_{ij}^{(n)}} \sin(2i\theta) \end{aligned} \tag{2.4.1}$$

where $\lambda_{ij}^{(n)}$ are defined in Eq. (2.3.10) and Eq. (2.3.11), and

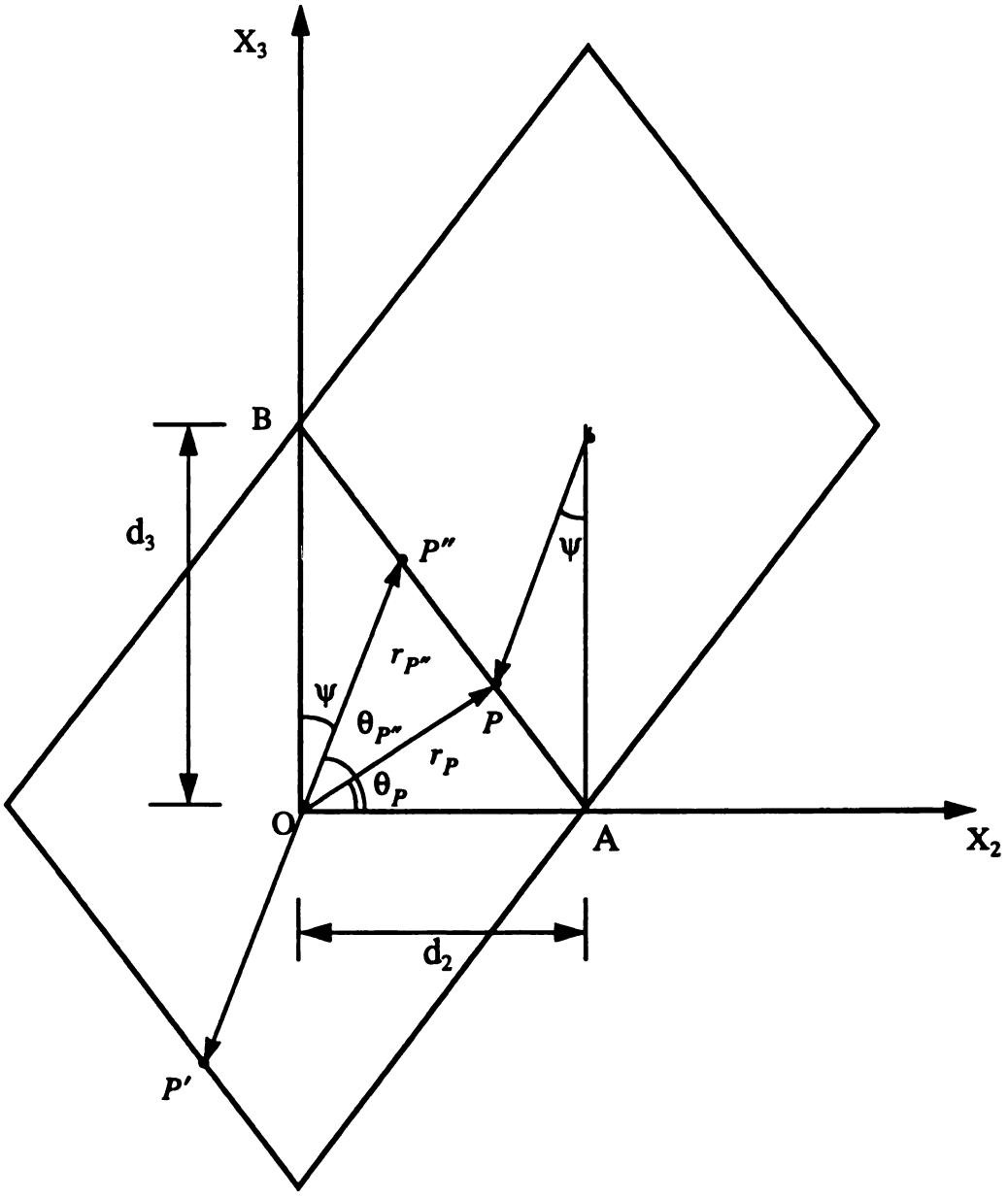

Figure 3. The determination of boundary condition from congruency and symmetry of repeating cells

$$\xi_{ij}^{(n)} = \frac{2i\lambda_{ij}^{(n)}\left(C_{23}^{(n)} + C_{44}^{(n)}\right) - 2i\left(C_{22}^{(n)} + C_{44}^{(n)}\right)}{-C_{22}^{(n)} + \left(\lambda_{ij}^{(n)}\right)^2 C_{33}^{(n)} - 4i^2 C_{44}^{(n)}} \tag{2.4.2}$$

$D_{ij}^{(n)}$ are constants, which are the unknown coefficients to be determined as follows, as in the symmetric loading case. In order for the solution to be bounded at $r = 0$, some of $D_{ij}^{(n)}$ are set to zero:

$$D_{02}^{(1)} = D_{i3}^{(1)} = D_{i4}^{(1)} = 0$$

The rest of coefficients are determined by the continuity condition Eq. (2.3.12) at each interface and the boundary conditions at the boundary of the repeating cell. In this case, the boundary conditions at the edge AB are:

$$\begin{aligned} (u_2)_P + (u_2)_{P''} &= \frac{1}{2}\hat{\gamma}_{23} d_3 \\ (u_3)_P + (u_3)_{P''} &= \frac{1}{2}\hat{\gamma}_{23} d_2 \\ (\sigma_n)_P &= (\sigma_n)_{P''} \\ (\tau_{nt})_P &= (\tau_{nt})_{P''} \end{aligned} \tag{2.4.3}$$

where points P and P'' are defined in Eq. (2.3.14), and $\hat{\gamma}_{23}$ is the applied shearing stain in the X_2-X_3 plane.

2.5 Solutions for Longitudinal Shear Loading

The deformation under longitudinal shear loading is governed by the first of Eqs. (2.2.8). In this case, the solution is divided into one for applied loading in the X_1 - X_3 plane and one for applied loading in the X_1 - X_2 plane.

The solution for longitudinal shear loading in the X_1 - X_3 plane ($\gamma_{13} = \hat{\gamma}_{13}, \gamma_{12} = 0$) is:

$$u^{(n)}(\theta, r) = \sum_{k=1}^{\infty} \left(F_{k1}^{(n)} r^{\lambda_{k1}^{(n)}} + F_{k2}^{(n)} r^{\lambda_{k2}^{(n)}} \right) \sin(k\theta) \tag{2.5.1}$$

where $\lambda_{k1}^{(n)} = k\sqrt{C_{66}^{(n)}/C_{55}^{(n)}}$, $\lambda_{k2}^{(n)} = -k\sqrt{C_{66}^{(n)}/C_{55}^{(n)}}$, and $F_{k1}^{(n)}$, $F_{k2}^{(n)}$ are constants. To eliminate the singular contribution, the following coefficient are set to zero:

$$F_{k2}^{(1)} = 0$$

The rest of coefficient $F_{k1}^{(n)}$ and $F_{k2}^{(n)}$ are determined by the similar procedure like previous cases. The continuity conditions are at each interface are:

$$\begin{aligned} u^{(n)}(\theta, r_n) &= u^{(n+1)}(\theta, r_n) \\ \tau_{xr}^{(n)}(\theta, r_n) &= \tau_{xr}^{(n+1)}(\theta, r_n) \end{aligned} \tag{2.5.2}$$

The boundary condition at the boundary AB are:

$$\begin{aligned} (u_2)_P + (u_2)_{P'} &= \hat{\gamma}_{13} d_3 \\ (\tau_{1t})_P &= (\tau_{1t})_{P'} \end{aligned} \tag{2.5.3}$$

where $\hat{\gamma}_{13}$ is the applied shearing strain in the X_1-X_3 plane, and 1 indicates X_1 direction.

The solution for longitudinal shear loading in the X_1 - X_2 plane ($\gamma_{12} = \hat{\gamma}_{12}, \gamma_{13} = 0$) is:

$$u^{(n)}(\theta, r) = \sum_{k=1}^{\infty} \left(G_{k1}^{(n)} r^{\lambda_{k1}^{(n)}} + G_{k2}^{(n)} r^{\lambda_{k2}^{(n)}} \right) \cos(k\theta) \tag{2.5.4}$$

where $\lambda_{k1}^{(n)}$, $\lambda_{k2}^{(n)}$ are the same ones as given above, and $G_{k1}^{(n)}$, $G_{k2}^{(n)}$ are constants. To eliminate the singular contribution, the following coefficient are set to zero:

$$G_{k2}^{(1)} = 0$$

The rest of coefficient $G_{k1}^{(n)}$ and $G_{k2}^{(n)}$ are determined by the similar procedure like previous cases. The continuity conditions are at each interface are:

$$\begin{aligned} u^{(n)}(\theta, r_n) &= u^{(n+1)}(\theta, r_n) \\ \tau_{xr}^{(n)}(\theta, r_n) &= \tau_{xr}^{(n+1)}(\theta, r_n) \end{aligned} \tag{2.5.5}$$

The boundary condition at the boundary AB are:

$$\begin{aligned} (u_2)_P + (u_2)_{P'} &= \hat{\gamma}_{12} d_3 \\ (\tau_{1t})_P &= (\tau_{1t})_{P'} \end{aligned} \tag{2.5.6}$$

where $\hat{\gamma}_{12}$ is the applied shearing strain in the X_1-X_3 plane, and 1 indicates X_1 direction.

2.6 Computation of Effective Composite Properties

For the composite material with a hexagonal array of the fibers, the composite constitutive relations in material coordinates are:

$$\begin{Bmatrix} \sigma_1 \\ \sigma_2 \\ \sigma_3 \end{Bmatrix} = \begin{bmatrix} C_{11} & C_{12} & C_{12} \\ C_{12} & C_{22} & C_{23} \\ C_{12} & C_{23} & C_{22} \end{bmatrix} \begin{Bmatrix} \varepsilon_1 - \phi_1 - \psi_1 \\ \varepsilon_2 - \phi_2 - \psi_2 \\ \varepsilon_3 - \phi_2 - \psi_2 \end{Bmatrix}$$

$$\tau_{23} = \frac{C_{22} - C_{23}}{2}\gamma_{23}, \quad \tau_{13} = C_{55}\gamma_{13}, \quad \tau_{12} = C_{55}\gamma_{12} \tag{2.6.1}$$

The effective composite properties are calculated by applying a single unit strain in one direction, setting all other strains and hygrothermal loads to zero, and calculating the resulting average stresses. For example, if $\varepsilon_1 = 1$ and all other strains are zero, then:

$$C_{11} = \bar{\sigma}_1, \; C_{12} = \bar{\sigma}_2 \tag{2.6.2}$$

Likewise the other effective composite properties can be determined in this way. The average stresses are calculated as follows:

$$\begin{aligned}
\bar{\sigma}_1 &= \frac{2}{d_2 d_3}\int_0^{\frac{\pi}{2}}\int_0^{\bar{r}(\theta)} \sigma_x(\theta, r)\, r dr d\theta \\
\bar{\sigma}_2 &= \frac{1}{d_3}\int_0^{d_3} \sigma_x\left(\frac{\pi}{2}, r\right) dr \\
\bar{\sigma}_3 &= \frac{1}{d_2}\int_0^{d_2} \sigma_\theta(0, r)\, dr \\
\bar{\tau}_{13} &= \frac{1}{d_2}\int_0^{d_2} \tau_{x\theta}(0, r)\, dr
\end{aligned} \tag{2.6.3}$$

where

$$\bar{r}(\theta) = d_2 \frac{\sin(\omega)}{\sin(\omega + \theta)}, \quad \omega = \operatorname{atan}(\sqrt{3}) \tag{2.6.4}$$

If the C_{ij} are obtained at a certain temperature and moisture level, the coefficients of thermal expansion and moisture expansion can be calculated by considering only constant thermal expansion or constant moisture expansion over their ranges (with all other strains zero). The procedures are very similar to that of getting C_{ij}. Then the coefficients of thermal expansion are obtained by setting $\Delta T = 1$ with all other strains set to zero:

$$\{\alpha\} = -[C]^{-1}\{\bar{\sigma}\} \tag{2.6.5}$$

The coefficient of moisture expansion are obtained by setting $\Delta M = 1$ with all other strains set to zero:

$$\{M\} = -[C]^{-1}\{\bar{\sigma}\} \tag{2.6.6}$$

where $\Delta\bar{M}$ is a small change in moisture content.

CHAPTER III
MICROMECHANICAL FAILURE THEORY

3.1 Introduction

The failure theory developed here utilizes the micromechanical elasticity solution obtained in the previous chapter, and the well-known failure criteria for isotropic as well as orthotropic materials to predict the failure in a given constituent.

In this chapter, a brief illustration will be given of a simple example of micromechanics based failure predictions. Detailed explanations will be given concerning the concept of the micromechanical failure theory and how the micromechanical elasticity solution and failure criteria are utilized here. Finally, the procedure for curve fitting of failure envelopes obtained by the micromechanical failure theory to polynomial type failure envelopes will be discussed.

3.2 An Example of Micromechanical Failure

Consider the following example where a compressive force is acting on composite material through a rigid body as shown in Figure 4. The composite material is composed of material A with cross sectional area S_A and material B with cross sectional area S_B. The total cross sectional area and length are S_t and L, respectively. The Young's modulus of composite, material A and material B are E_t, E_A and E_B respectively. From the equilibrium

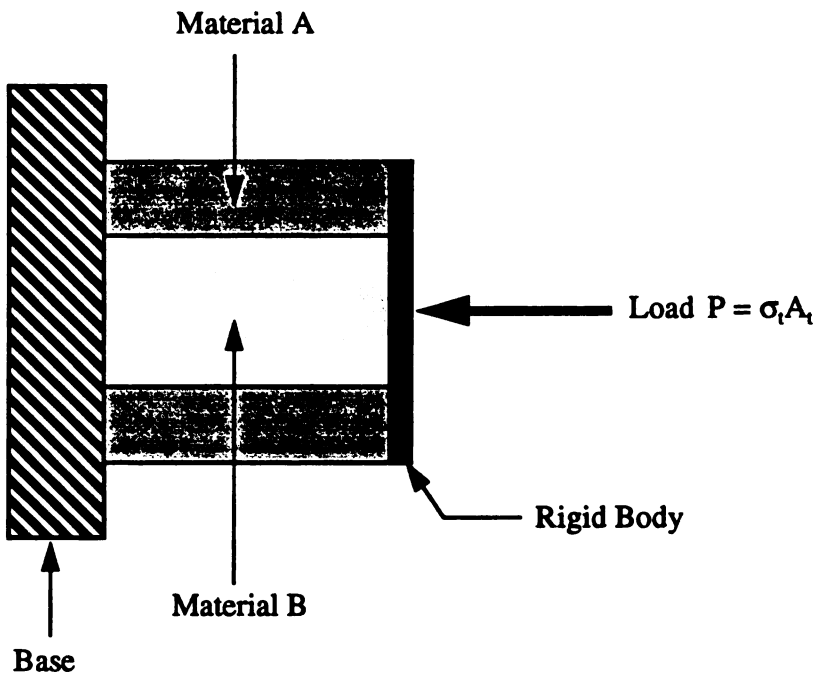

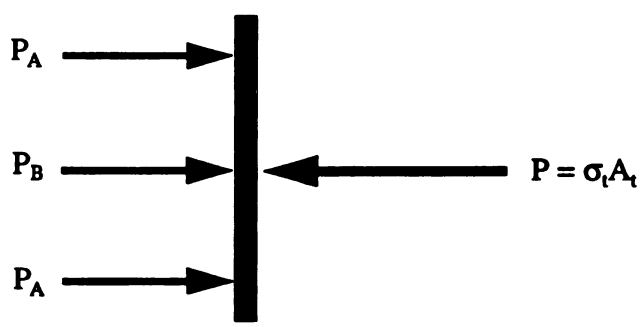

Figure 4. The illustration of a simple composite body subjected to compressive force and the free body diagram

of horizontal forces, we can get:

$$2P_A + P_B = P \tag{3.2.1}$$

The strain and displacement of each constituent are:

for constituent A, $$\varepsilon_A = \frac{\delta_A}{L} = \frac{\sigma_A}{E_A} = \frac{P_A}{E_A S_A}$$

$$\delta_A = \frac{P_A L}{E_A S_A} \tag{3.2.2}$$

for constituent B, $$\varepsilon_B = \frac{\delta_B}{L} = \frac{\sigma_B}{E_B} = \frac{P_B}{E_B S_B}$$

$$\delta_B = \frac{P_B L}{E_B S_B} \tag{3.2.3}$$

Since material A and B are compressed through a rigid body, it can be assumed that the displacements are same. Therefore, by equating Eq. (3.2.2) and Eq. (3.2.3):

$$\delta_A = \delta_B = \delta$$

$$P_A = \frac{E_A S_A}{E_B S_B} P_B \tag{3.2.4}$$

The substitution of Eq. (3.2.4) into Eq. (3.2.1) leads to:

$$P_B = \frac{E_B S_B}{2E_A S_A + E_B S_B} P \tag{3.2.5}$$

Substituting of Eq. (3.2.5) into Eq. , P_A is obtained:

$$P_A = \frac{E_A S_A}{2E_A S_A + E_B S_B} P \tag{3.2.6}$$

Then, the stress state of each constituent and the combined material, respectively, when only the compressive load P is acting is obtained as follows:

$$\sigma_t = \frac{P}{S_t} \tag{3.2.7}$$

$$\sigma_A = \frac{P_A}{S_A} = \frac{E_A P}{2E_A S_A + E_B S_B} \tag{3.2.8}$$

$$\sigma_B = \frac{P_B}{S_B} = \frac{E_B P}{2E_A S_A + E_B S_B} \tag{3.2.9}$$

If the applied load is increased, the stress in constituent A and/or constituent B will eventually reach its ultimate value. Failure of the composite may be defined as failure of either constituent A or B. The stress in the composite at that time is:

$$\sigma_t^u = \frac{P^u}{S_t} \tag{3.2.10}$$

and we have either

$$\sigma_A^u = \frac{P_A^u}{S_A} = \frac{E_A P^u}{2E_A S_A + E_B S_B} \tag{3.2.11}$$

or

$$\sigma_B^u = \frac{P_B^u}{S_B} = \frac{E_B P^u}{2E_A S_A + E_B S_B} \tag{3.2.12}$$

where σ_t^u, P^u, σ_A^u, P_A^u, σ_B^u, and P_B^u are the stresses and loads in the composite material and its constituents, respectively, when the failure occurs. In this case, the stress in each constituent can be calculated, and a proper failure criterion for each constituent has to be chosen to predict failure. Here, it can be observed that the (average) stress state of the composite material is different from that of each constituent from Eq. (3.2.10), Eq. (3.2.10) and Eq. (3.2.12), when the failure occurs in some constituent.

In order adopt this concept to failure of fiber reinforced composite materials, we need to 1) set up an appropriate RVE (Representative Volume Element), 2) perform stress analysis in RVE for a given set of external loads, and 3) choose the proper failure criterion for each constituent to predict the onset of failure. Steps 1 and 2 were discussed in the previous chapter. Below, some common failure criteria are discussed.

3.3 Failure Criteria

Failure criteria can be roughly divided into those for isotropic materials and those for orthotropic materials. Failure criteria play a very important role in the micromechanical failure theory, because failure criteria predict whether or not failure occurs at the selected points in the R.V.E. Thus, the several failure criteria useful for prediction of the failure in fiber, matrix and fiber/matrix interface will be described briefly.

3.3.1 Failure Criteria for Isotropic Material

Maximum Principal Stress Theory, or Rankine Theory

The maximum principal stress criterion assumes that failure occurs when one of the principal stresses is equal to or greater than the value of the uniaxial yield stress in tension, σ_u^T, or is equal to or less than the value of the uniaxial yield stress in compression, σ_u^C. This criterion asserts that yielding will occur when any one of the following conditions is reached:

In tension, $\sigma_1 \geq \sigma_u^T$, or $\sigma_2 \geq \sigma_u^T$, or $\sigma_3 \geq \sigma_u^T$

In compression, $\sigma_1 \geq \sigma_u^C$, or $\sigma_2 \geq \sigma_u^C$, or $\sigma_3 \geq \sigma_u^C$

This theory assumes that only the maximum principal stress causes failure, and the contribution of stress interaction is disregarded [39].

Maximum Principal Strain Theory, or Saint-Venant Theory

The maximum principal strain criterion assumes that failure occurs when one of the principal strains is equal to or greater than the value of the uniaxial yield strain in tension, ε_u^T, or is equal to or less than the value of the uniaxial yield strain in compression, ε_u^C. The ε_u^T and ε_u^C are related to the ultimate stresses by:

$$\varepsilon_u^T = \frac{1}{E}\sigma_u^T \text{ and } \varepsilon_u^C = \frac{1}{E}\sigma_u^C$$

where E is the elastic modulus of the material. This criterion asserts that yielding will occur when any one of the following conditions is reached:

In tension, $\varepsilon_1 \geq \varepsilon_u^T$, or $\varepsilon_2 \geq \varepsilon_u^T$, or $\varepsilon_3 \geq \varepsilon_u^T$

In compression, $\varepsilon_1 \geq \varepsilon_u^C$, or $\varepsilon_2 \geq \varepsilon_u^C$, or $\varepsilon_3 \geq \varepsilon_u^C$

In this theory, the role of the interaction of the principal stress is accounted for failure [39].

Maximum Shear Stress Criterion, or Tresca Criterion

The maximum shear stress criterion (sometimes called the Coulomb theory) assumes that failure occurs when the maximum shear stress is equal to or greater than the value of the maximum shear stress, $\tau_u = \frac{1}{2}\sigma_u$, which is occurring under uniaxial tension. The maximum shear stress is equal to half of the difference between the maximum and minimum principal stresses. This criterion asserts that failure will occur when any one of the following conditions is reached:

$$|\sigma_1 - \sigma_2| = \sigma_u,$$

$$|\sigma_2 - \sigma_3| = \sigma_u,$$

$$|\sigma_3 - \sigma_1| = \sigma_u$$

In this theory, some interaction of the principal stresses is included, but this theory is not applicable for the material whose tensile and compressive strengths are different [39].

Distortion Energy Criteria, or the Von Mises Criterion

The distortion energy theory assumes that failure begins when the distortion energy is equal to or greater than the distortion energy at failure in uniaxial tension. This criterion asserts that yielding will occur when the following condition is reached:

$$\frac{1}{2}\left[(\sigma_1 - \sigma_2)^2 + (\sigma_2 - \sigma_3)^2 + (\sigma_3 - \sigma_1)^2\right] = \sigma_u^2$$

The distortional energy criterion accounts for interaction of the principal stresses [39].

3.3.2 Failure Criteria for Orthotropic Material

Independent Maximum Stress Criterion

The independent maximum stress criterion assumes that failure will occur when any of the stress components referred to the principal material axes is equal to or greater than its corresponding allowable strength in that direction. Thus, this criterion asserts that failure would occur when any one of the following conditions is reached:

$$\sigma_{11} = X_1^T, \qquad -\sigma_{11} = X_1^C$$

$$\sigma_{22} = X_2^T, \qquad -\sigma_{22} = X_2^C$$

$$\sigma_{33} = X_3^T, \qquad -\sigma_{33} = X_3^C$$

$$\sigma_{23} = X_{23}, \qquad \sigma_{31} = X_{31}, \qquad \sigma_{12} = X_{12}$$

where σ_{ij} are the stress components referred to the material axes, and X_i^T, X_i^C and X_{ij} are the tensile, compressive and shear strengths, respectively, of the material in its i^{th} principal direction. This theory does not account for stress interaction [40].

Independent Maximum Strain Criterion

The independent maximum strain criterion assumes that failure will occur when any of the strain components referred to the principal material axes is equal to or greater than its corresponding allowable strain in that direction. Thus, this criterion asserts that failure would occur when any one of the following condition is reached:

$$\varepsilon_{11} = e_1^T, \qquad -\varepsilon_{11} = e_1^C$$

$$\varepsilon_{22} = e_2^T, \qquad -\varepsilon_{22} = e_2^C$$

$$\varepsilon_{33} = e_3^T, \qquad -\varepsilon_{33} = e_3^C$$

$$\varepsilon_{23} = e_{23}, \qquad \varepsilon_{31} = e_{31}, \qquad \varepsilon_{12} = e_{12}$$

where ε_{ij} are the strain components referred to the material axes, and e_i^T, e_i^C and e_{ij} are the tensile, compressive and shear strengths, respectively, of the material in its i^{th} principal direction. This theory accounts for the stress interaction but disregards any strain interaction [40].

3.4 Micromechanical Failure Theory

Failure criteria for composite materials have been developed on the basis of the aforementioned micromechanics elasticity solution and failure criteria for isotropic and orthotropic materials. They can be cast in several forms in either stress- or strain- space, and require only stiffness properties and uniaxial strength data of each constituent

The failure of composite materials is predicted when stress or strain states of a point in any of the constituents (e.g., fiber, matrix and interface) exceed a critical level as predicted by a properly chosen failure criterion for each constituent. When a lamina (composite) load gives rise to a micromechanical stress state that causes failure in some constituent, then that load state is assumed to lie on the failure envelope for the composite material. When a failure criterion for each constituent is chosen, the mechanical properties of each constituent and the failure characteristics of each constituent in the composite material should be taken into account. Since the primary emphasis here was on polymer matrix composite materials, the details to be discussed are most suitable for these material systems.

Fiber

Fibers in composite materials are used as a reinforcing agent. In polymer matrix composite materials, the longitudinal Young's modulus of the fibers is often 10 times greater than that of the matrix [4]. If a unidirectional lamina is subjected to a tensile or a compressive longitudinal load, the failure of the lamina is usually a result of the fracture of fiber in tension or fiber buckling/kinking in compression, and the failure modes and the failure stresses for each case are quite different. When a tensile longitudinal load is acting on a lamina, the axial strain of each constituent in the lamina is the same, since it was assumed that fibers are perfectly bonded to the matrix through fiber/matrix interface:

$$\varepsilon^{f}_{x_1} = \varepsilon^{m}_{x_1} = \varepsilon^{l}_{x_1} \tag{3.4.1}$$

where $\varepsilon^{f}_{x_1}$, $\varepsilon^{m}_{x_1}$ and $\varepsilon^{l}_{x_1}$ are the longitudinal strains of fibers, matrix and lamina, respectively. However, generally, the fibers have a lower ultimate strain than matrix, and lamina fracture occurs at the fiber ultimate strain [41]. When a lamina is subjected to a compressive longitudinal load, the failure of a lamina is often caused by buckling or kinking of fibers in out-of phase mode or in-phase [42]. But, according to Hashin [22], the dependence of both fiber failure modes on the axial shear stresses is not identified clearly. Hence, it is concluded that axial tensile and compressive strains of fiber dominate the composite longitudinal strength. Thus, the maximum strain criterion was chosen as the fiber failure criterion in this research. Failure modes such as fiber buckling/kinking are assumed to initiate at some critical level of axial strain, and so are accounted for in indirectly. In addition, it is assumed that the fiber never fails due to transverse and shear strains ($\varepsilon_2, \varepsilon_3, \gamma_{23}, \gamma_{31}$ and γ_{12}), therefore, the much bigger values than that of

longitudinal strength are assigned to transverse and shear strength components.

Fiber/matrix interface

Generally, the fiber/matrix interface is a vanishingly thin region in the composite between the fiber and matrix, and is formed during the composite manufacturing process. It transfers the load between the fiber and matrix in composites, so that it affects the mechanical response of composite materials.

If the interface region has a small but finite thickness, it is often referred to as an interphase. The interphase may have distinct elastic properties, and it was shown in references [43, 44] that the elastic moduli and the thickness of the interphase have an influence on the effective elastic properties. But the elastic moduli and the thickness are often not available for many composite systems. Thus, in the current study, an interphase region was not considered, though the model is sufficiently general to have considered one.

Furthermore, its normal and shearing strengths are difficult to measure experimentally. So, in the current research, the normal and shearing strengths were determined using the following procedure [45]. With all other applied loads being zero, the lamina ultimate transverse strength was applied to the micromechanical model. Then, normal and shearing stresses were computed in the matrix at the fiber/matrix interface region, and principal stresses were computed elsewhere in the matrix. If the maximum principal stress in the matrix due to the load was less than the tensile strength of the matrix material in the bulk state, then it was assumed that failure occurred at the fiber/matrix interface and the maximum normal stress at the fiber/matrix interface region represents the normal strength of interface. Otherwise, it was assumed that failure occurred in the matrix, and the normal strength of interface is equal to or greater than the computed maximum normal stress at

the interface. The shear strength of interface was calculated in a similar way by applying the lamina ultimate inplane shearing stress. It was assumed that interface was perfectly bonded to both fiber and matrix, and failed due to tensile transverse normal stress or shear stresses ($\sigma_{r\theta}$, σ_{xr}). Hence independent maximum stress criterion was applied to predict the failure in the interface. [28, 32]

Matrix:

When a lamina is subjected to a longitudinal load, the matrix plays the role of both protecting the fibers and distributing load between and among the fibers. However, when a transverse tensile load is applied to the lamina, the fibers do not serve as a load-carrying constituent in the lamina, but act as solid inclusions in matrix. Due to the existence of solid inclusions in the matrix, the local stresses and strains in the matrix are higher than the applied stress [4]. In addition, even though the region with maximum stress in the composites is often located in some other phase, failure generally occurs in the matrix first. Furthermore, a uniaxial load acting on a composite material in any direction can cause a three dimensional stress state in the matrix, which causes the stress components to interact. So, it is assumed that the transverse and shear strength of composite material is dominated by the strength of the matrix. The suitability of a matrix failure criterion depends on the properties of the matrix - ductile, brittle, etc. In this work, the following criteria are considered: maximum principal stress, maximum principal strain, Von-Mises and Tresca criterion, wherein the Tresca failure criterion is applicable to matrices of which the tensile strength and the compressive strength are the same.

The stress evaluation points are carefully selected as shown Figure 5 in order not to miss the locations of high stress. The stress evaluation points at the interface region and

near the interface region in the matrix should be densely distributed, because not only do the highest stresses often exist in that region, but also the stress gradient in that region is very large. In the current research, 249 points in the RVE were chosen at which to evaluate the stresses as shown in Figure 5. The interface is treated as a finite region, but is so thin that the stress evaluation points in that region appear to overlap with those in the other regions.

Lamina Strength Components

The uniaxial normal strengths of a lamina are determined if a uniaxial lamina load acting along a principal material of a lamina creates a micromechanical stress state that causes some constituent to fail, and the lamina load is assumed to be the unidirectional strength of the lamina in that direction. Constituent failure due to the micromechanical stress state caused by a lamina load is predicted by the failure criterion chosen for the constituent. The shear strengths of a lamina are obtained in the same way as the longitudinal normal strength are found.

But more attention and insight should be paid to determine the transverse normal strength and the longitudinal shear strength. In reality, the arrangement of fibers in continuous fiber-reinforced composite materials is random, therefore these materials can be regarded to be transversely isotropic in both stiffness and strength. The assumption of hexagonal packing of fibers, as used in the current elasticity solution, gives a rise to transverse isotropy of elastic moduli, but not strength. Thus, the transverse normal load and the longitudinal shear load causing failure of some constituent should be applied and averaged over a range of loading directions from 0 degrees loading direction to 360 degrees (or 0 degrees to 30 degrees due to symmetry) to obtain the transverse normal and the

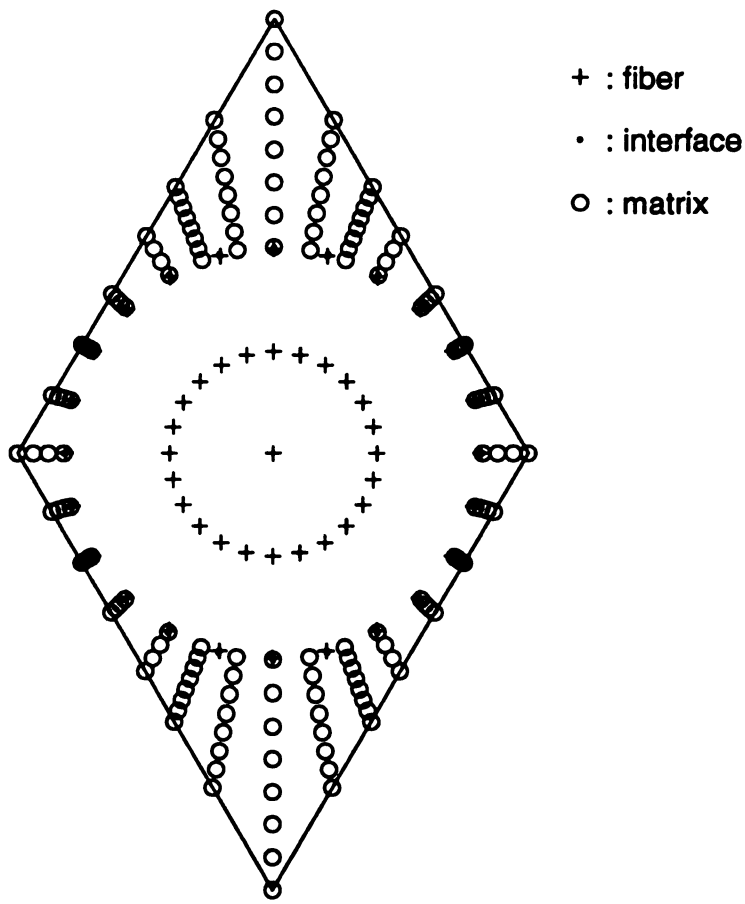

Figure 5. The stress evaluation points in RVE

longitudinal shear strength of the lamina. To perform these processes, a uniaxial stress load acting on the model at a certain angle should be transformed to the reference axes by using the stress transformation law.

When a stress load is acting on the lamina at a certain angle as shown in Figure 6, by stress transformation laws, the stress tensor $\bar{\sigma}$ in the Cartesian coordinate $P\bar{X}_1\bar{X}_2\bar{X}_3$, of which components are $\bar{\sigma}_{ij}$ $i,j = 1, 2, \ldots, 6$, can be expressed in terms of the stress tensor σ in the Cartesian coordinate $PX_1X_2X_3$, which has σ_{ij} $i,j = 1, 2, \ldots, 6$ as components, as follows [47]:

$$\sigma = A^T \bar{\sigma} A \tag{3.4.2}$$

where A is a proper transformation matrix, and A^T is the transpose matrix of A. The A and A^T matrices are written as:

$$A = [a_{ij}] = \begin{bmatrix} 1 & 0 & 0 \\ 0 & \cos(-\theta) & \sin(-\theta) \\ 0 & -\sin(-\theta) & \cos(-\theta) \end{bmatrix} \tag{3.4.3}$$

$$A^T = [a_{ij}]^T = \begin{bmatrix} 1 & 0 & 0 \\ 0 & \cos(-\theta) & -\sin(-\theta) \\ 0 & \sin(-\theta) & \cos(-\theta) \end{bmatrix} \tag{3.4.4}$$

The tensors σ, $\bar{\sigma}$ are:

$$\sigma = [\sigma_{ij}] = \begin{bmatrix} \sigma_{11} & \sigma_{12} & \sigma_{31} \\ \sigma_{12} & \sigma_{22} & \sigma_{23} \\ \sigma_{31} & \sigma_{23} & \sigma_{33} \end{bmatrix}, \qquad \bar{\sigma} = [\bar{\sigma}_{ij}] = \begin{bmatrix} \bar{\sigma}_{11} & \bar{\sigma}_{12} & \bar{\sigma}_{31} \\ \bar{\sigma}_{12} & \bar{\sigma}_{22} & \bar{\sigma}_{23} \\ \bar{\sigma}_{31} & \bar{\sigma}_{23} & \bar{\sigma}_{33} \end{bmatrix} \tag{3.4.5}$$

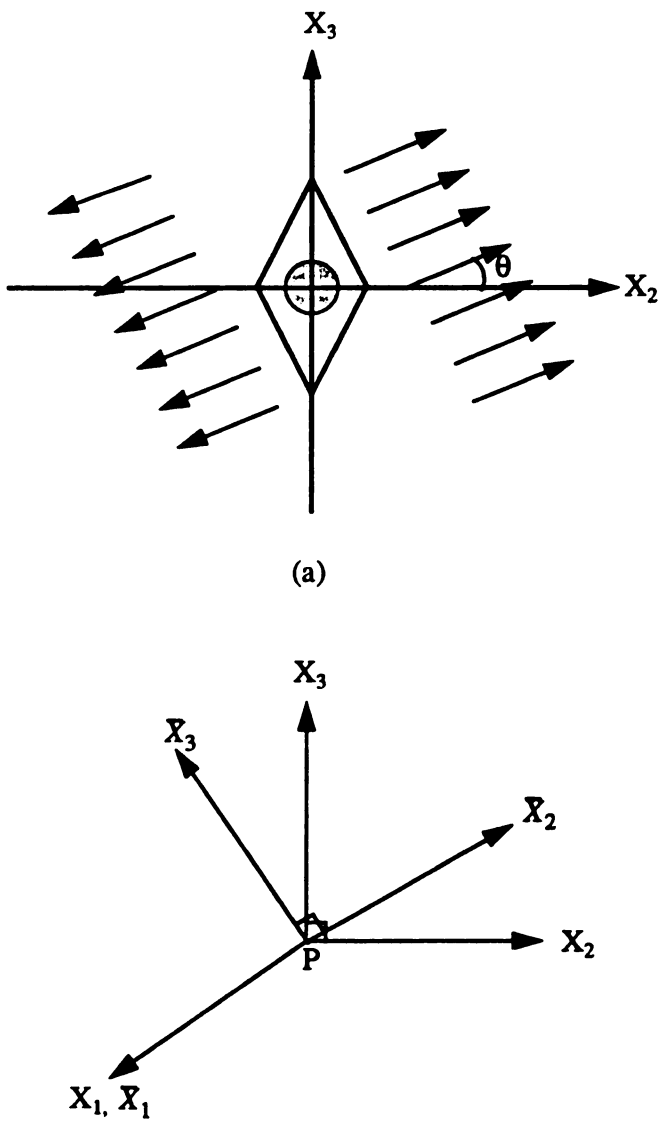

Figure 6. (a) The RVE subjected to an off-axis load
(b) The reference axes and the rotated axes

Substituting Eq. (3.4.3), Eq. (3.4.4) and Eq. (3.4.5) into Eq. (3.4.2), stress tensor $\bar{\sigma}$ in the Cartesian coordinate $PX_1X_2X_3$ is transformed into the stress tensor σ in the Cartesian coordinate $PX_1X_2X_3$ as follows:

$$\begin{aligned}\left[\sigma_{ij}\right] &= \left[a_{ij}\right]^T\left[\bar{\sigma}_{ij}\right]\left[a_{ij}\right] \\ &= \begin{bmatrix}1 & 0 & 0\\ 0 & \cos(-\theta) & -\sin(-\theta)\\ 0 & \sin(-\theta) & \cos(-\theta)\end{bmatrix}\begin{bmatrix}\bar{\sigma}_{11} & \bar{\sigma}_{12} & \bar{\sigma}_{31}\\ \bar{\sigma}_{12} & \bar{\sigma}_{22} & \bar{\sigma}_{23}\\ \bar{\sigma}_{31} & \bar{\sigma}_{23} & \bar{\sigma}_{33}\end{bmatrix}\begin{bmatrix}1 & 0 & 0\\ 0 & \cos(-\theta) & \sin(-\theta)\\ 0 & -\sin(-\theta) & \cos(-\theta)\end{bmatrix}\end{aligned}$$

$$\begin{aligned}\sigma_{11} &= \bar{\sigma}_{11}\\ \sigma_{12} &= \bar{\sigma}_{12}\cos\theta + \bar{\sigma}_{31}\sin\theta\\ \sigma_{31} &= -\bar{\sigma}_{12}\sin\theta + \bar{\sigma}_{31}\cos\theta\\ \sigma_{22} &= \bar{\sigma}_{22}\cos\theta^2 + 2\bar{\sigma}_{23}\sin\theta\cos\theta + \bar{\sigma}_{33}\sin\theta^2\\ \sigma_{23} &= -\bar{\sigma}_{22}\cos\theta\sin\theta + \bar{\sigma}_{23}\left(\cos\theta^2 - \sin\theta^2\right) + \bar{\sigma}_{33}\cos\theta\sin\theta\\ \sigma_{33} &= \bar{\sigma}_{22}\sin\theta^2 - 2\bar{\sigma}_{23}\cos\theta\sin\theta + \bar{\sigma}_{33}\cos\theta^2\end{aligned} \tag{3.4.6}$$

Eq. (3.4.6) gives us the relationships between the stresses in reference axes and those in certain rotated axes. Therefore, an off-axis stress load can be transformed into the reference axes (the Cartesian coordinate $PX_1X_2X_3$ shown in Figure 6) by using Eq. (3.4.6). The transformed stresses are taken as a stress load acting on the model, and cause a micromechanical stress state in each constituent. If the failure of some constituent is predicted by the failure criterion chosen for that constituent, then the stress load is taken as the strength of lamina at that angle, and all the lamina loads at each angle from 0 degrees to 360 degrees are obtained. The lamina transverse normal and longitudinal shear strengths are obtained by averaging the obtained lamina loads from 0 degrees to 360 degrees.

Failure Envelopes

The failure envelopes in X_1 - X_2 plane, i.e., when the biaxial loads in X_1 and X_2 directions are acting together, are obtained in the following way. First, the longitudinal lamina load is fixed at some value which is less than or equal to the longitudinal normal strength of the lamina, then the transverse lamina load giving rise to failure in some constituent is sought and averaged from 0 degrees to 360 degrees. Accordingly, the lamina fails at the biaxial load, and the longitudinal and transverse normal loads are assumed to lie on the failure envelope. Then, the longitudinal lamina load is incremented, and the transverse normal lamina load that causes failure is again obtained. After the above processes are repeated over the range from the tensile longitudinal strength to compressive longitudinal strength of the lamina, the failure envelope for biaxial loading in stress space is obtained. The failure envelope in strain space can be obtained by converting the stress states in failure envelope to strain states by means of the constitutive law for an orthotropic body [48]:

$$\begin{aligned}
\varepsilon_{11} &= \frac{1}{E_1}\sigma_{11} - \frac{\nu_{12}}{E_1}\sigma_{22} - \frac{\nu_{13}}{E_1}\sigma_{33} \\
\varepsilon_{22} &= \frac{1}{E_2}\sigma_{22} - \frac{\nu_{12}}{E_1}\sigma_{11} - \frac{\nu_{23}}{E_2}\sigma_{33} \\
\varepsilon_{33} &= \frac{1}{E_3}\sigma_{33} - \frac{\nu_{13}}{E_1}\sigma_{11} - \frac{\nu_{23}}{E_2}\sigma_{2} \\
2\varepsilon_{23} &= \frac{1}{G_{23}}\sigma_{23}, \quad 2\varepsilon_{13} = \frac{1}{G_{13}}\sigma_{13}, \quad 2\varepsilon_{12} = \frac{1}{G_{12}}\sigma_{12}
\end{aligned} \tag{3.4.7}$$

where σ_{ij} is Cauchy stress tensor, ε_{ij} is infinitesimal strain tensor, and E_i and G_{ij} are Young's moduli and shear moduli, respectively. When converting a failure envelope from stress space to strain space, it should be noted that a biaxial stress state creates a tri - axial strain state due to Poisson's effect. This phenomenon can be easily verified from Eq. (3.4.7).

If we expand the concept for obtaining the failure envelope for biaxial loading, we can get the failure envelope when the longitudinal normal, transverse normal and inplane shear loads are acting on the lamina at the same time. In this case, the maximum loads in longitudinal and transverse directions should be obtained first. Then, similar to the biaxial case, the longitudinal shear load is applied, with the longitudinal normal load fixed at some value equal to or less than the maximum load in the longitudinal direction. Then the transverse load causing failure in some constituent is averaged from 0 degrees to 360 degrees. Thus the transverse load is determined by averaging the obtained transverse loads from 0 degrees to 360 degrees as before. The longitudinal normal and shear loads, and the averaged transverse load are assumed to be on the 3 dimensional failure surface.

3.5 Curve Fitting of Failure Envelopes

The failure envelope obtained by the micromechanical failure theory for biaxial lamina loading can be fit to a polynomial type failure theory by using the predicted unidirectional strengths and nonlinear regression. Among the polynomial type failure criteria for orthotropic materials, Tsai - Wu's failure criterion is widely used, and includes interaction among the stress components analogous to the Von - Mises criterion for isotropic materials [21]. The general form of Tsai - Wu's failure criterion is [12]:

$$F_i\sigma_i + F_{ij}\sigma_i\sigma_j = 1 \qquad i,j = 1,2,\ldots,6 \tag{3.5.1}$$

where summation on the repeated subscripts is implied, σ_i are the components of the Cauchy stress tensor and F_i , F_{ij} are strength parameters. If we expand the Eq. (3.5.1), then we have:

$$F_1\sigma_1 + F_2\sigma_2 + F_3\sigma_3 + F_4\sigma_4 + F_5\sigma_5 + F_6\sigma_6 + F_{11}\sigma_1^2 + F_{22}\sigma_2^2 + F_{33}\sigma_3^2 + F_{44}\sigma_4^2 + F_{55}\sigma_5^2 + F_{66}\sigma_6^2 + 2F_{12}\sigma_1\sigma_2 + 2F_{13}\sigma_1\sigma_3 + 2F_{14}\sigma_1\sigma_4 + 2F_{15}\sigma_1\sigma_5 + 2F_{16}\sigma_1\sigma_6 2F_{23}\sigma_2\sigma_3 + 2F_{24}\sigma_2\sigma_4 + 2F_{25}\sigma_2\sigma_5 + 2F_{26}\sigma_2\sigma_6 + 2F_{34}\sigma_3\sigma_4 + 2F_{35}\sigma_3\sigma_5 + 2F_{36}\sigma_3\sigma_6 + 2F_{45}\sigma_4\sigma_5 + 2F_{46}\sigma_4\sigma_6 + 2F_{56}\sigma_5\sigma_6 = 1 \quad (3.5.2)$$

In the above equation, the linear stress terms provide for strength difference and sign reversal of normal stresses in tension and compression, respectively, which is extremely important for a lamina. But the sign reversal is unsubstantial for the shear stresses, because the strength of a lamina should not be affected by the direction or the sign of the shear stress components. So the terms pertaining to the first order shear stresses must vanish. The relevant terms are:

$$F_4\sigma_4,\ F_5\sigma_5,\ F_6\sigma_6,\ 2F_{14}\sigma_1\sigma_4,\ 2F_{15}\sigma_1\sigma_5,\ 2F_{16}\sigma_1\sigma_6,\ 2F_{24}\sigma_2\sigma_4,\ 2F_{25}\sigma_2\sigma_5$$
$$2F_{26}\sigma_2\sigma_6,\ 2F_{34}\sigma_3\sigma_4,\ 2F_{35}\sigma_3\sigma_5,\ 2F_{36}\sigma_3\sigma_6,\ 2F_{45}\sigma_4\sigma_5,\ 2F_{46}\sigma_4\sigma_6,\ 2F_{56}\sigma_5\sigma_6$$

Since the stress components are in general not zero, the only way to make the relevant terms vanish is to set the strength parameters zero:

$$F_4 = F_5 = F_6 = F_{14} = F_{15} = F_{16} = F_{24} = F_{25} = F_{26} = F_{34} = F_{35} = F_{36} = F_{45} = F_{46} = F_{56} = 0 \quad (3.5.3)$$

Now the Eq. (3.5.2) can be rewritten as:

$$F_1\sigma_1 + F_2\sigma_2 + F_3\sigma_3 + F_{11}\sigma_1^2 + F_{22}\sigma_2^2 + F_{33}\sigma_3^2 + F_{44}\sigma_4^2 + F_{55}\sigma_5^2 + F_{66}\sigma_6^2 + 2F_{12}\sigma_1\sigma_2 + 2F_{13}\sigma_1\sigma_3 + 2F_{23}\sigma_2\sigma_3 = 1 \quad (3.5.4)$$

$$F_1 = \frac{1}{X_1^T} - \frac{1}{X_1^C}, \qquad F_2 = \frac{1}{X_2^T} - \frac{1}{X_2^C}, \qquad F_3 = \frac{1}{X_3^T} - \frac{1}{X_3^C},$$

$$F_{11} = \frac{1}{X_1^T X_1^C}, \qquad F_{22} = \frac{1}{X_2^T X_2^C}, \qquad F_{33} = \frac{1}{X_3^T X_3^C}, \tag{3.5.5}$$

$$F_{44} = \frac{1}{X_4^2}, \qquad F_{55} = \frac{1}{X_5^2}, \qquad F_{66} = \frac{1}{X_6^2}$$

The other strength parameters will be discussed later.

For the case of biaxial stress state, $(i, j = 1, 2)$, the only non - zero stress components are σ_1 and σ_2. Consequently, the Eq. (3.5.4) is simplified to:

$$F_1\sigma_1 + F_2\sigma_2 + F_{11}\sigma_1^2 + F_{22}\sigma_2^2 + 2F_{12}\sigma_1\sigma_2 = 1 \tag{3.5.6}$$

The non - zero strength parameters F_i and F_{ii} can be determined in terms of strength measured by simple tension or compression or shear tests. The non - zero strength parameters of F_{ij} $(i \neq j)$ i.e., F_{12}, F_{23} and F_{31} give an account of the interaction between the two normal stress components. For example, among the interaction terms, F_{12} can be obtained from Eq. (3.5.6):

$$F_{12} = \frac{1}{2}\left\{1 - \left(\frac{1}{\sigma_2}F_1 + \frac{1}{\sigma_1}F_2 + \frac{\sigma_1}{\sigma_2}F_{11} + \frac{\sigma_2}{\sigma_1}F_{22}\right)\right\} \tag{3.5.7}$$

The Eq. (3.5.7) shows us that F_{ij} are functions of the ratio of σ_i to σ_j. The only way that the interaction parameter can be evaluated experimentally is to perform the biaxial tests with every possible ratio of σ_i to σ_j. However, this experimental task is unhappily not as easy and simple as the uniaxial test or shear test. In addition, even if F_{ij} are very small, they play an important role in the failure criterion in that small changes in F_{ij} can signifi-

cantly affect the predicted strength and its failure envelope. In Figure 7, the influence of F_{12} among the interaction terms is shown. To ensure that the failure envelope is closed and finite, Tsai and Wu suggest [12]:

$$F_{ij} = \frac{F_{ij}^*}{\sqrt{F_{ii}F_{jj}}} \tag{3.5.8}$$

where $-1 \le F_{ij}^* \le 1$.

Tsai and Hahn suggest [19]:

$$F_{ij}^* = -0.5 \tag{3.5.9}$$

to make the failure envelope similar to that of Von Mises failure criterion.

In this study, the problematical interaction strength parameters, F_{ij}, are obtained by making the failure envelope obtained by micromechanical failure theory fit to the polynomial type failure theory by means of the nonlinear regression method[15, 49]. For example, the interaction strength parameter F_{12} is obtained as follows.

Let the left hand side of Eq. (3.5.6) be Y_i and the right hand side of Eq. (3.5.6) be y_i:

$$\begin{aligned} Y_i &= F_1\sigma_{1i} + F_2\sigma_{2i} + F_{11}\sigma_{1i}^2 + F_{22}\sigma_{2i}^2 + 2F_{12}\sigma_{1i}\sigma_{2i} \\ y_i &= 1 \end{aligned} \tag{3.5.10}$$

F_{12} which is the regression coefficient in this nonlinear regression procedure can be calculated by minimizing a deviation function S defined as follows:

$$S = \sum_{i=1}^{N} (Y_i - y_i)^2 \tag{3.5.11}$$

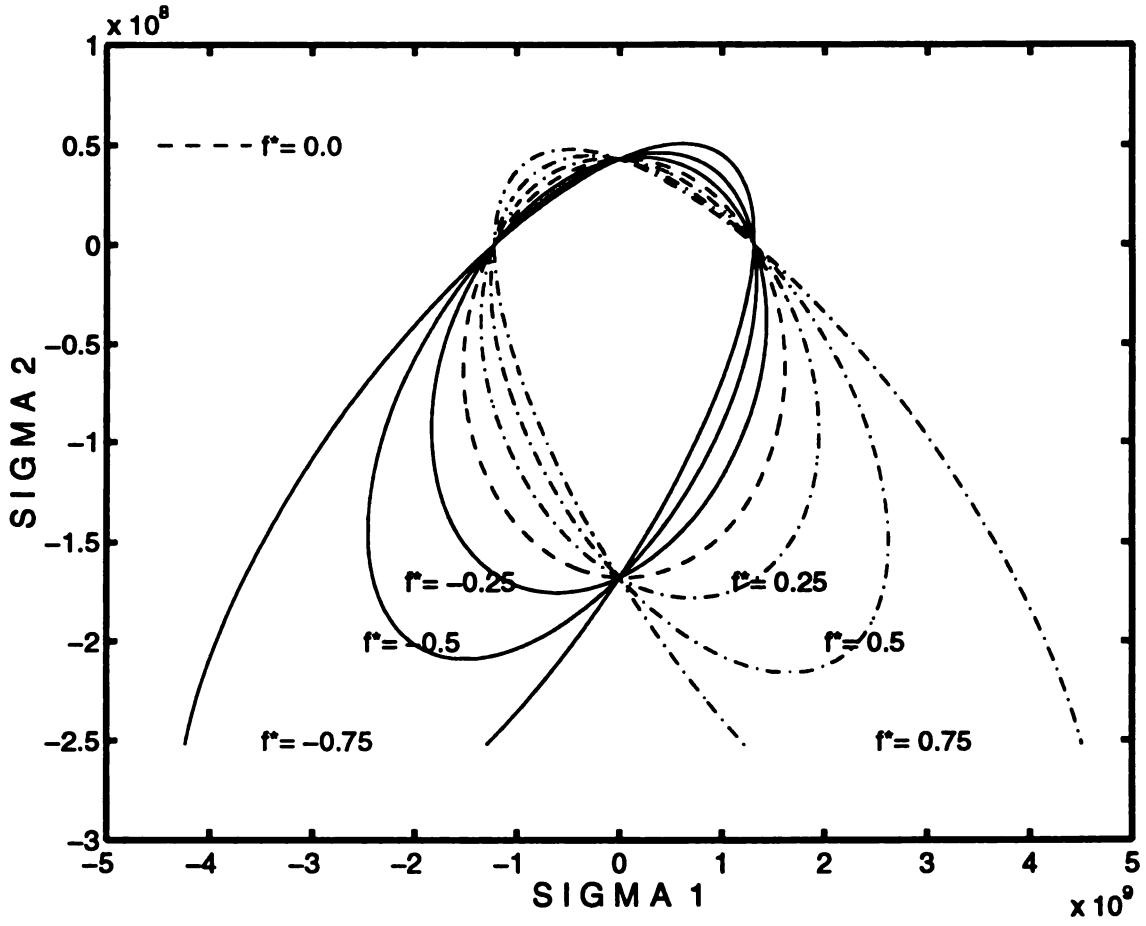

Figure 7. The variation of failure Envelopes due to change in the interaction term F_{12} in $\sigma_1 - \sigma_2$ domain

$$= \sum_{i=1}^{N} \left(F_1\sigma_{1i} + F_2\sigma_{2i} + F_{11}\sigma_{1i}^2 + F_{22}\sigma_{2i}^2 + 2F_{12}\sigma_{1i}\sigma_{2i} - 1 \right)^2 \qquad (3.5.12)$$

where N is the number of data points. Using the method of calculus, we can minimize the function given by Eq. (3.5.11) as shown below:

$$\frac{\partial S}{\partial F_{12}} = 0 \qquad (3.5.13)$$

Substituting Eq. (3.5.11) into Eq. (3.5.13) gives:

$$\frac{\partial S}{\partial F_{12}} = \sum_{i=1}^{N} \frac{\partial}{\partial F_{12}} \left(F_1\sigma_{1i} + F_2\sigma_{2i} + F_{11}\sigma_{1i}^2 + F_{22}\sigma_{2i}^2 + 2F_{12}\sigma_{1i}\sigma_{2i} - 1 \right)^2 = 0 \qquad (3.5.14)$$

If we take the partial derivative of Eq. (3.5.14), we have:

$$\frac{\partial S}{\partial F_{12}} = \sum_{i=1}^{N} \{4\sigma_{1i}\sigma_{2i} \left(F_1\sigma_{1i} + F_2\sigma_{2i} + F_{11}\sigma_{1i}^2 + F_{22}\sigma_{2i}^2 - 1 \right) + 8F_{12}(\sigma_{1i}\sigma_{2i})^2\} = 0 \qquad (3.5.15)$$

If we solve for the regression coefficient, F_{12}, from Eq. (3.5.15), then we obtain the coefficient as follows:

$$F_{12} = \frac{X}{Y} \qquad (3.5.16)$$

where

$$X = \sum_{i=1}^{N} \sigma_{1i}\sigma_{2i} - \sum_{i=1}^{N} F_1\sigma_{1i}^2\sigma_{2i} - \sum_{i=1}^{N} F_2\sigma_{1i}\sigma_{2i}^2 - \sum_{i=1}^{N} F_{11}\sigma_{1i}^3\sigma_{2i} - \sum_{i=1}^{N} F_{22}\sigma_{1i}\sigma_{2i}^3$$

$$Y = 2\sum_{i=1}^{N} \sigma_{1i}^2\sigma_{2i}^2$$

Hence, the problematical interaction terms are determined without the need for any biaxial experiments.

With the determined strength parameters and the uniaxial strengths of lamina, it is possible to plot the polynomial type failure envelope in two ways, when a biaxial stress state is applied to the lamina. One of the approaches is to find a set of σ_1 and σ_2 to satisfy Eq. (3.5.6) by trial and error method. That is, σ_1 (say) is fixed at some value first which is equal to or less than the ultimate strength in X_1 or X_2 direction, and then σ_2 is sought to satisfy the Eq. (3.5.6) by varying it from its uniaxial tensile strength to its compressive strength. By repeating the above process, the set of points on the failure envelope is calculated.

The other method is to obtain an equation for σ_1 or σ_2 from Eq. (3.5.6) by means of the discriminant formula for a quadratic equation. Rearranging Eq. (3.5.6) with regard to σ_2 in the descending order gives:

$$F_{22}\sigma_2^2 + (F_2 + 2F_{12}\sigma_1)\sigma_2 + F_1\sigma_1^2 + F_1\sigma_1 - 1 = 0 \tag{3.5.17}$$

Solving Eq. (3.5.17) for σ_2 gives:

$$\sigma_2 = \frac{-(F_2 + 2F_{12}\sigma_1) + \sqrt{(F_2 + 2F_{12}\sigma_1)^2 - 4F_{22}\left(F_1\sigma_1^2 + F_1\sigma_1 - 1\right)}}{2F_{22}} \tag{3.5.18}$$

$$\sigma_2 = \frac{-(F_2 + 2F_{12}\sigma_1) - \sqrt{(F_2 + 2F_{12}\sigma_1)^2 - 4F_{22}\left(F_1\sigma_1^2 + F_1\sigma_1 - 1\right)}}{2F_{22}} \tag{3.5.19}$$

At a value of σ_1, Eq. (3.5.18) represents points in one half of the failure envelope, and Eq. (3.5.19) represents points in the other half of the failure envelope. Therefore, a set of σ_2

and σ_1 on the failure envelope, which satisfy Eq. (3.5.6), is obtained by varying σ_1 from the tensile strength to the compressive strength of the lamina.

CHAPTER IV
INDEPENDENT MODE FAILURE CRITERIA

4.1 Introduction

A lot of researches have been carried out to predict the failure envelope more realistically, on the assumption that the failure envelope is a piecewise smooth curve, since the mechanical behavior of composite material is anisotropic. Some researchers established separate failure criteria in each quadrant of stress space by defining a different functions, in order to obtain piecewise smooth curve [23, 16]. In this chapter, it will be discussed how to obtain a more realistic and applicable failure criterion by considering the failure mode of each constituent [22].

4.2 The Concept of Independent Mode Failure Criteria

The stress distribution in each constituent is affected by the magnitude of applied load and/or the ratio of the applied loads in each direction. The change in the magnitude of applied loads causing failure in some constituent leads to changing only the magnitude of all the existing stress components at the same rate, but does not affect the relative magnitude of all the existing stress components. Thus it makes a contribution to the first occurrence of failure in the same constituent. But the change in the ratio of applied loads causing failure changes the distribution of stress components in the constituents, and may

induce a change in the failure mode. This fact implies that the failure mode of all the points on the failure envelopes are not the same. In other words, the failure envelope of a composite material is represented by the intersected area of the failure envelopes of each constituent. Moreover, it would be unreasonable that the entire failure envelope can be represented by a single equation, which gives a mathematically smooth curve, since each failure mode is entirely different. Thus, it is very useful to establish a separate failure criterion for each constituent in terms of lamina loads by supposing that failure takes place in only the constituent under consideration, rather than using a single equation for entire failure envelope.

4.3 Independent Mode Failure Criteria

The failure envelope of each constituent in a given composite material system can be written as function of macro (lamina) load. This function is obtained via the micromechanical model by allowing failure to occur in only the constituent under consideration. All other constituents are assigned strength values that are orders of magnitude larger than the actual strength to ensure that failure will not be predicted to occur in these constituents. Then the failure envelopes are predicted in terms of lamina loads, using the micromechanical failure theory. By repeating this process for each constituent, the failure envelope of each constituent can be calculated as a function of the macro (composite) stress state. The inner intersected area of the failure envelopes is regarded as the failure envelope for the lamina.

Since both the failure load and the mode of failure are predicted in the current scheme, it is possible to cast the failure model in a simple mathematical form with separate criteria

for each mode of failure. For example, if a polynomial form is desired, the criteria can be written as follows:

For fiber:

$$F_i^f \sigma_i^l + F_{ij}^f \sigma_i^l \sigma_j^l = 1 \tag{4.3.1}$$

If the lamina loading is biaxial, Eq. (4.3.1) is expanded to:

$$F_1^f \sigma_1^l + F_2^f \sigma_2^l + F_{11}^f \left(\sigma_1^l\right)^2 + F_{22}^f \left(\sigma_2^l\right)^2 + 2F_{12}^f \sigma_1^l \sigma_2^l = 1 \tag{4.3.2}$$

For matrix:

$$F_i^m \sigma_i^l + F_{ij}^m \sigma_i^l \sigma_j^l = 1 \tag{4.3.3}$$

If the lamina load is biaxial, Eq. (4.3.3) is expanded to:

$$F_1^m \sigma_1^l + F_2^m \sigma_2^l + F_{11}^m \left(\sigma_1^l\right)^2 + F_{22}^m \left(\sigma_2^l\right)^2 + 2F_{12}^m \sigma_1^l \sigma_2^l = 1 \tag{4.3.4}$$

For fiber/matrix interface:

$$F_i^{in} \sigma_i^l + F_{ij}^{in} \sigma_i^l \sigma_j^l = 1 \tag{4.3.5}$$

If the lamina load is biaxial, Eq. (4.3.5) is expanded to:

$$F_1^{in} \sigma_1^l + F_2^{in} \sigma_2^l + F_{11}^{in} \left(\sigma_1^l\right)^2 + F_{22}^{in} \left(\sigma_2^l\right)^2 + 2F_{12}^{in} \sigma_1^l \sigma_2^l = 1 \tag{4.3.6}$$

where the superscripts *m*, *f*, *in* and *l* refer to matrix, fiber, interface and lamina, respectively, F_i^k and F_{ij}^k are the strength parameters in terms of the lamina load as shown in Eq.

(3.5.5), and σ_i^l represents the components of stress in the lamina. The strength parameters of each constituent in Eqs. (4.3.1 - 4.3.6) should be computed as functions of the lamina loads using the micromechanical failure theory. Then, the strength parameters (i.e., F_i and F_{ii}) can be calculated as in Eq. (3.5.5).

Alternatively, other mathematical forms of the failure criterion may be used. For example, an appropriate form for fiber failure may be:

in tension:

$$\frac{\varepsilon_1^f}{\varepsilon_{1u_T}^l} = 1 \tag{4.3.7}$$

in compression:

$$\frac{-\varepsilon_1^f}{\varepsilon_{1u_T}^l} = 1 \tag{4.3.8}$$

Once the shape of the failure envelope for each constituent is known, an appropriate mathematical expression to describe each surface can be chosen.

CHAPTER V
THE INDEPEDENT MODE FAILURE CRITERION BASED ON "IN-SITU" CONSTITUENT STRENGTH

5.1 Introduction

The accuracy of the micromechanical failure theory depends largely on the degree of error in the material properties of each constituent in the composite system. The geometry, stiffness and strength of each constituent in a composite system are inherently randomly varied during the manufacturing processes of a composite system, and are usually different from those of each constituent in bulk state [31]. For this reason, the use of bulk mechanical properties in the micromechanical failure theory may lead to poor failure predictions in composite systems. Especially, the mechanical properties of polymers which are commonly used as matrix are time - dependent, so that the mechanical properties of polymers in a composite system are possibly different from its bulk mechanical properties.

For example, the creep function of an epoxy matrix is given by the four-parameter model [52]:

$$J(t) = \frac{1}{E_0} + \frac{1}{E_1}\left(1 - e^{-\lambda t}\right) + \frac{t}{\mu_0} \tag{5.1.1}$$

where E_0, E_1, λ and μ_0 are constants, and t is time. A plot of the creep function for 934 resin and the epoxy matrix used in glass/epoxy composites is shown in Figure 8. If the

applied loading, σ, is constant with time, the strain will be [53]:

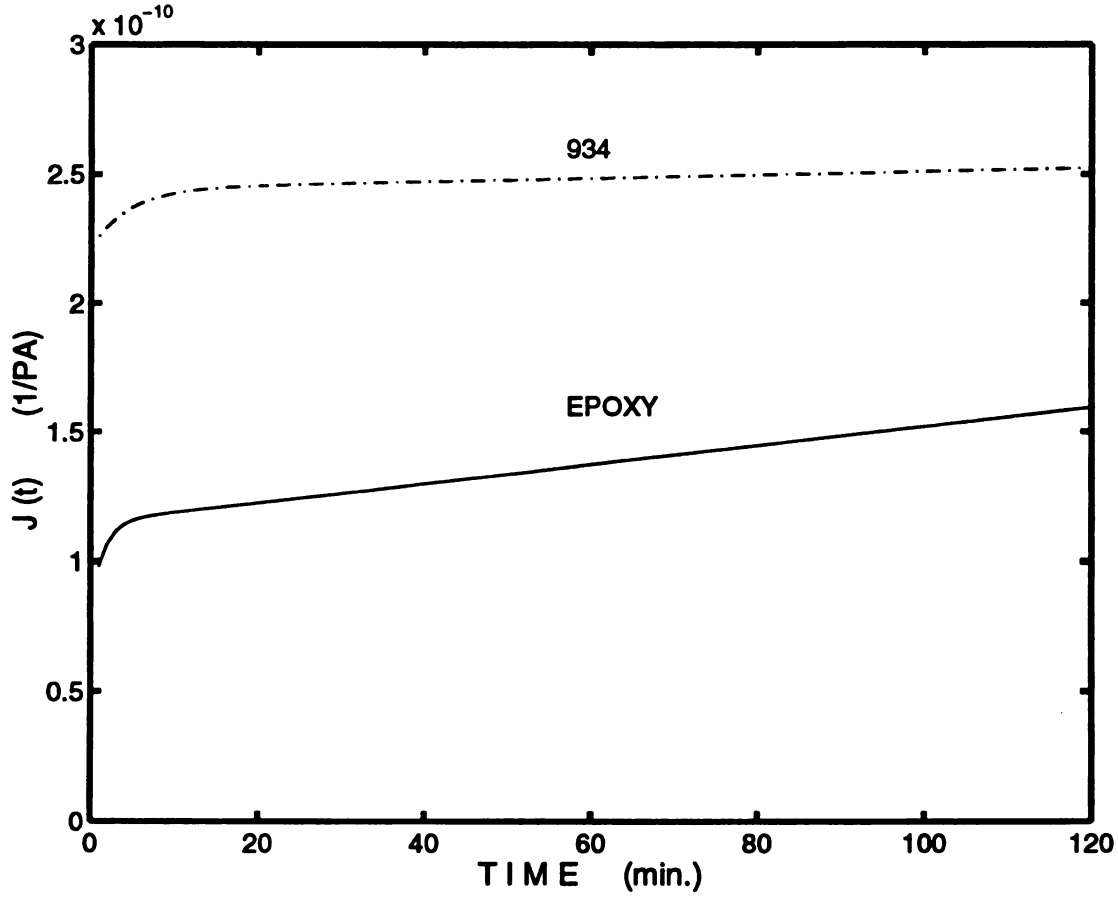

Figure 8. The creep behavior of some materials used as matrix

$$\varepsilon(t) = \sigma J(t) \tag{5.1.2}$$

This visco-elastic behavior of matrix leads to poor prediction of the transverse strength of a lamina, since matrix failure dominates the transverse strength of a lamina.

Another obstacle to using micromechanical models is that some mechanical properties of constituents are not commonly available. For example, the compression strength of a matrix material, which is sometimes different from the tension strength, is often not readily available. Hence, the current model includes the option to extract average "in-situ" constituent strength properties using unidirectional composite strength data, so that it indirectly accounts for the above variations as well as thermal residual stresses, voids, and other processing effects.

5.2 The In-situ Constituent Strengths

To obtain the in-situ strength of each constituent, a failure mode must be assumed for a given applied uniaxial loading state. For example, transverse lamina strength is often dominated by matrix strength, while failures due to longitudinal loads usually occur in the fiber. Thus, the processes to obtain the in-situ strength of each constituent are different.

Fiber Strength

Since the longitudinal tension and compression strengths of a composite material are dominated by the tension and compression strengths of fiber, the longitudinal strength of a composite material is applied as a load. The resulting maximum strain in the fiber at that

load is taken as the ultimate strain of the fiber.

Matrix Strength

The transverse tensile and compressive strength of a composite are dominated by the tensile and compressive strengths of the matrix or by the strengths of the interface. According to Kominar and Wagner [50], the failure of unidirectional composites with very stiff resins can take place without significant preliminary interfacial debonding but as the result of matrix crack nucleation and growth. Moreover, Folias [51] found that if the debonding at the interface does not occur, there exists a stress magnification factor in the matrix which attains a maximum between the fibers. If a crack does initiate at the interface, then it commonly propagates through the matrix to connect with cracks at other interfaces, eventually leading to lamina failure. When a transverse load is applied to a unidirectional lamina, it is difficult to distinguish between the load at initial failure and the ultimate load, because the cracks often propagate so rapidly. Consequently, in the current model, the transverse strength of the composite is applied as a load in the model at each angle from 0 degrees to 360 degrees, and the maximum principal stress in the matrix is determined for each angle, and averaged from 0 degrees to 360 degrees. The averaged maximum principal stress is taken as the ultimate strength of the matrix. Note that this value of matrix strength may also be related to the interface strength, depending upon the mode of failure in the experimental tests employed for mechanical characterization of the lamina.

5.3 The Independent Mode Failure Model Using "In-Situ" Properties

The obtained in-situ strengths are used as constituent strengths in the failure criterion for each constituent. In this independent mode failure criterion, the interface mode of failure is excluded, because the transverse strength of the composite was assumed to be dominated by matrix strengths. In polynomial form, the failure criteria can be written as:

Fiber

$$F_i^f \sigma_i^l + F_{ij}^f \sigma_i^l \sigma_j^l = 1 \tag{5.3.1}$$

where F_i^f and F_{ii}^f are obtained in terms of macro by substituting "in-situ" strengths of the matrix into Eq. (3.5.5) and the interaction terms F_{ij}^f are obtained by nonlinear regression like Eq. (3.5.16).

Matrix

$$F_i^m \sigma_i^l + F_{ij}^m \sigma_i^l \sigma_j^l = 1 \tag{5.3.2}$$

where F_i^m and F_{ii}^m are obtained by substituting "in-situ" strengths of the matrix into Eq. (3.5.5) and the interaction terms F_{ij}^m are obtained by nonlinear regression like Eq. (3.5.16).

This technique enables us to match the predicted and experimental unidirectional strengths as well as to obtain more realistic failure envelope under multi-axial loading conditions, because much of the inherent randomness and processing effects are effectively accounted for.

CHAPTER VI
NUMERICAL IMPLEMENTATION AND DISCUSSION OF RESULTS

6.1 Numerical Algorithms

The numerical procedure used in this research consists of conversion of macro stress loading to macro strain loading, micromechanical stress analysis, micromechanical failure prediction, prediction of uniaxial strengths, and the failure envelope for multiaxial loading, and curve fitting of the failure envelopes. The used algorithm is depicted in Figure 9 in detail and is described as follows:

1. Using the micromechanical elasticity solutions, compute the effective lamina material properties and store the micromechanical stresses due to each of the six single components of unit macro strain (lamina strain).

2. Convert 1 MPa of unidirectional lamina load to the corresponding lamina strain state and apply the strain state to the micromechanical model. Compute stresses at the desired points within each constituent (i.e., fiber, matrix, or interface) of the material system due to the uniaxial lamina load.

3. Evaluate the chosen failure criterion at each point within each constituent of the material, store the failure information, and determine the maximum failure index (ψ_{max}) for all the points.

4. Check for failure (ψ_{max}). If the failure criterion is not Von - Mises criterion among

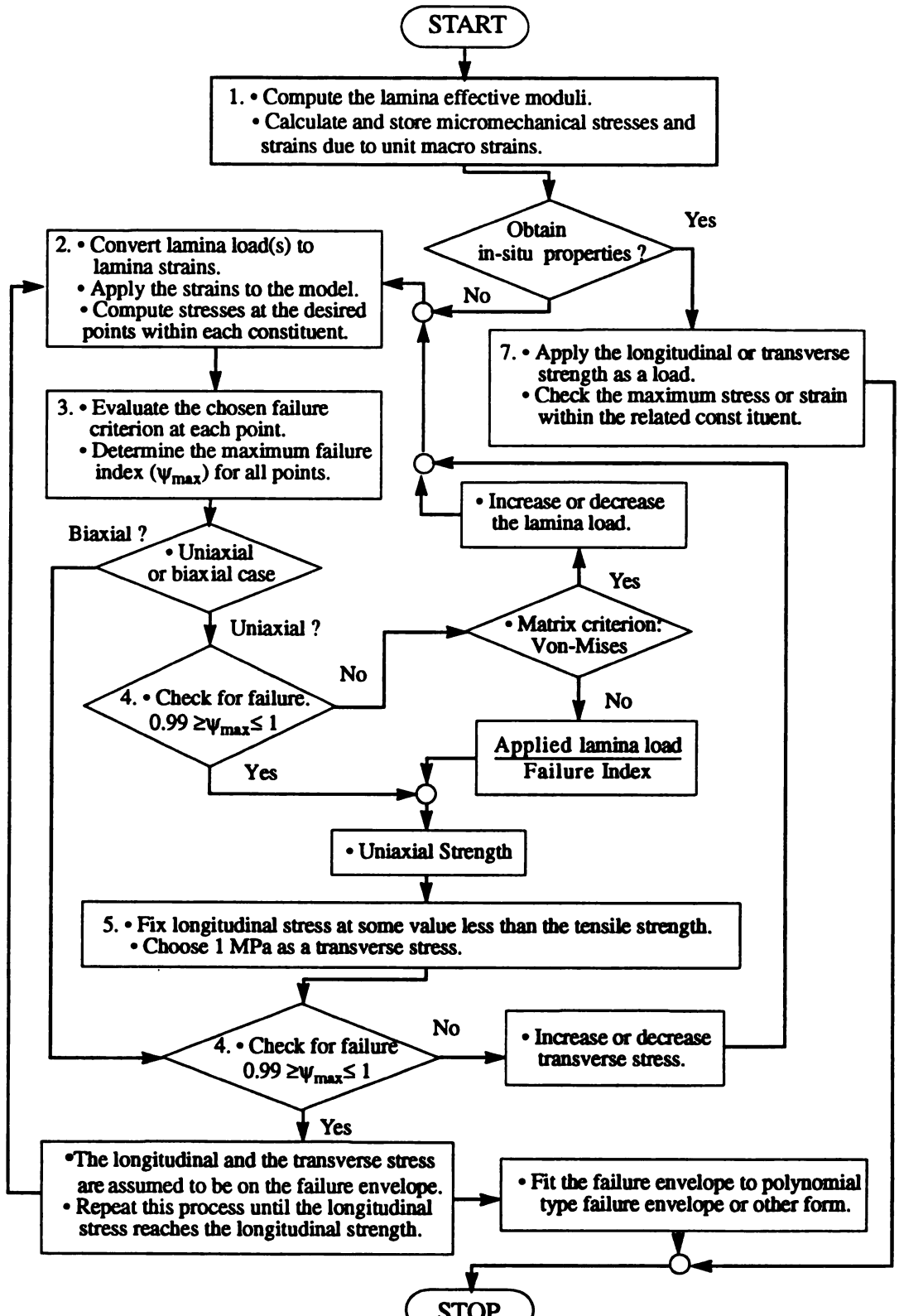

Figure 9. The flow chart

the aforementioned failure criteria, the uniaxial strength is determined as:

$$Uniaxial\ Strength = \frac{\text{Applied lamina load}}{\text{Failure Index}} \tag{6.1.1}$$

If Von - Mises criterion is chosen as the failure criterion, the acting lamina load is regarded as the uniaxial strength, when $1-\varepsilon < \psi_{max} < 1+\varepsilon$, where ε is a failure tolerance. If $\psi_{max} < 1-\varepsilon$ or $\psi_{max} > 1+\varepsilon$, increase or decrease the lamina load, and return to step 2. Thus, the uniaxial lamina strength is determined in an iteration fashion.

5. On the basis of the uniaxial strengths of the lamina, calculate the biaxial strength as follows. First, vary the longitudinal stress of the lamina from the value of tensile strength to the compressive strength. Then find the transverse stress for the fixed longitudinal stress that satisfies $1-\varepsilon < \psi_{max} < 1+\varepsilon$, using steps 2, 3 and 4. If $1-\varepsilon < \psi_{max} < 1+\varepsilon$, the longitudinal stress and the transverse stress are considered to be on the failure envelope.

6. Using a nonlinear regression procedure and the uniaxial strengths of the lamina, the failure envelope is fit to a polynomial type failure envelope or some other mathematical form.

7. To get the in-situ strengths of each constituent, perform step 1 first. Then apply the longitudinal or transverse strengths as a load to the model, and check the maximum principal stress or maximum strain for the load among each related constituent.

The failure envelope and uniaxial strength of the lamina based on the in-situ strengths of each constituent are obtained by inputting the in-situ strengths as the strength of each constituent and performing steps 1 - 6 again.

6.2 The Numerical Results and Discussion

The Verification of the Micromechanics Solution

In the simulation, the composite material T300/934 system was used, and the material properties are listed in the Tables 1 - 3.

The solution for each loading case consists of a series summation, so that it is very important to see how many terms are needed for the solution to converge. From Figure 10, it can be observed that 9 terms are not sufficient for σ_3 to converge. But, using 19 terms, all stress components converge with acceptable errors. Here, the convergence of the solution is checked along line 2 in Figure 11 in terms of stresses, not displacements, because the stress is of greatest interest. The stresses at or near the interface also converge within about 19 terms.

The point matching technique or collocation was applied to obtain some constant terms in the solution for each loading case, at some selected points along the diagonal boundary AB of the RVE. Therefore, it needs to be assessed whether or not the behavior of stress components along the diagonal boundary AB changes abruptly or becomes singular. Figure 12 shows that the predicted principal stresses on the diagonal boundary and lines parallel to the diagonal boundary as shown Figure 11 are changing very smoothly as expected.

The effective material properties are determined by Eqs. (2.6.1) - (2.6.6), based on the average stresses. The obtained effective material properties are compared with those proposed by Chamis [2]. The formulae used by Chamis are:

$$E_{11} = E_{f1} V_f + E_m (1 - V_f) \tag{6.2.1}$$

TABLE 1. Material properties of fiber used in calculation

	T300	AS4
E_1 (GPa)	233.000	235.0000
E_2 (GPa)	23.1000	14.0000
E_3 (GPa)	23.1000	14.0000
nu_{23}	0.4000	0.250
nu_{13}	0.2000	0.2000
nu_{12}	0.2000	0.2000
G_{23} (GPa)	8.2700	5.5000
G_{13} (GPa)	8.9600	28.0000
G_{12} (GPa)	8.9600	28.0000
alpha1 (1/deg. °C)	-5.4000E-07	-3.6000E-07
alpha2 (1/deg. °C)	1.0080E-05	1.8000E-05
alpha3 (1/deg. °C)	1.0080E-05	1.8000E-05
allow. axial strain (tension)	0.0118	0.0153
allow. axial strain (comp.)	0.0094	0.0145

T300, AS4: as used in [46]

TABLE 2. Material properties of matrix used in calculation

	934	3501-6
E_1 (GPa)	4.6500	4.3000
E_2 (GPa)	4.6500	4.3000
E_3 (GPa)	4.6500	4.3000
nu_{23}	0.3630	0.3400
nu_{13}	0.3630	0.3400
nu_{12}	0.3630	0.3400
G_{23} (GPa)	1.7000	1.6000
G_{13} (GPa)	1.7000	1.6000
G_{12} (GPa)	1.7000	1.6000
alpha1 (1/deg. °C)	0.414E-04	0.4000E-04
alpha2 (1/deg. °C)	0.414E-04	0.4000E-04
alpha3 (1/deg. °C)	0.414E-04	0.4000E-4
ult. tensile stress (MPa)	58.8000	83.0000
ult. comp. stress (MPa)	58.8000	207.0000

934, 3501-6: as used in [46]

TABLE 3. Material properties of composites measured in experiment

	T300/934	AS4/3501-6
E_1 (GPa)	148.0000	145.0000
E_2 (GPa)	9.6500	10.6000
nu_{12}	0.3000	0.2700
G_{12} (GPa)	4.5500	7.6000
tens. long. strength (MPa)	1314.0000	2090.0000
comp. long. strength (MPa)	1220.0000	1440.0000
tens. trans. strength (MPa)	43.0000	64.0000
comp. trans. strength (MPa)	168.0000	228.0000
long. shear strength (Mpa)	48.0000	71.0000
fiber vol. fraction (%)	60.0	65.0

T300/934 [54]

AS4/3501-6 [56]

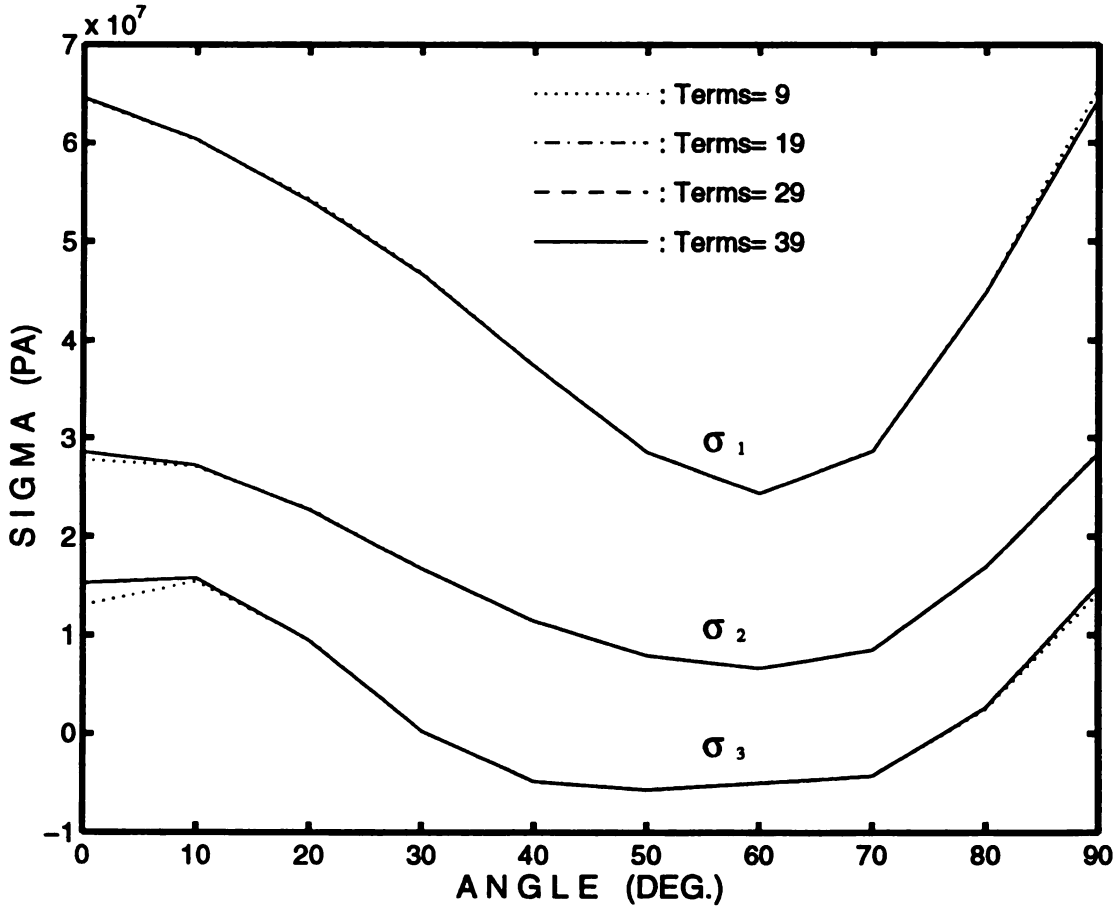

Figure 10. The convergence of stresses according to the number of terms

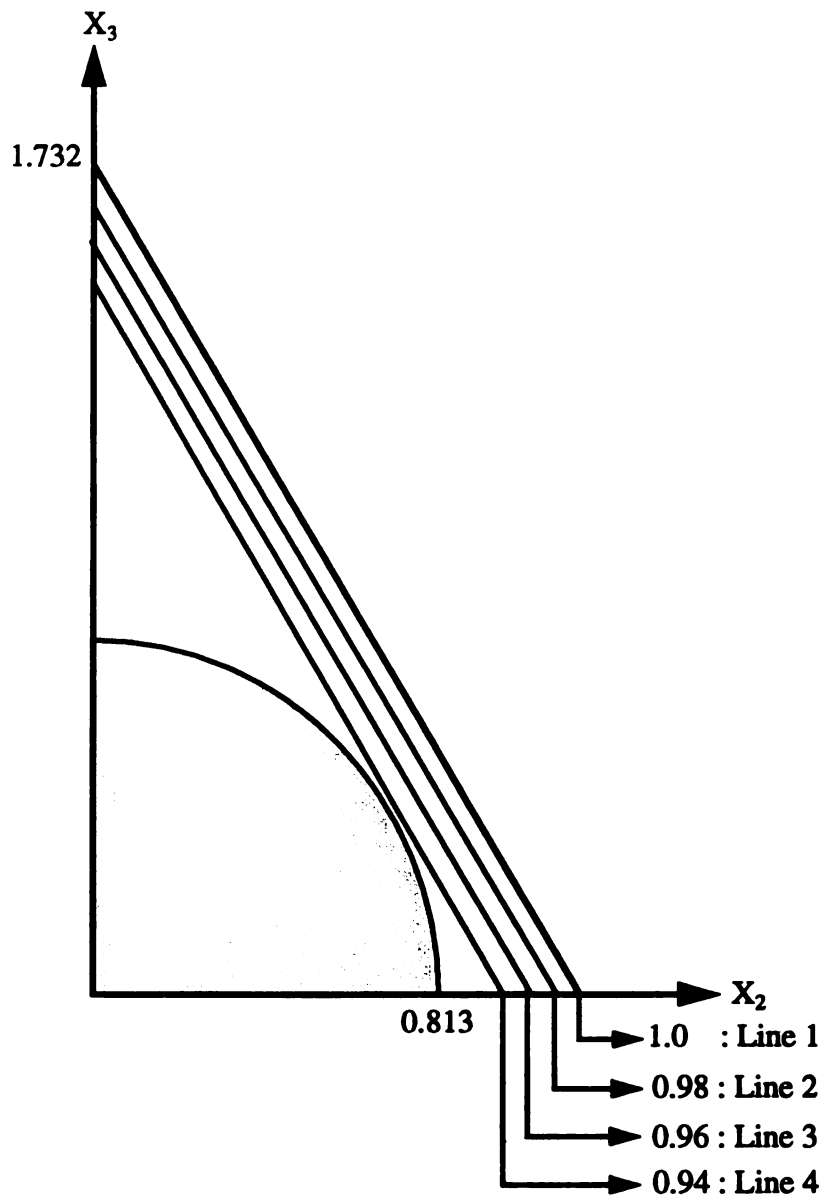

Figure 11. The stress evaluation position

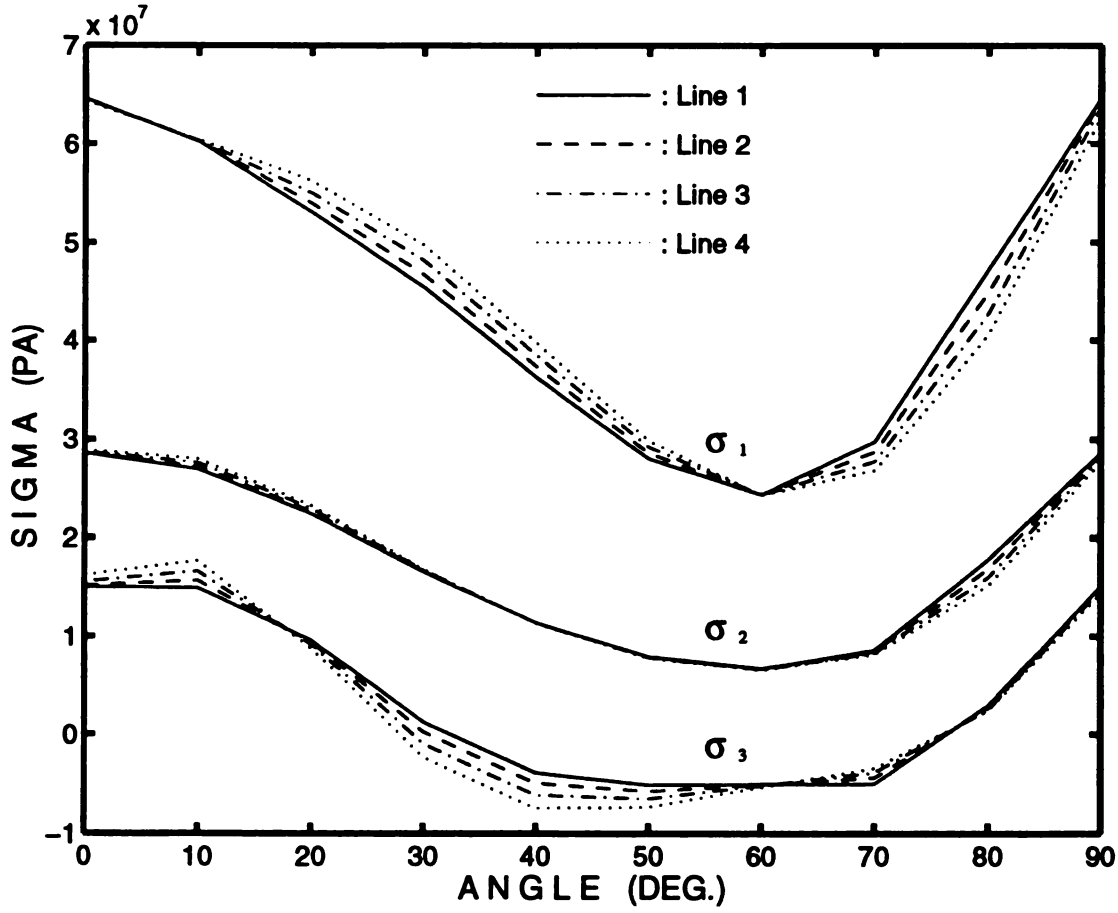

Figure 12. The Stress distribution near boundary

$$E_{22} = E_{33} = \frac{E_m}{1 - \sqrt{V_f}(1 - E_m/E_{f2})}$$

$$G_{12} = G_{13} = \frac{G_m}{1 - \sqrt{V_f}(1 - G_m/G_{f2})}$$

$$G_{23} = \frac{G_m}{1 - \sqrt{V_f}(1 - G_m/G_{f23})}$$

$$\nu_{12} = \nu_{13} = \nu_{f12} V_f + \nu_m (1 - V_f)$$

$$\nu_{23} = \frac{E_{22}}{2G_{23}} - 1$$

where E, G and ν are Young's modulus, shear modulus and Poisson's ratio, the arabic subscripts stand for the material directions, and the subscript f and m mean fiber and matrix, respectively.

It is shown in Figure 13 that the prediction of longitudinal and transverse Young's modulus, E_1 and E_2, respectively, by the current model has a better agreement with experiments than that by Chamis. It is observed in Figure 14 and Figure 15 that the longitudinal shear modulus and Poisson's ratio, G_{12} and ν_{12}, respectively, predicted by the current model have some deviation with the experimental results. But the transverse shear modulus and Poisson's ratio, G_{23} and ν_{23} are difficult to measure reliably, so the source of the difference is difficult to identify.

Results using the Micromechanical Failure Theory

In Figure 16, the lamina loads leading to failure in some constituent applied in the direction varying from 0 degrees to 360 degrees are plotted by adopting the maximum principal stress criterion for the matrix. It can be observed that there exists an axes of symmetry every 30 degrees, and the axes of symmetry for transverse normal strengths coincides with that for longitudinal shear strength. The absolute maximum value of transverse

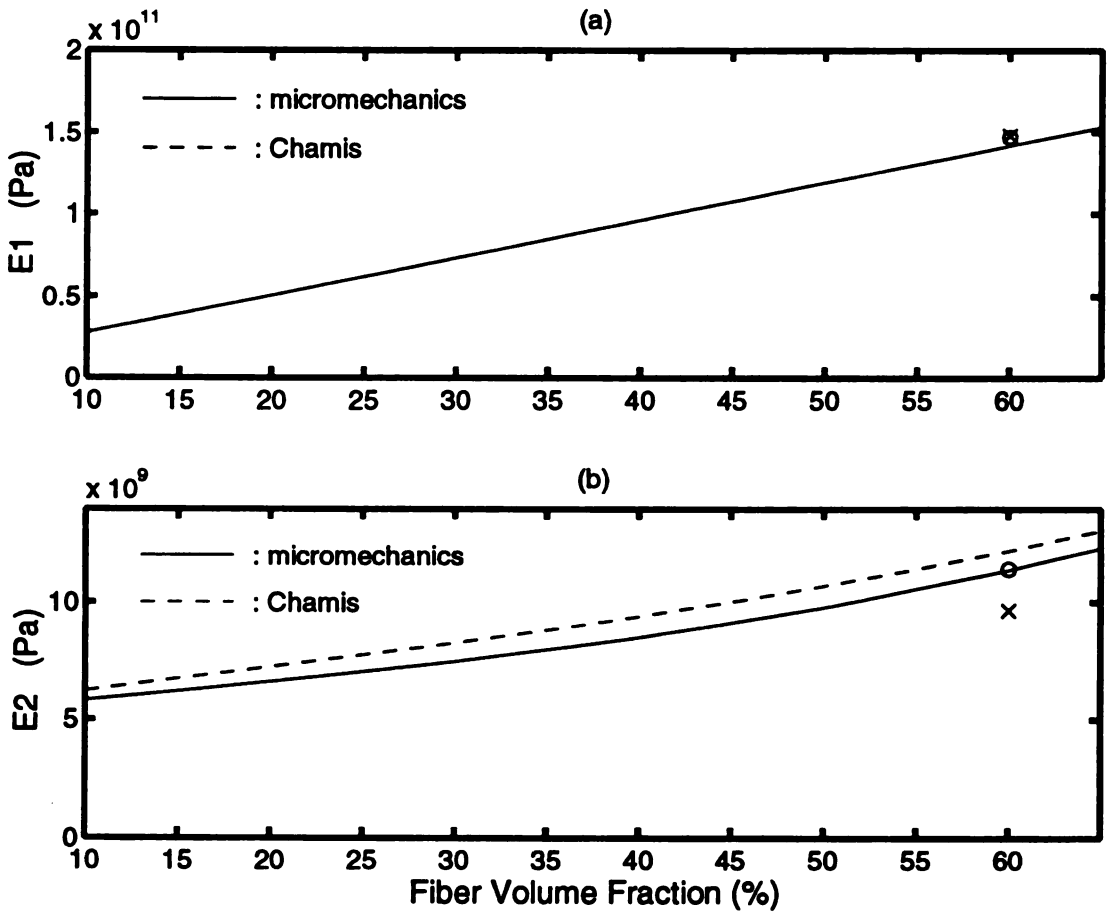

o : Tsai [54]

x : Chang-Kutlu [55]

Figure 13. The Variations of E1 and E2 with fiber volume fraction

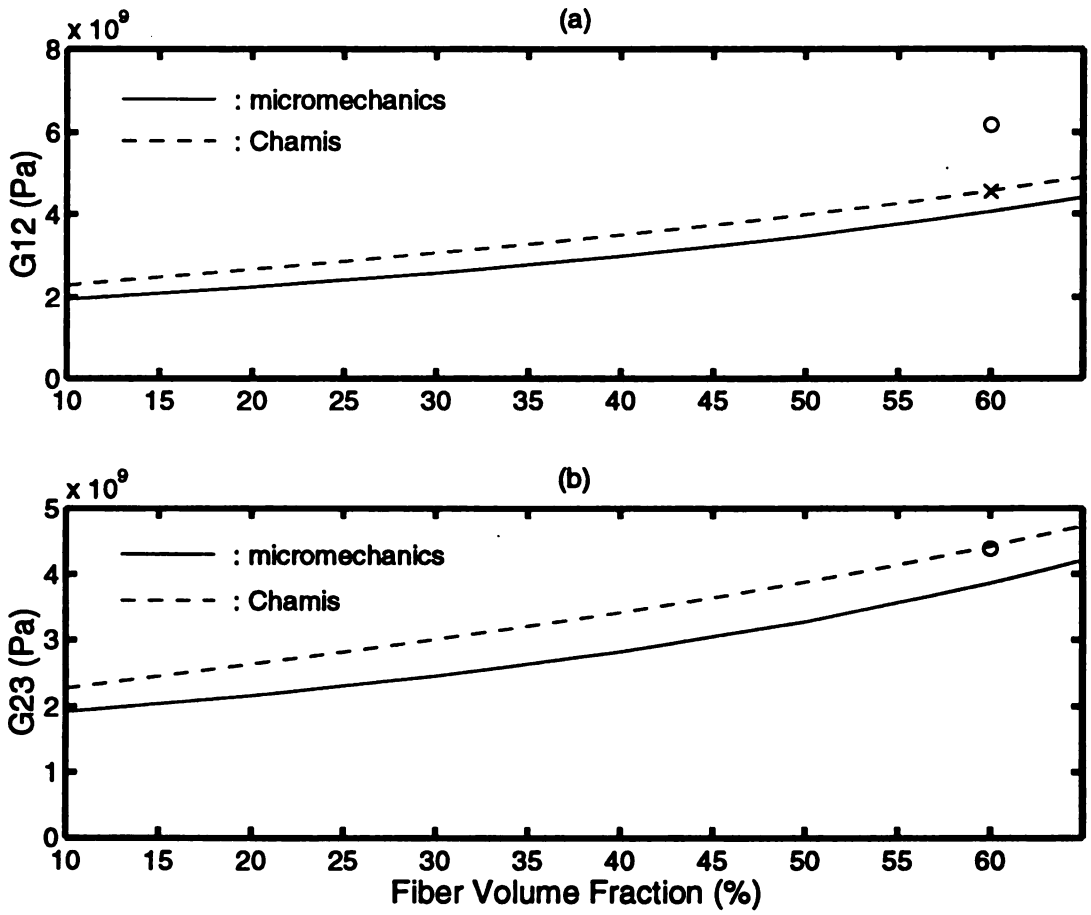

o : Tsai [54]

x : Chang-Kutlu [55]

Figure 14. The Variations of G12 and G23 with Fiber Volume Fraction

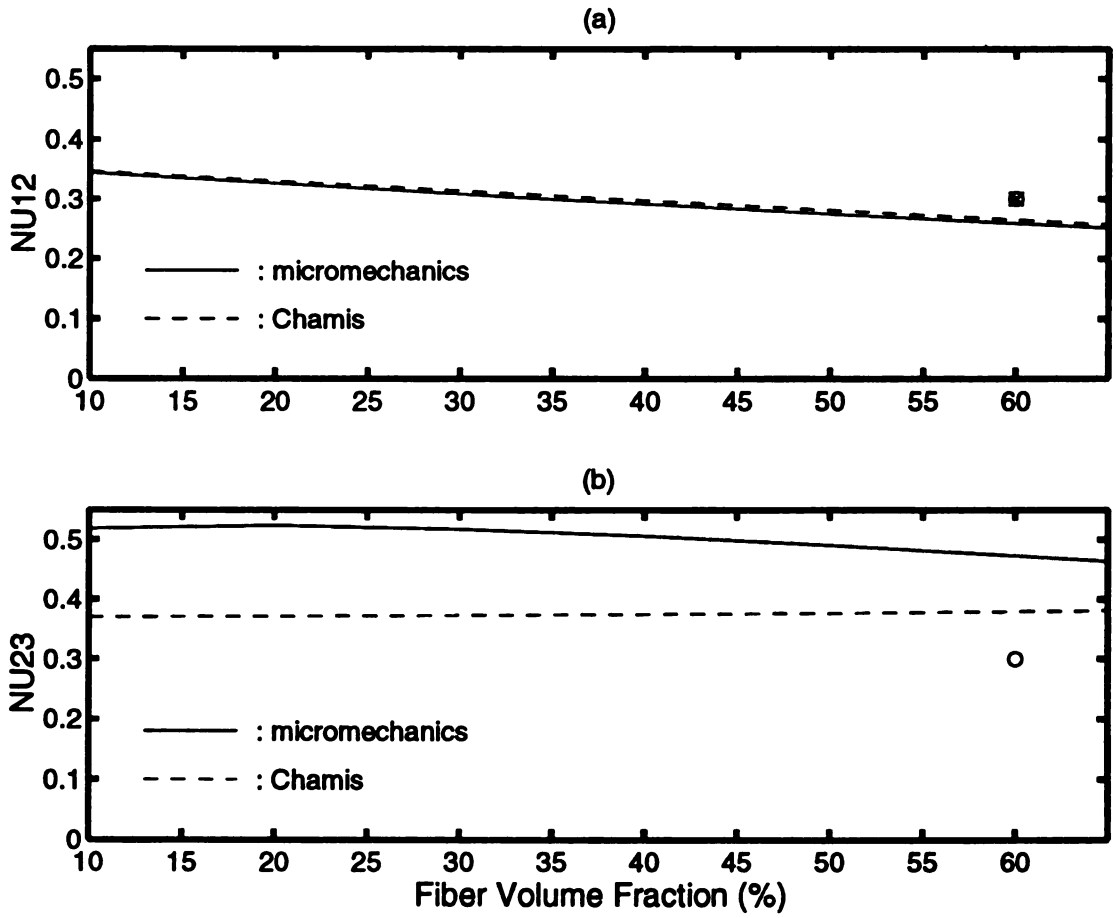

o : Tsai [54]

x : Chang-Kutlu [55]

Figure 15. The Variations of ν_{12} and ν_{23} with Fiber Volume Fraction

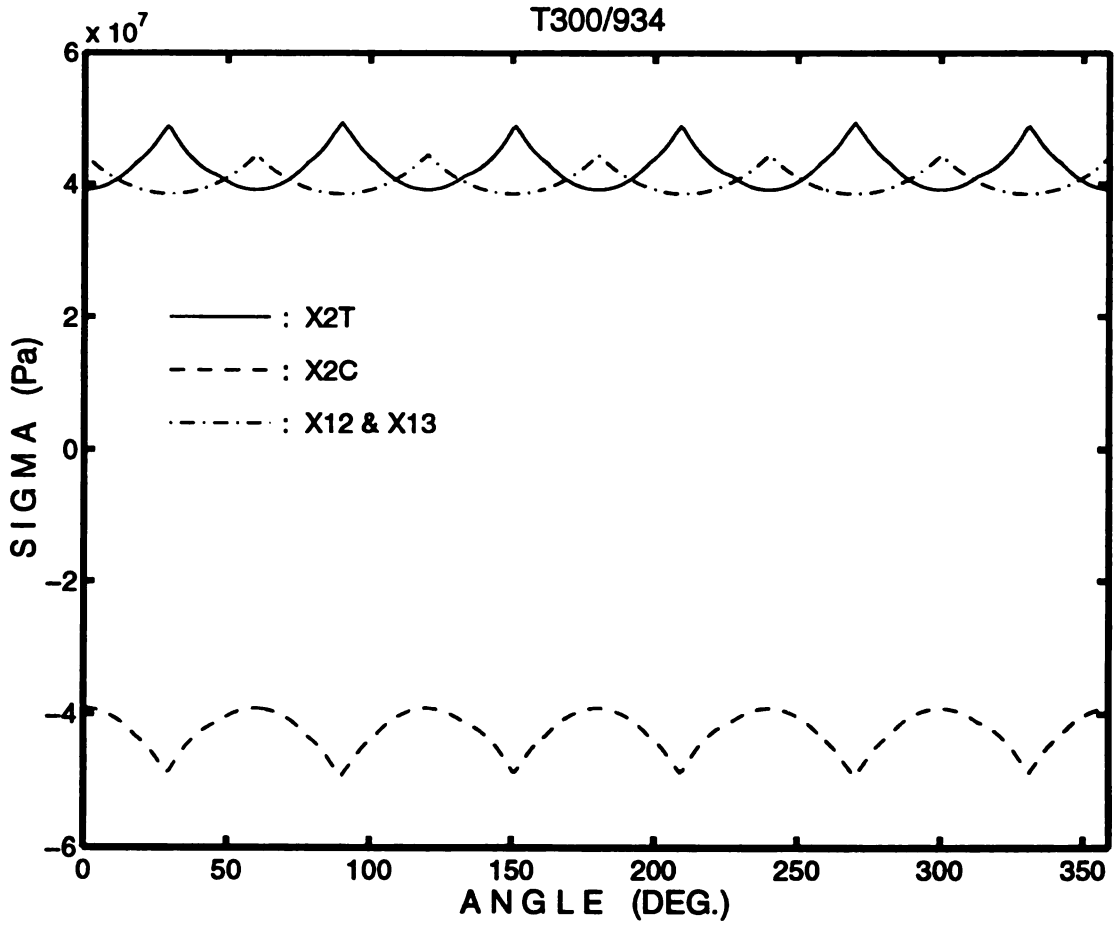

Figure 16. The Variation of maximum loads causing failure in transverse direction as the applied angle changes

tensile and compressive lamina loads causing failure are found out at 30, 90, 150... degrees, but the maximum value of longitudinal shearing lamina load bringing about failure are found at 0, 60, 120... degrees. The axes of symmetry can be expected from the assumed arrangement of fibers in the composite.

The predicted unidirectional strengths are compared with the experimental results in Figures 17 - 22. To determine the unidirectional strengths of a lamina, the maximum strain criterion was adopted for fiber, the maximum stress criterion was used for interface, and one of the following failure criteria were used for matrix as discussed in Chapter 3: maximum principal strain criterion, maximum principal stress criterion, Tresca criterion, and Von - Mises criterion. Hereafter, the only failure criterion for matrix will be mentioned, since the failure criteria for the other constituents are fixed. In each case, bulk matrix properties used.

As shown in Figures 17 and 20, the predicted transverse tensile strengths for both T300/934 and AS4/3501-6 by maximum principal stress criterion, Tresca criterion and Von - Mises criterion were in good agreements with experimental results, but by maximum principal strain criterion were relatively poor. The maximum principal stress criterion rendered the strength closest to the experimental results for both composite systems. For AS4/3501-6, Tresca criterion is not applicable, because the tensile strength of matrix is different from the compressive strength. It was observed that all the predicted transverse tensile strengths were lower than the those of matrices. This phenomenon comes from the fact that the fibers are acting as solid inclusions and give rise to higher stress than the applied stress load, when loading is applied in the transverse direction.

No matter what criterion was used, the prediction of transverse compressive strength as shown in Figures 18 and 21 was very poor, when compared with the experimental

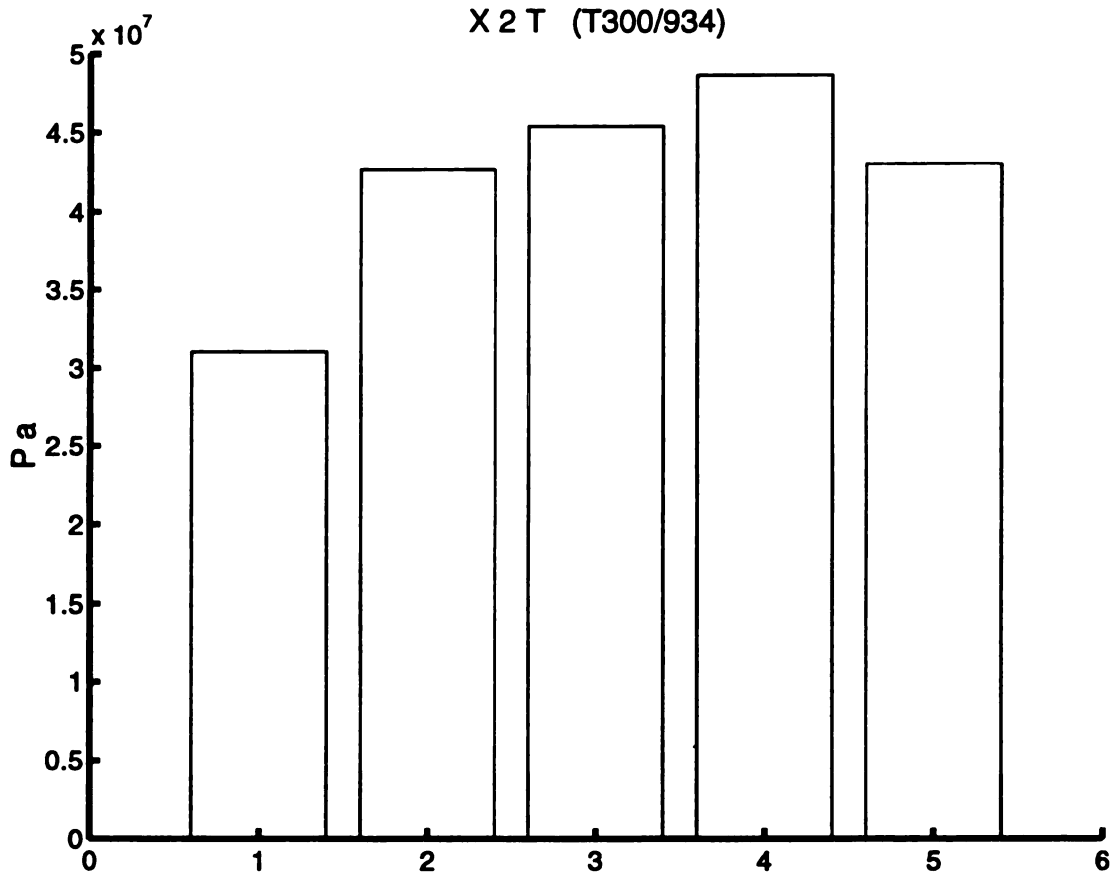

1. Maximum principal strain criterion
2. Maximum principal stress criterion
3. Tresca criterion
4. Von - Mises criterion
5. Experimental result [54]

Figure 17. The predicted tensile transverse strengths by micromechanical failure theory (T300/934)

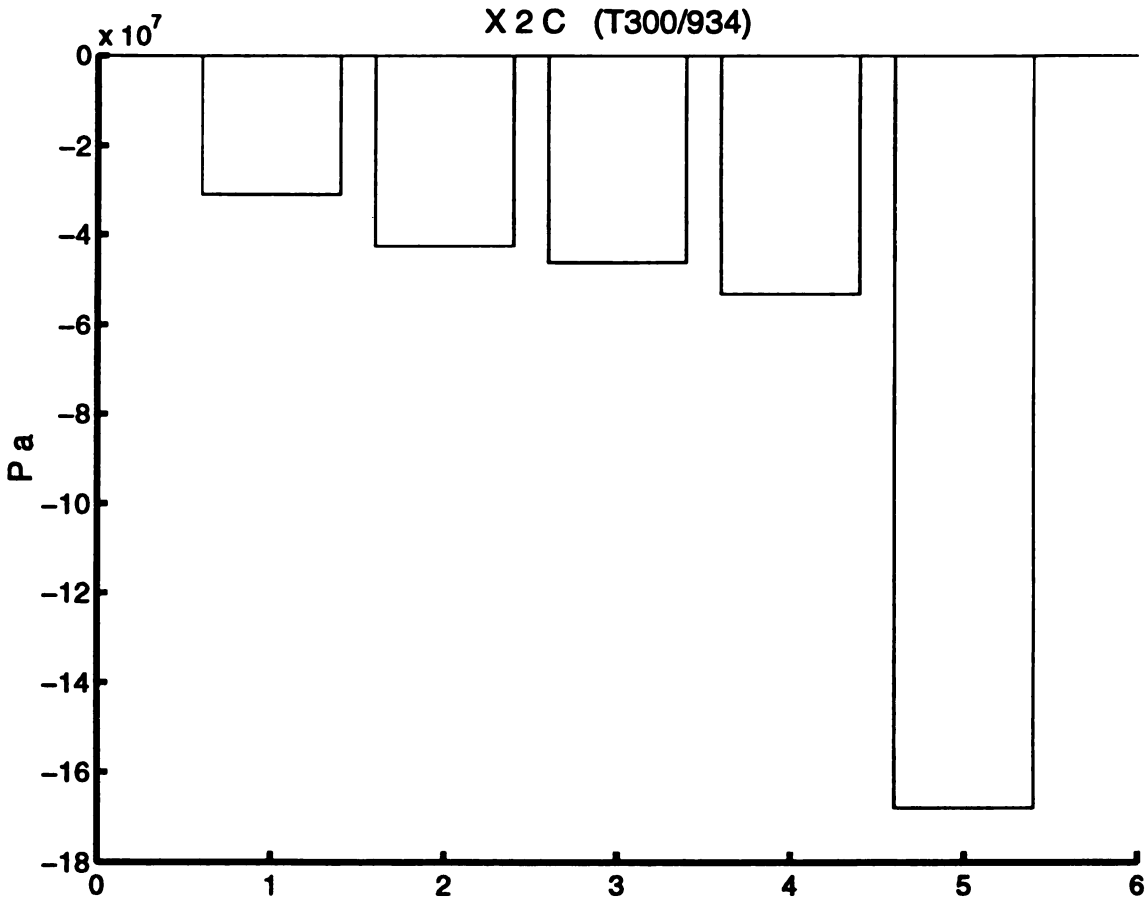

1. Maximum principal strain criterion 2. Maximum principal stress criterion
3. Tresca criterion 4. Von - Mises criterion
5. Experimental result [54]

Figure 18. The predicted compressive transverse strengths by micromechanics failure theory (T300/934)

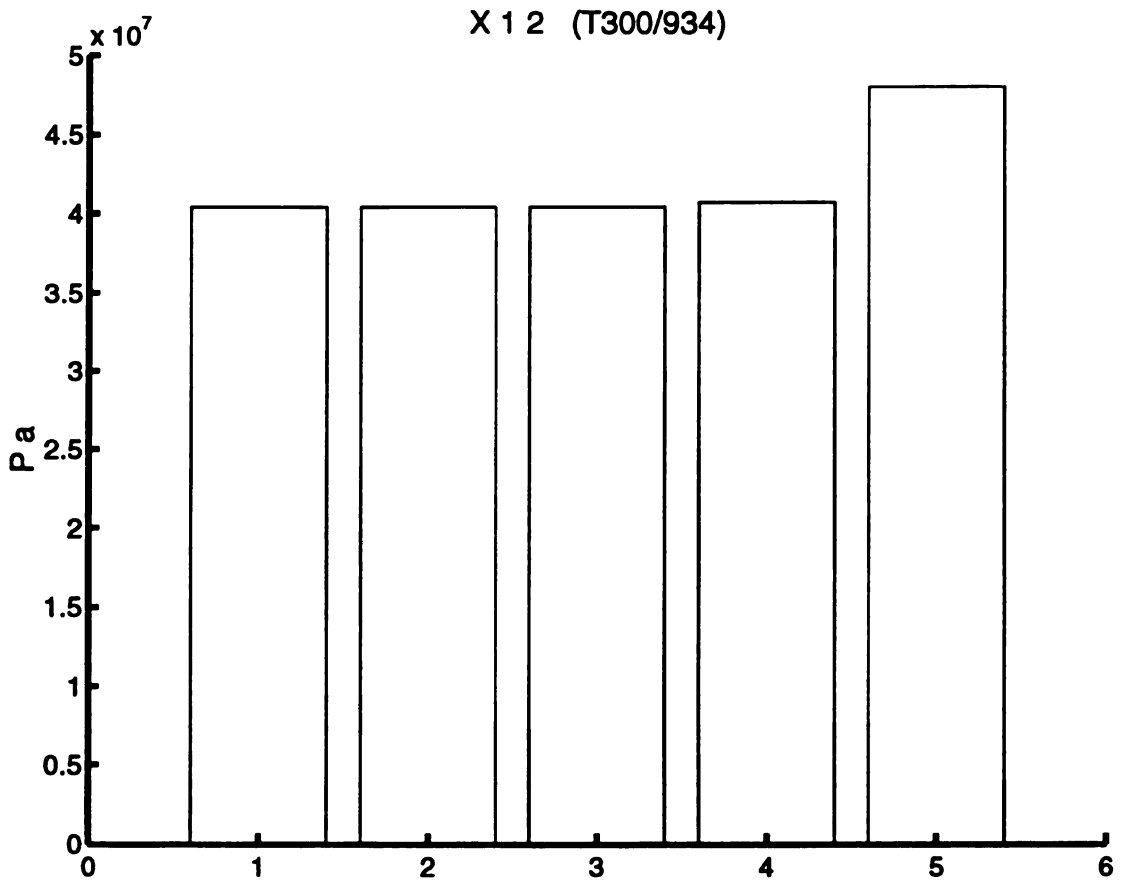

1. Maximum principal strain criterion 2. Maximum principal stress criterion
3. Tresca criterion 4. Von - Mises criterion
5. Experimental result [54]

Figure 19. The predicted longitudinal shear strengths by micromechanics failure theory (T300/934)

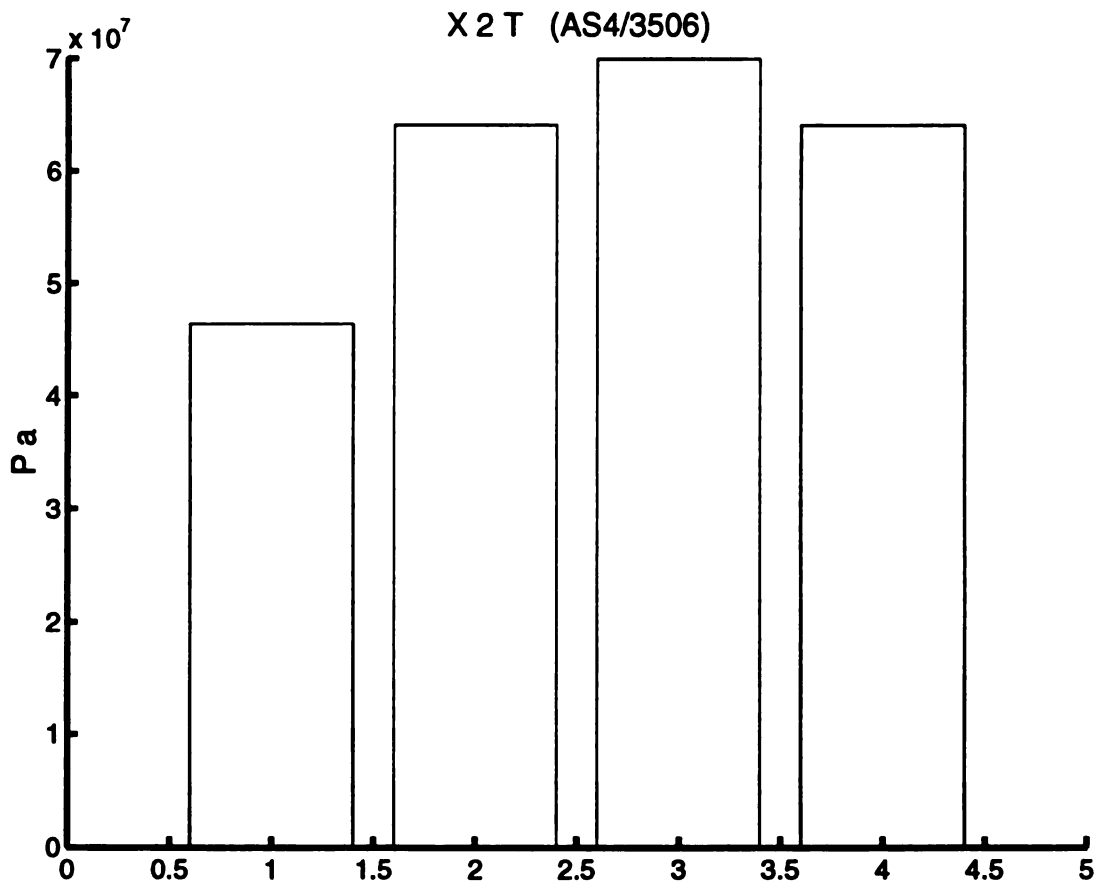

1. Maximum principal strain criterion 2. Maximum principal stress criterion
3. Von - Mises criterion 4. Experimental result [56]

Figure 20. The predicted tensile transverse strengths by micromechanics failure theory (AS4/3501-6)

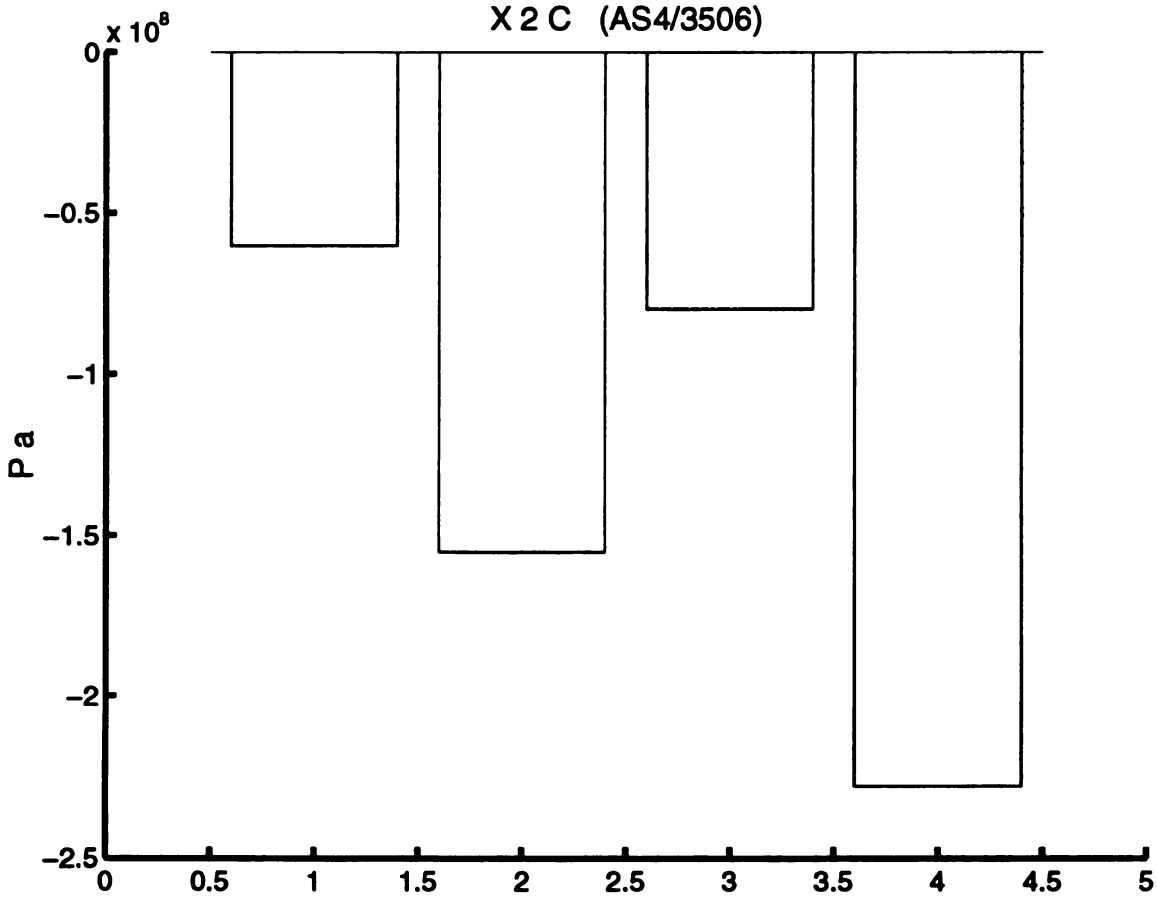

1. Maximum principal strain criterion 2. Maximum principal stress criterion
3. Von - Mises criterion 4. Experimental result [56]

Figure 21. The predicted compressive transverse strengths by micromechanics failure theory (AS4/3501-6)

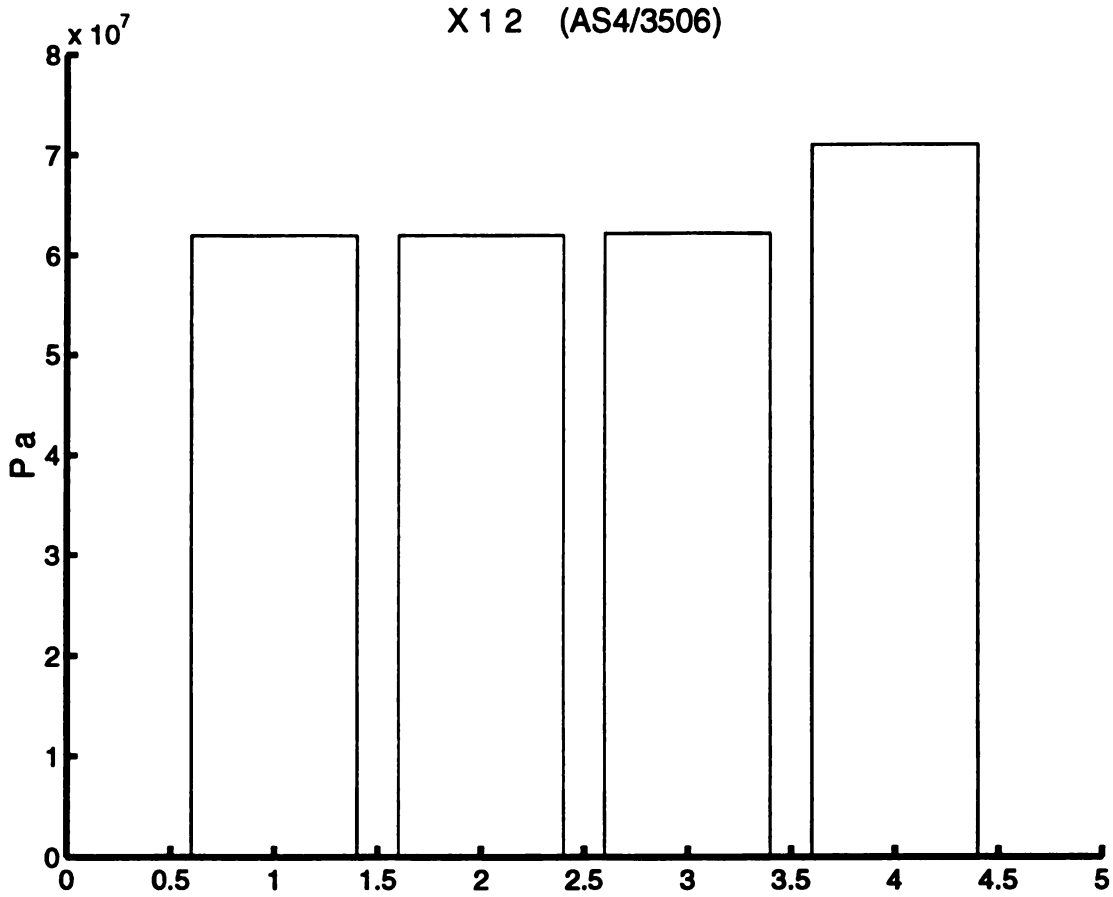

1. Maximum principal strain criterion 2. Maximum principal stress criterion
3. Von - Mises criterion 4. Experimental result [56]

Figure 22. The predicted longitudinal shear strengths by micromechanics failure theory (AS4/3501-6)

results. This may originate from the fact that the compressive strength of the matrix in a composite is different from that in bulk state. For T300/934, Von - Mises criterion predicted better transverse compressive strength than the other criteria. For AS4/3501-6, the prediction by maximum principal stress criterion was much better than any other criteria, because the absolute compressive strength of matrix is greater than the absolute tensile strength.

In Figures 19 and 22, the predicted longitudinal shear strength is depicted. The obtained longitudinal shear strengths by maximum principal strain criterion, maximum principal stress criterion and Tresca criterion are exactly same, but the shear strength by Von - Mises criterion is slightly bigger than those by the other method. When the predicted shear strength was compared with the experimental results for both cases, the error was less than about 15 percent.

Since it was supposed that the longitudinal strength of a lamina is dominated by the fibers, and fibers are brittle, the ultimate longitudinal strain of the fiber was taken to be the same as that of the lamina. Therefore, the longitudinal strength predicted from the micromechanics failure theory is exactly the same as the experimental result.

In the process of obtaining unidirectional strengths, it was found that the matrix strength can influence the axial strength of composite. When the axial load is applied, tensile or compressive stress is developed in the matrix due to the Poisson's effect, and a lamina may fail by failure of matrix, not in the fiber. This implies that, to obtain higher strength of composite, the strengths of all constituents should be considered. Thus, this micromechanical failure criterion can be used in designing composite systems.

The failure envelopes for T300/934 in stress space predicted by the micromechanical failure theory are shown in Figure 23, and the failure envelope by maximum principal

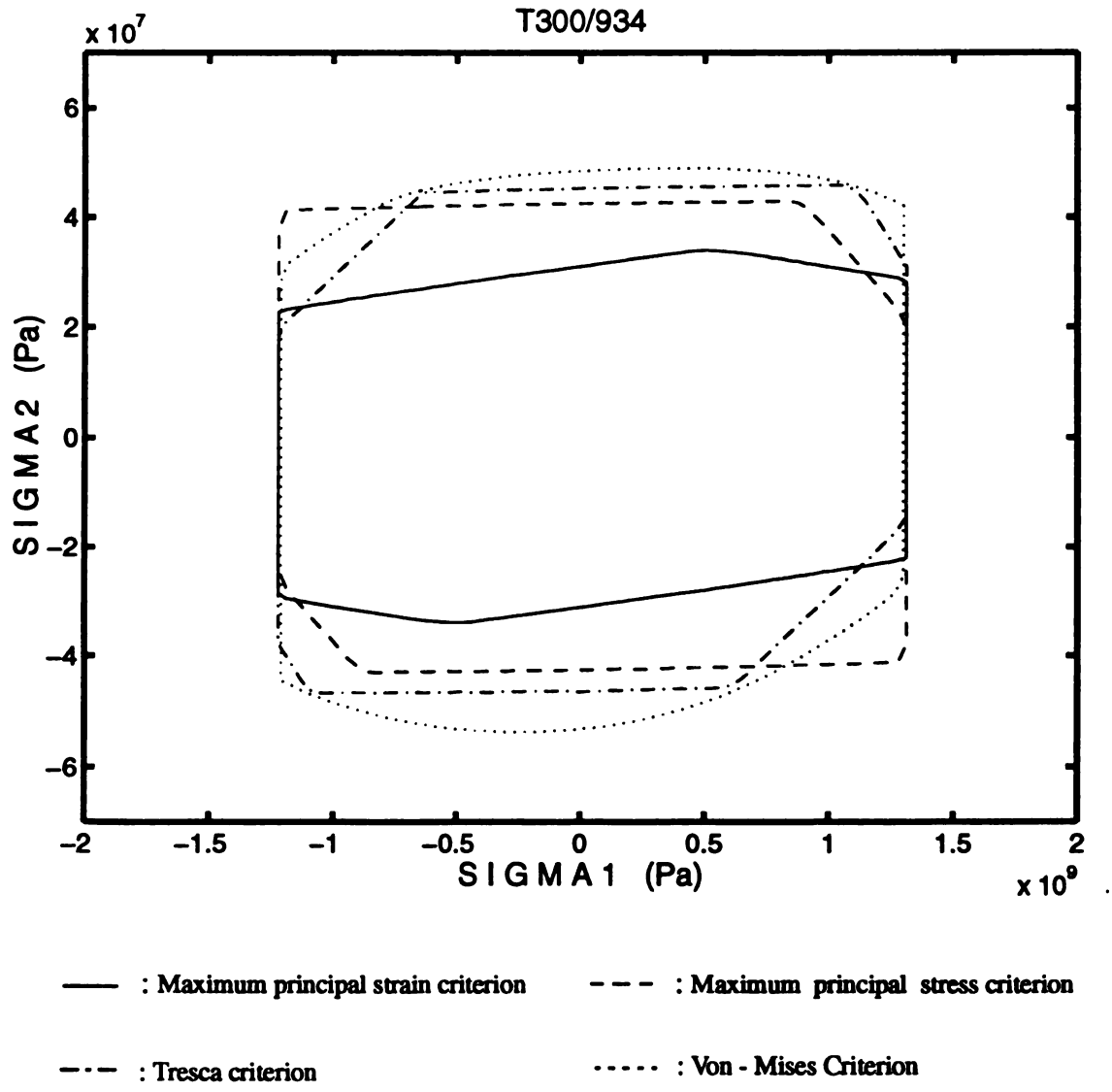

Figure 23. Failure envelope in stress space (T300/934)

strain criterion is most conservative among the predicted failure envelopes. Considering the different scales of σ_1 axis and σ_2 axis in the plot, it is noticed that the failure envelopes are long and thin along the σ_1-axis. The conversion of the failure envelopes in biaxial stress state to strain space gives rise to three-dimensional strain state due to Poisson's effect by stresses in X_1 and X_2 directions. The failure envelopes in 3 dimensional strain space are shown in Figure 24, and are inclined to ε_3 axis. If they are replotted in the ε_1 and ε_2 space, the envelopes will be the same as shown in Figure 25.

For AS4/3501-6, the failure envelopes in stress space are shown in Figure 26, and the failure envelopes in the two-dimensional strain space are shown in Figure 27. Since the compressive strength of the matrix in this composite system is much larger than its tensile strength, the maximum principal stress criterion gives better results than any other criteria in this research, while the maximum principal strain failure criterion provided poor results.

In Figure 28, the failure envelope for T300/934 was plotted by choosing the Von-Mises failure criterion for the matrix, then it was fit to the polynomial type failure envelope by using nonlinear regression and unidirectional strengths of the lamina as discussed in Chapter 3, Section 5. In this process, the interaction strength parameter, F_{12}, was obtained. The failure envelopes obtained by the micromechanical failure theory and the nonlinear regression are compared with the Tsai-Wu failure envelope which is obtained using experimental results and the interaction strength parameter suggested by Tsai-Hahn as in Eq. (3.5.9). The interaction strength parameters predicted by the two methods are shown in Table 4 below:

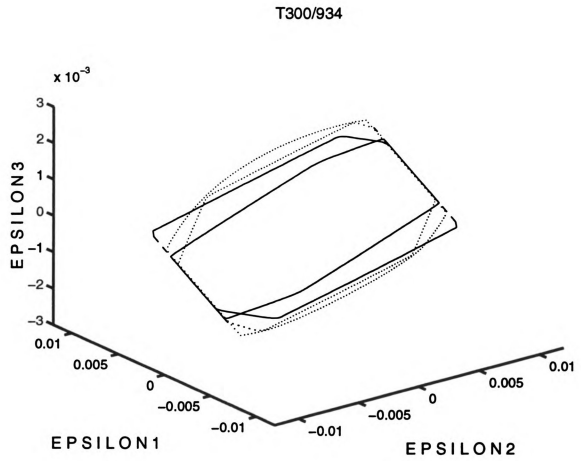

Figure 24. Failure envelopes in 3 dimensional strain space

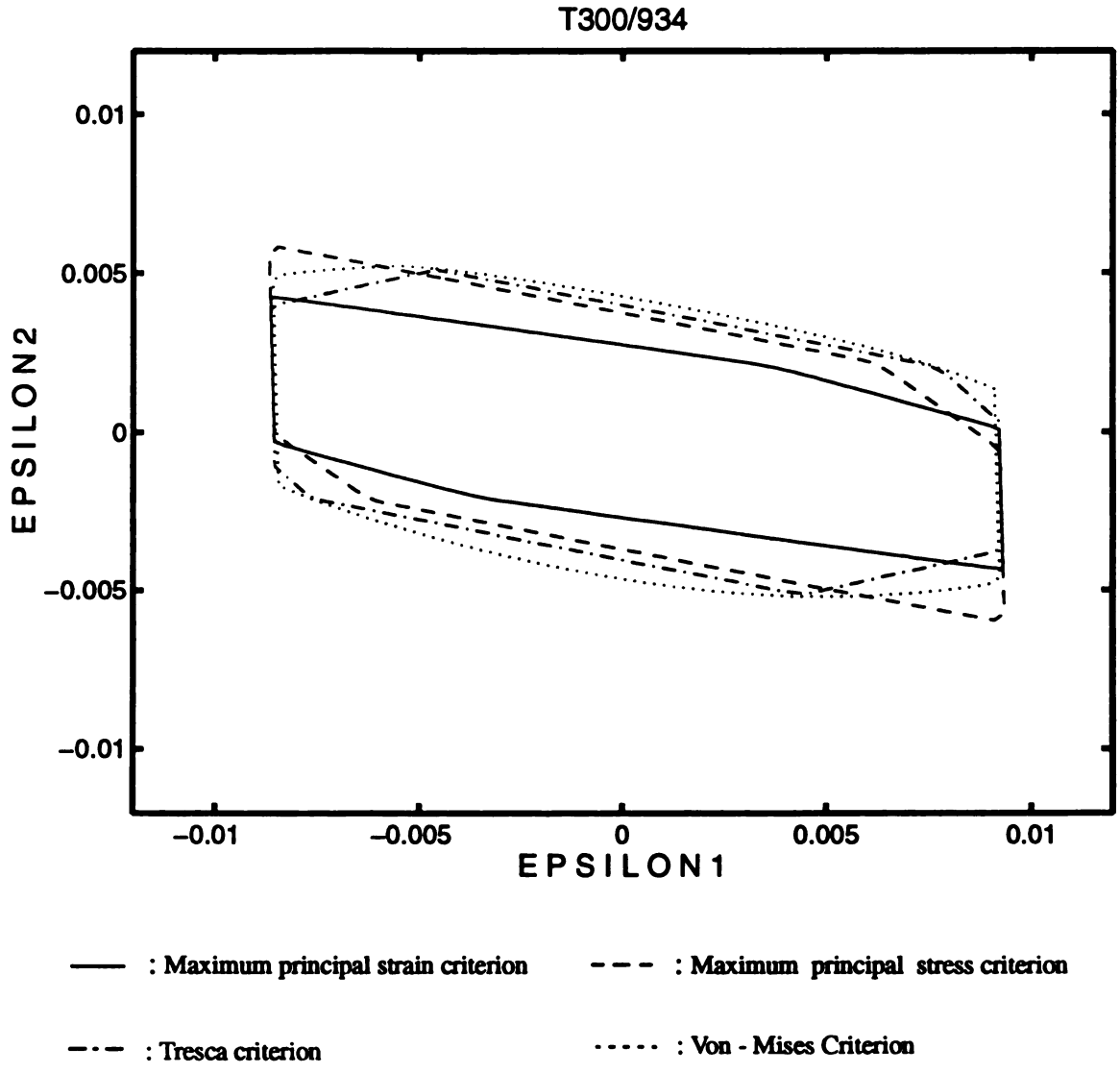

Figure 25. Failure envelopes in strain space (T300/934)

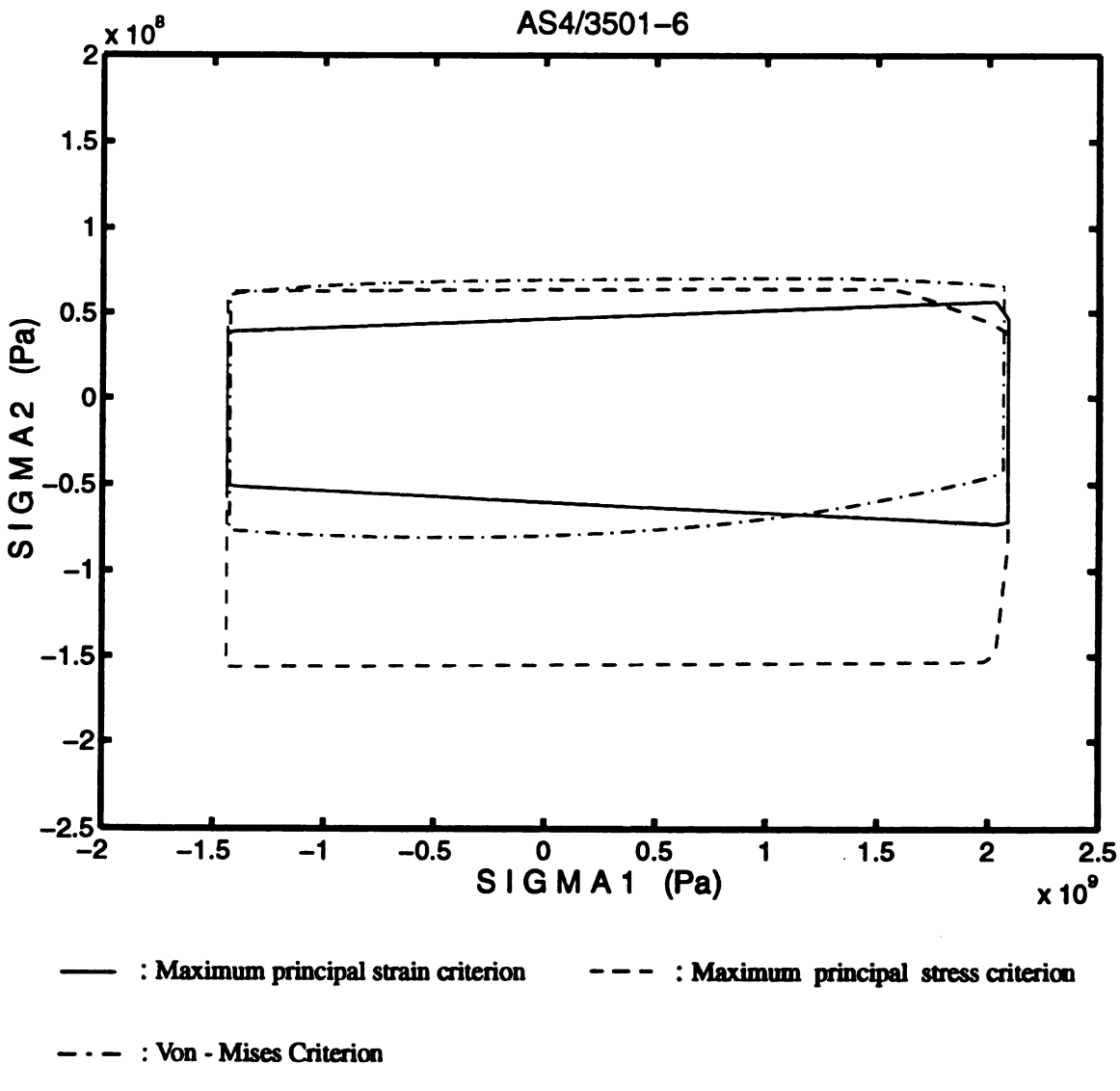

Figure 26. Failure envelopes in stress space (AS4/3501-6)

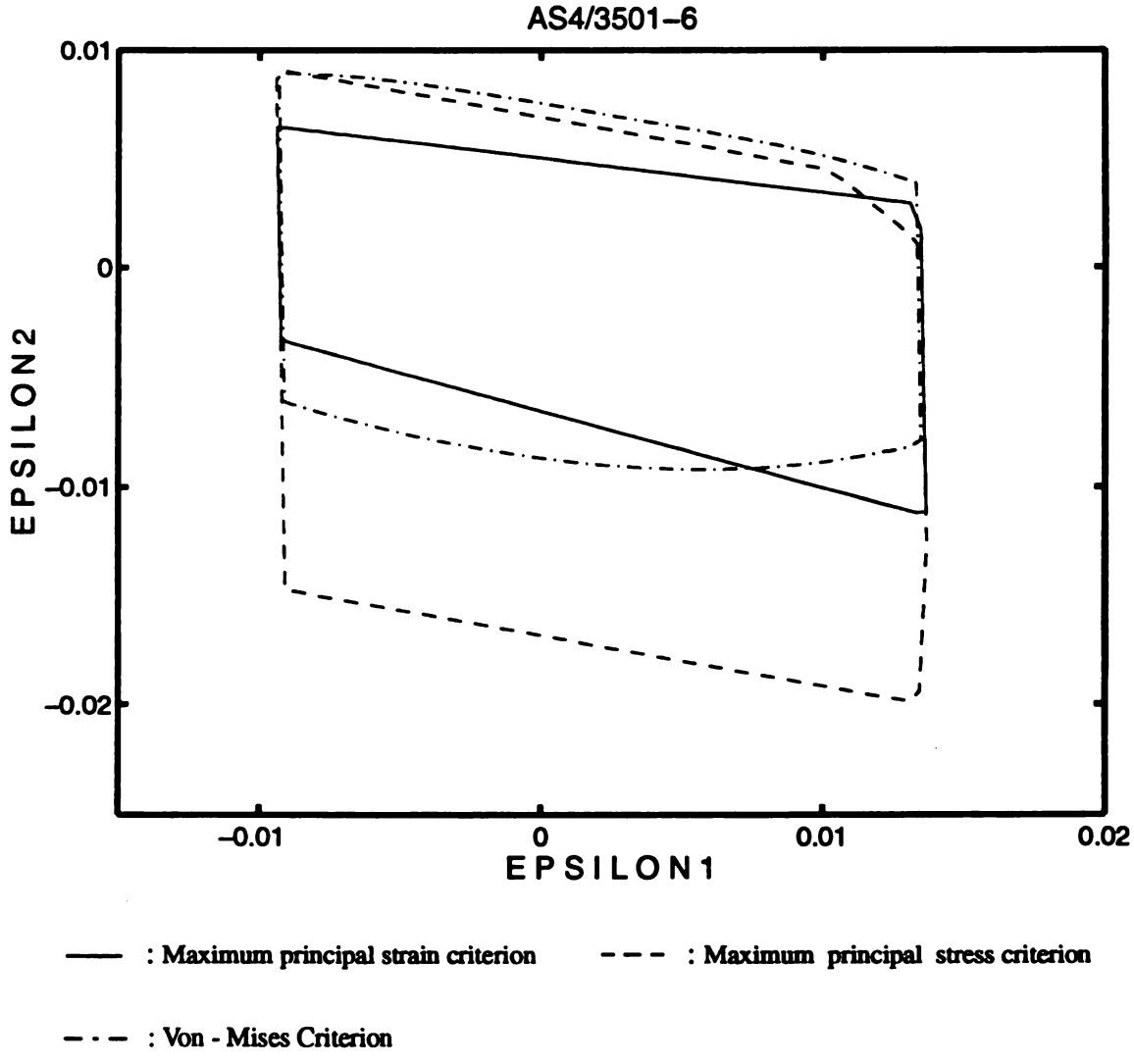

Figure 27. Failure envelopes in strain space (AS4/3501-6)

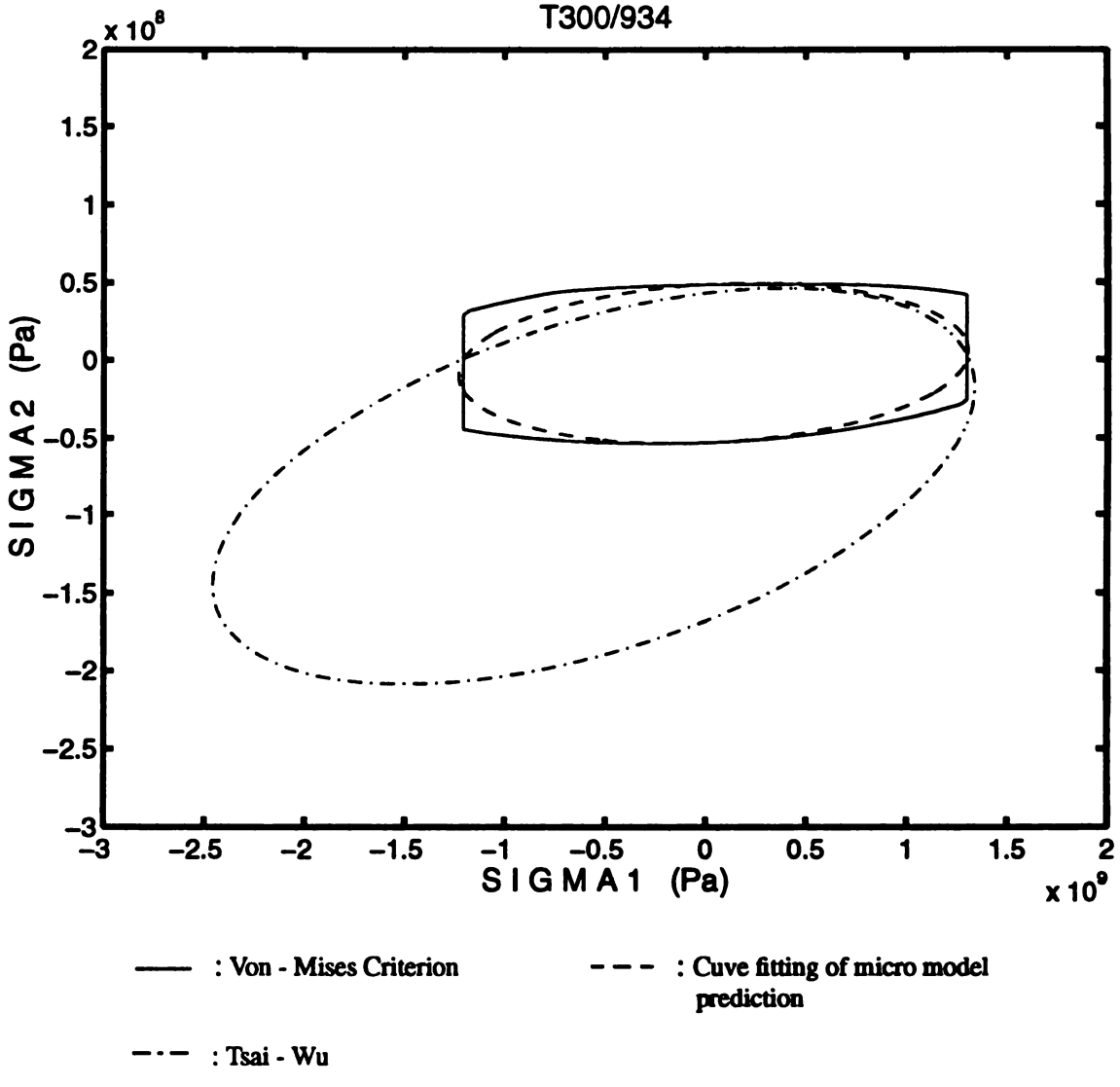

Figure 28. Fitting failure envelope to polynomial type failure envelope and the failure envelopes using Tsai-Wu theory and experimental results (T300/934)

TABLE 4. Comparison of interaction strength parameter

	Nonlinear regression	Tsai - Hahn
Strength Parameter	-0.235339655944E-17	-0.46462603093E-17

In tension - tension space the failure envelope obtained by the micromechanical failure theory is very close to the Tsai-Wu's failure envelope obtained using experimental values. The deviation between the computed Tsai-Wu type and the experimental Tsai-Wu envelopes mainly comes from the differences in interaction term F_{12} for each envelope and the transverse compressive strength.

Figure 29 shows the failure envelopes for AS4/3501-6 where the maximum principal stress failure criterion was used for the matrix to get the failure envelope from the micromechanical failure theory. In tension - tension space, the failure envelopes from the micromechanical failure theory are in good agreement with the Tsai-wu's failure envelope using experimental results.

Thus, unidirectional strengths as well as strengths under multiaxial loading of the lamina are determined. The predicted strengths of the lamina by the model are in reasonably good agreement with experimental results.

The fiber volume fraction in composites has an influence on the strengths of composites, so the failure envelope varies as the fiber volume fraction changes. The variations in failure envelope due to the changes in fiber volume fraction are shown in Figures 30 and 31 for T300/934. From Figure 30, it can be observed that the longitudinal strength of a lamina is proportional to the fiber volume fraction, that is, the longitudinal strength increases as fiber volume fraction increases. But the transverse strength is not influenced as much as the longitudinal strength as shown in Figure 30. The transverse strength

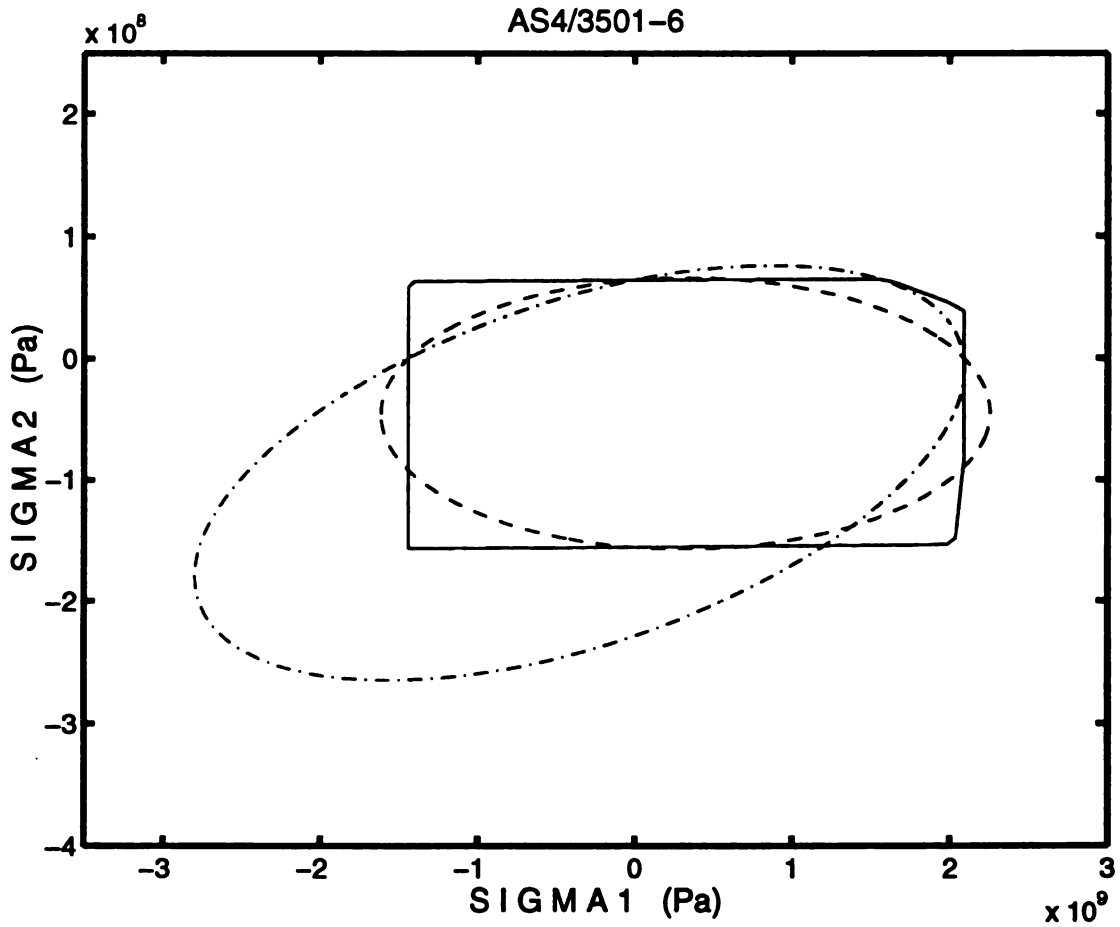

Figure 29. Fitting failure envelope to polynomial type failure envelope and the failure envelopes using Tsai-Wu theory and experimental results (AS4/3501-6)

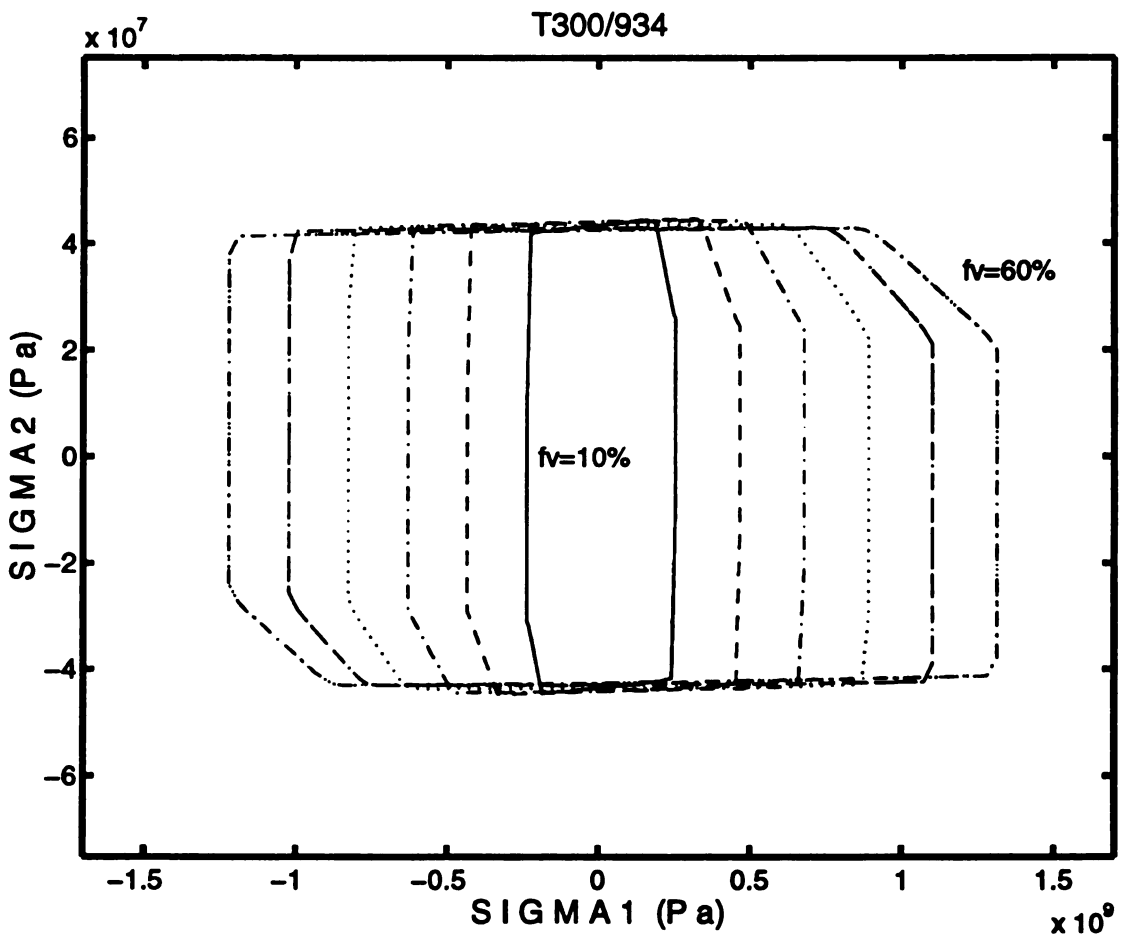

Figure 30. The changes in failure envelope in stress space due to the change in fiber volume fraction

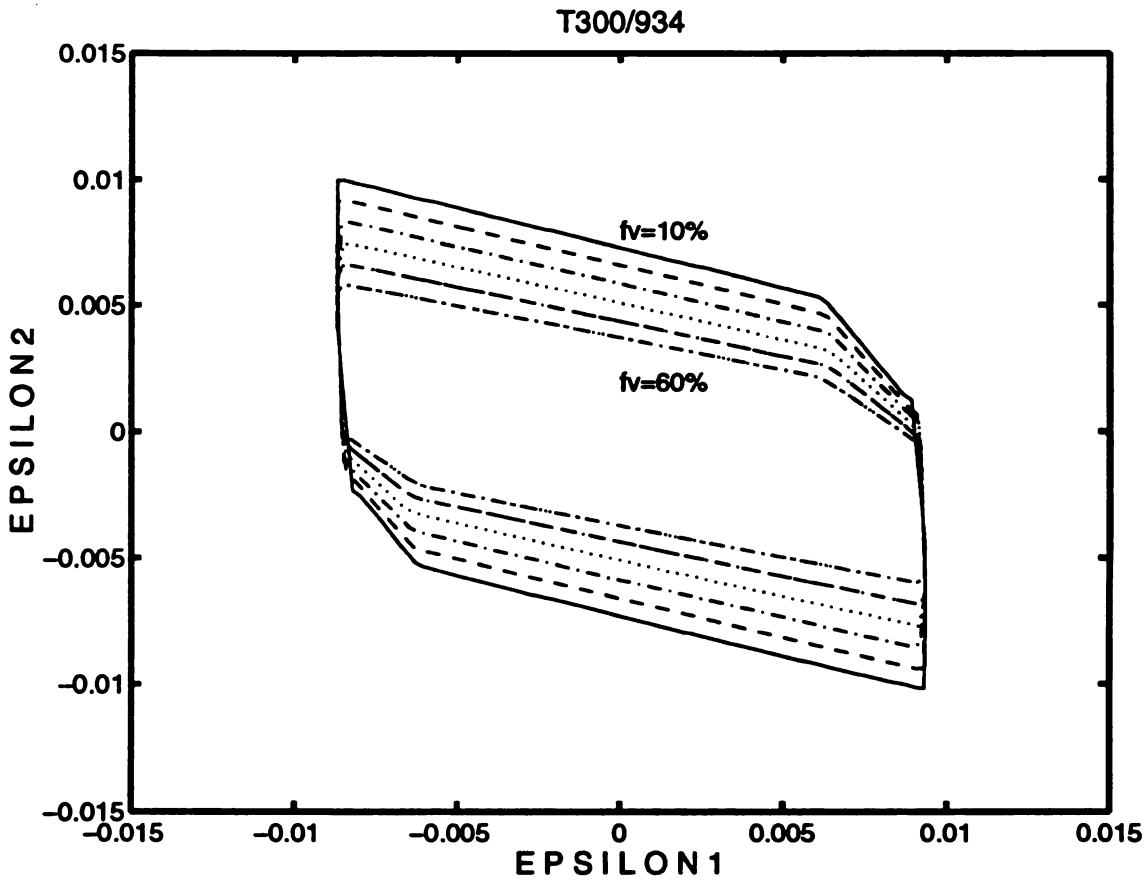

Figure 31. The changes in failure envelope in strain space due to the change in fiber volume fraction

increases a little bit, and then decreases slightly as fiber volume fraction increases. The failure strain in the transverse direction decreases as fiber volume fraction increases.

When a lamina is subjected to a plane stress state, the failure envelope is plotted in three-dimensional space which takes longitudinal, transverse, and longitudinal shear stresses as axes. In this case, since the strength of a lamina is finite, the failure surface should be closed. It is shown in Figure 32 that the failure surface is closed and symmetric about the plane in which the longitudinal shear stress is zero. The failure surface is obtained by using the maximum principal stress criterion for the matrix. When the shearing load is applied on the lamina, the influence of shearing stress on lamina strength is shown in Figure 33. The longitudinal strength is not affected up to about 20 MPa of longitudinal shear stress, but when the longitudinal shearing stresses exceed about 20 MPa, the longitudinal strength decreases very fast. On the other hand, the transverse strength decreases steadily as the shearing load increases.

The Results of Independent Mode Failure Criteria

The failure envelope of each constituent in a lamina is predicted in terms of lamina loads by using the micromechanical failure theory and allowing failure to occur in only the constituent under consideration. A typical result is shown in Figure 34, which was obtained by choosing the Von - Mises criterion for the matrix. The intersected part of each constituent is regarded as the failure envelope for the composite (T300/934). To see more clearly, the failure envelope is replotted in Figure 35, and it can be ascertained that fiber dominates the longitudinal strength, while interface and/or matrix govern the transverse strength. If Tresca failure criterion is used for matrix, only the matrix dominates the transverse strength as shown in Figure 36. For AS4/3501-6, the independent failure envelopes

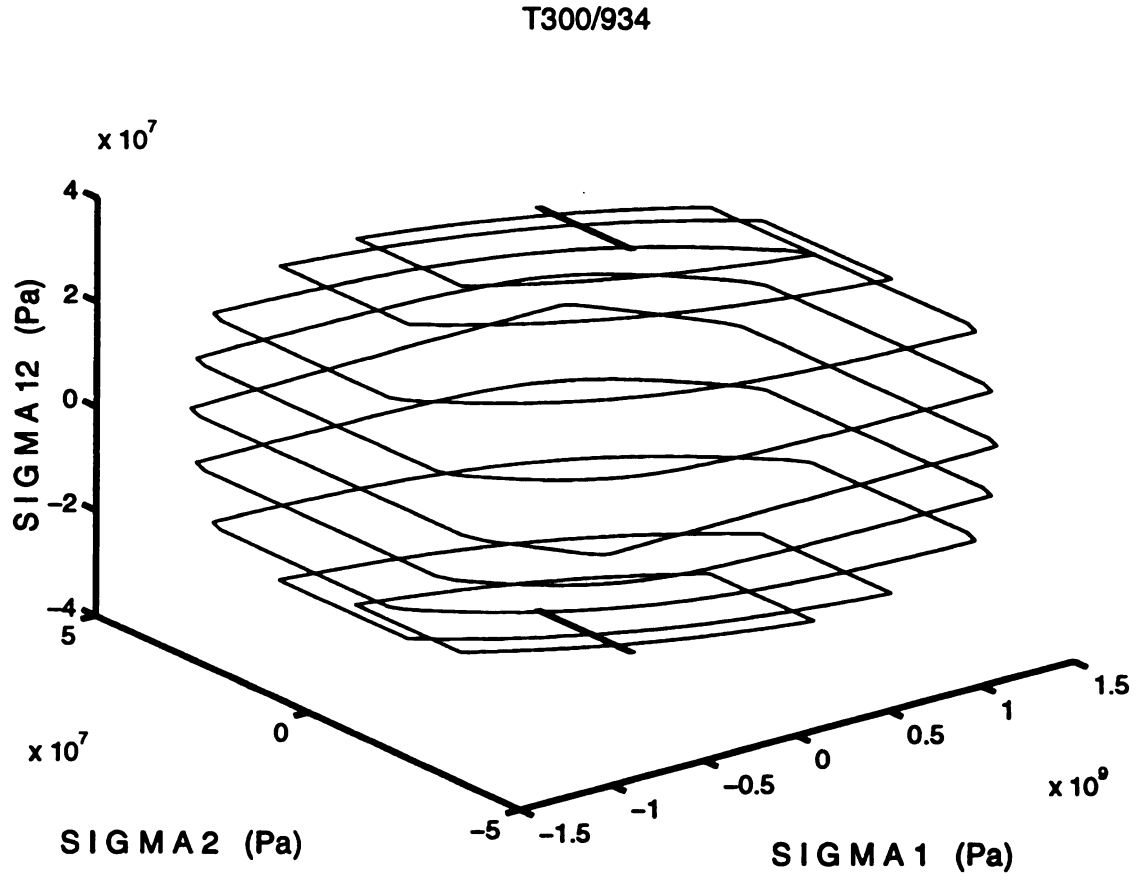

Figure 32. The failure envelopes in three dimensions when shear loading is applied.

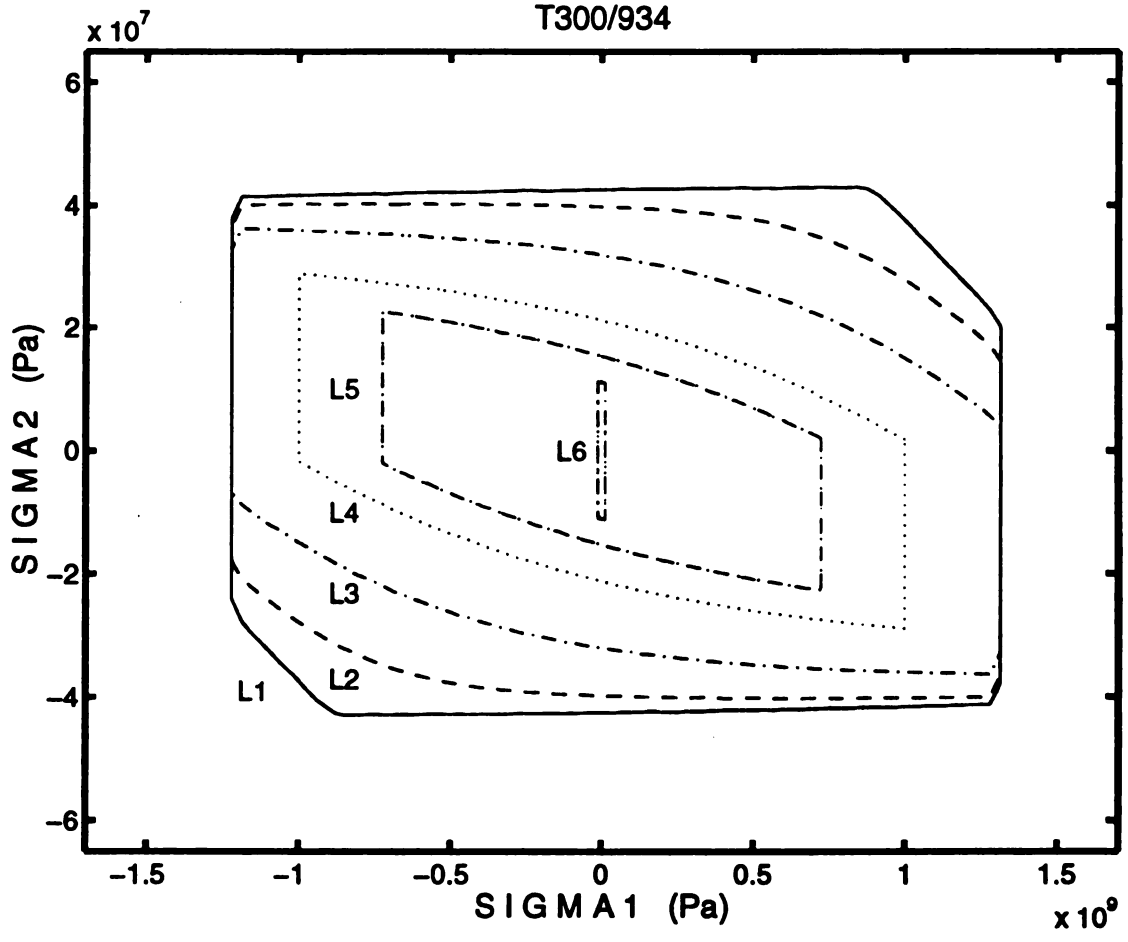

Shear load: L1: 0 MPa L2: 10 MPa L3: 20 MPa
L4: 30 MPa L5: 35 MPa L6: 38.5 MPa

Figure 33. The failure envelopes in two dimensions when shear loading is applied.

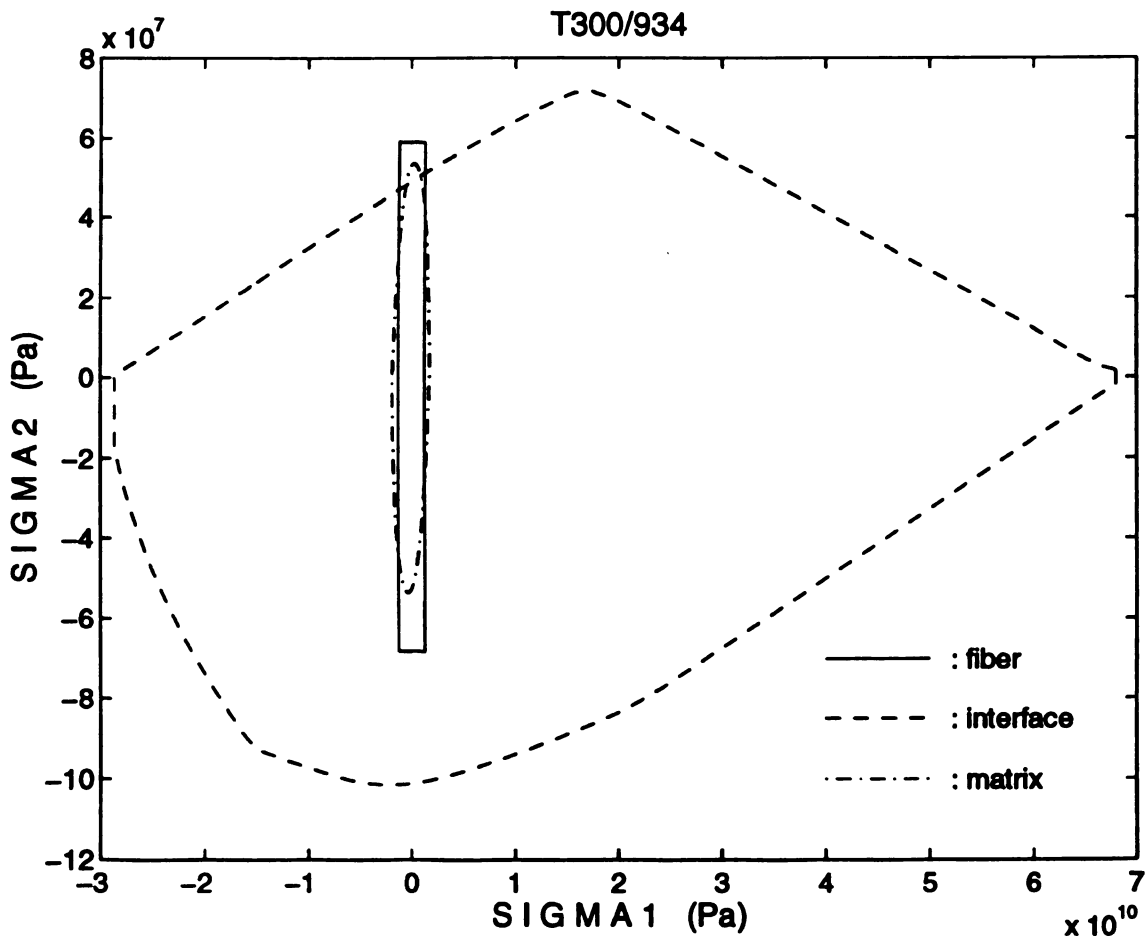

Figure 34. Independent mode failure envelope in stress space(T300/934)

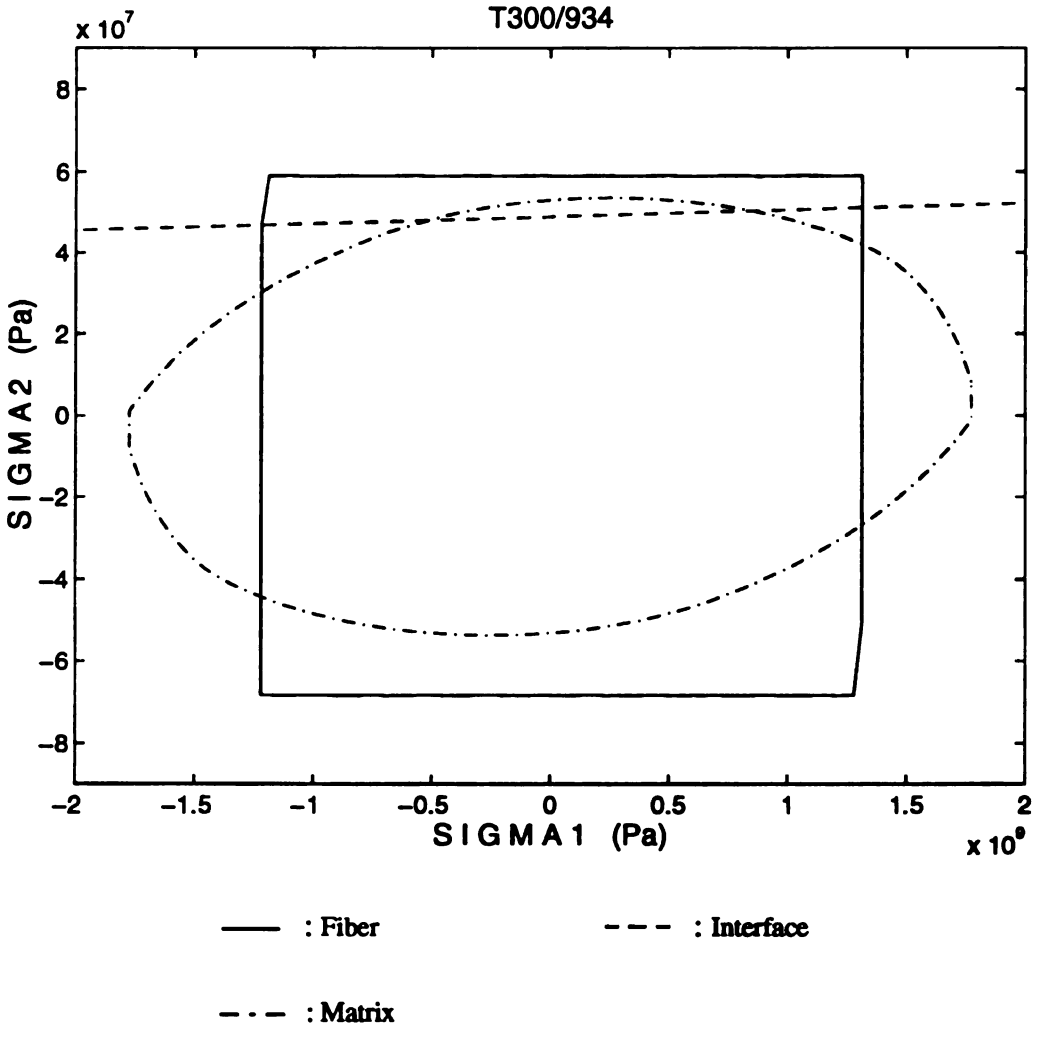

Figure 35. The zoom of the independent mode failure envelopes

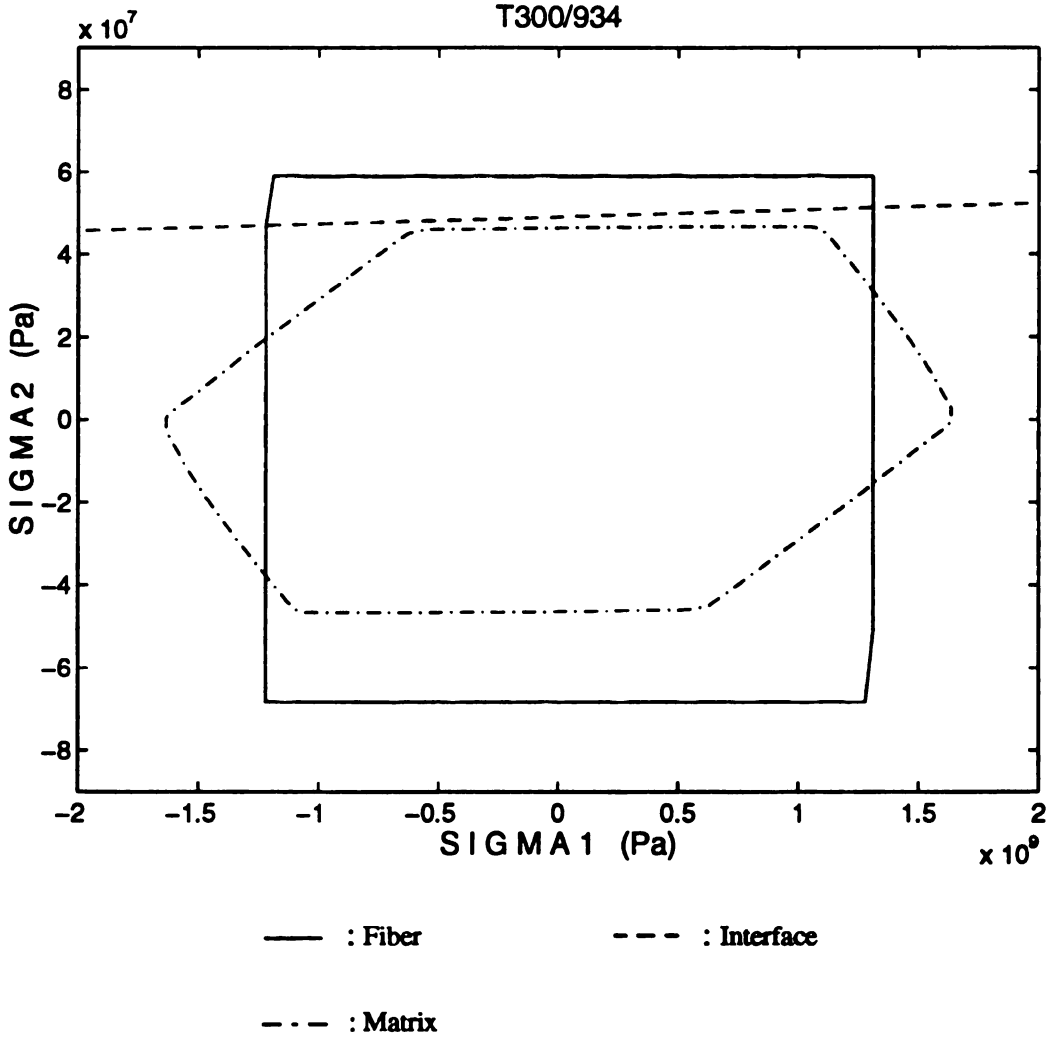

Figure 36. The independent failure envelopes (Tresca criterion)

are shown in Figures 37 and 38 by adopting maximum principal stresses failure criterion for matrix, and it is also confirmed that the matrix dominates the transverse strength of the composite.

Making use of the uniaxial strengths of each constituent in terms of lamina load, and fitting the failure envelope of each constituent to a polynomial type failure criterion, the strength parameters are obtained for the independent mode failure criteria as functions of macro loads. The obtained strength parameters of each constituent for a plane stress state are listed in Table 5. But the strength parameters for matrix can be changed by the choice of failure criterion for the matrix. If the strength parameters are substituted into Eqs. (4.3.2), (4.3.4) and (4.3.6), the failure envelope of each constituent are obtained as shown in Figures 39 and 40. In the figures, as expected, the fiber dominates the longitudinal strength of lamina, and interface and/or matrix dominates the transverse strength. The prediction in tension and tension space has good agreement with the Tsai - Wu failure envelope based on experimental results.

The independent mode failure criterion based on "in-situ" constituent strengths

Thus far, the AS4/3501-6 and T300/934 composite systems were simulated to assess theory, but the prediction of transverse strengths did not have good agreement with the experimental results. This may be due to the reasons discussed in Section 5.1. Thus, to make the failure envelopes more realistic, the in-situ matrix strength can be used instead of the bulk strength. Table 6 shows the comparison between the in-situ strength and the bulk strength of 3501-6 and 934 resins. In Figure 41, the failure envelope based on in-situ strength of matrix are shown and compared with Tsai-Wu failure envelope using experimental results. In the tension - tension region, the current failure envelope based on in-situ

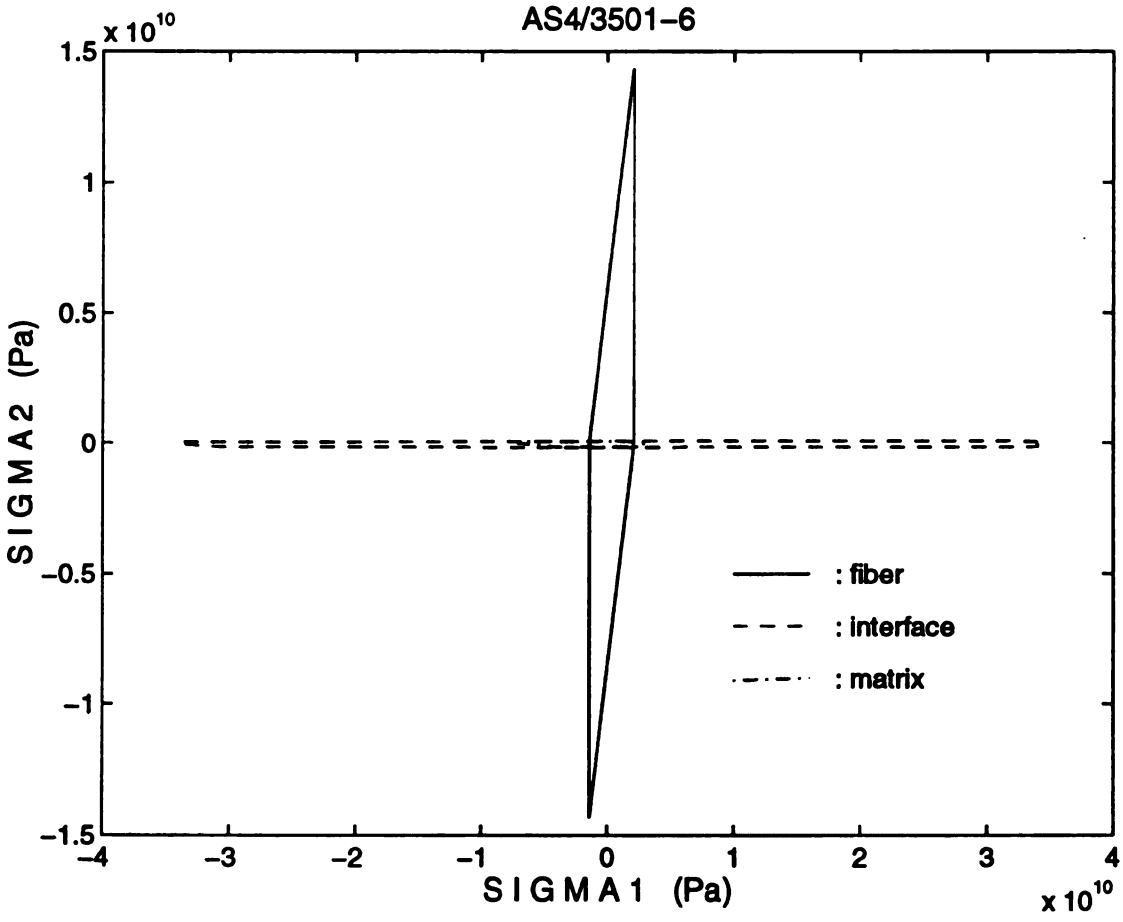

Figure 37. The independent failure envelopes in stress space (AS4/3501-6)

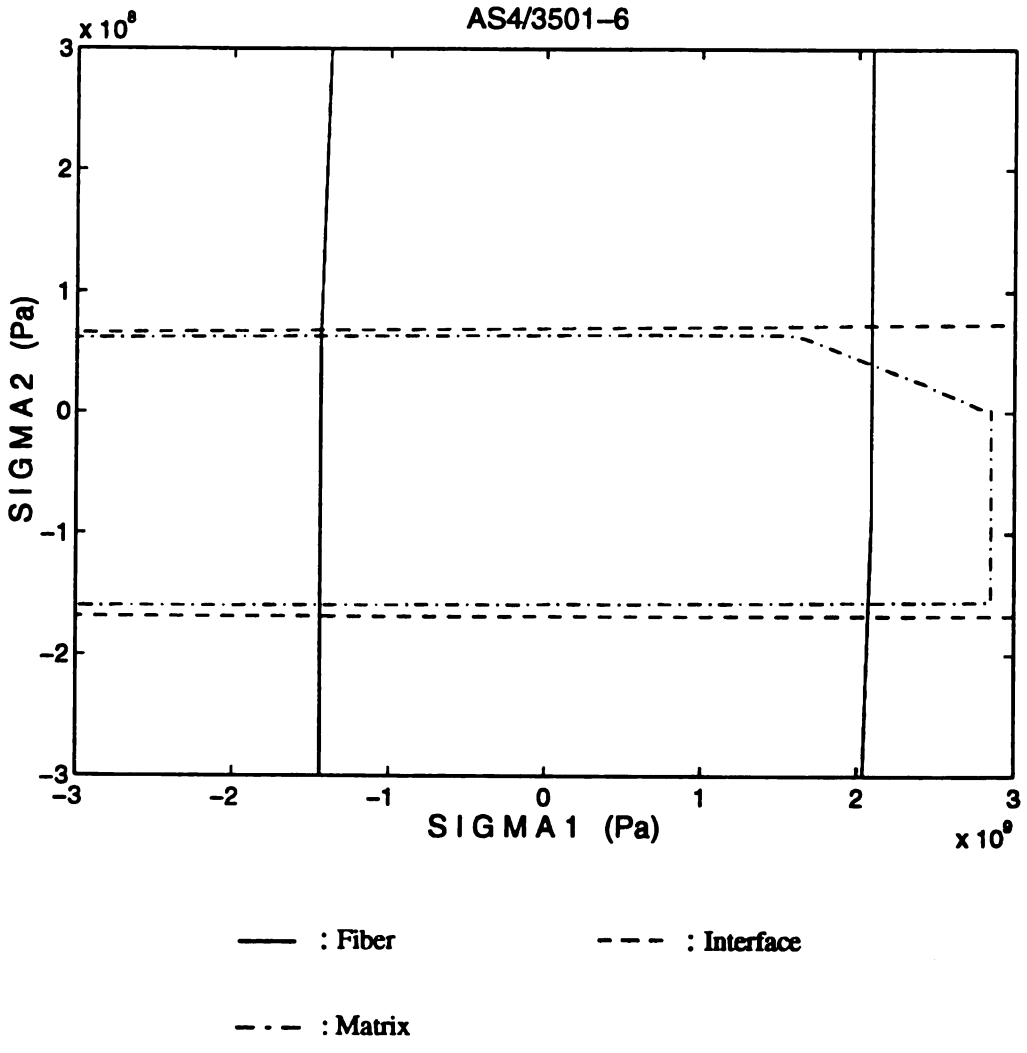

Figure 38. The zoom of the independent mode failure envelopes

TABLE 5. The strength parameters for independent failure criterion

	T300/934	AS4/3501-6
F_1^f	-0.586385108445E-10	-0.215978453212E-09
F_{11}^f	0.623829307604E-18	0.332278910265E-18
F_2^f	0.230417004521E-08	0.529573725026E-10
F_{22}^f	0.248058914102E-15	0.199772076128E-19
F_{12}^f	-0.242261961673E-18	-0.818557039821E-19
F_{66}^f	0.910411205632E-15	0.568826873132E-23
F_1^{in}	-0.201801474273E-10	0.000000000000E+00
F_{11}^{in}	0.512993473221E-21	0.865685248847E-21
F_2^{in}	0.104603918702E-07	0.835030761877E-08
F_{22}^{in}	0.201807946708E-15	0.845712457806E-16
F_{12}^{in}	-0.225731392658E-18	-0.623613958904E-19
F_{66}^{in}	0.604565155100E-15	0.258876386798E-16
F_1^m	0.00000000000E+00	0.210148107289E-09
F_{11}^m	0.318131154099E-18	0.493464634521E-19
F_2^m	0.00000000000E+00	0.935305955771E-08
F_{22}^m	0.353761427543E-15	0.977490324149E-16
F_{12}^m	-0.360073205736E-17	0.455226648330E-18
F_{66}^m	0.9104079092589E-55	0.227530749253E-60

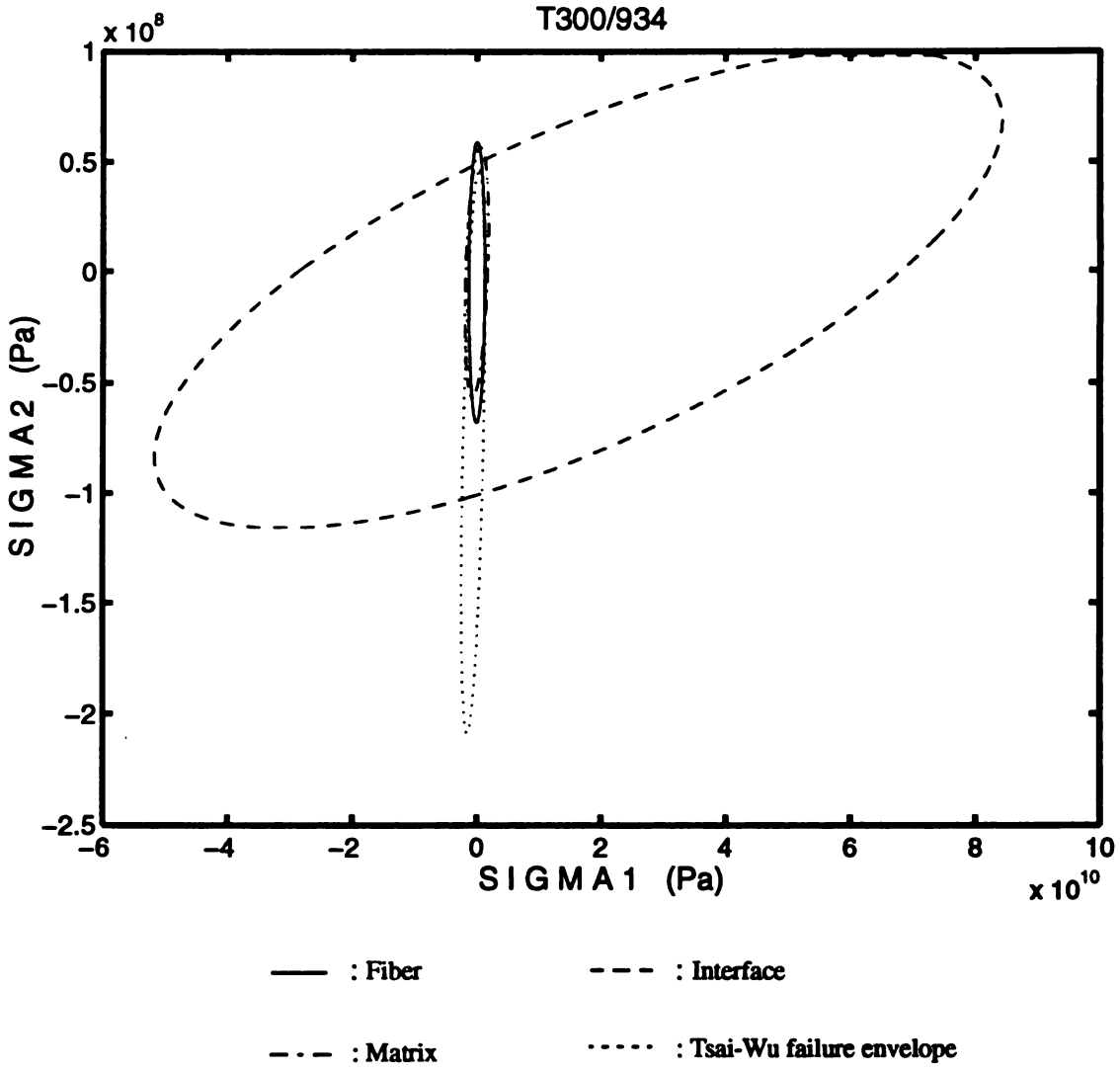

Figure 39. The curve fitting of independent mode failure envelopes (T300/934)

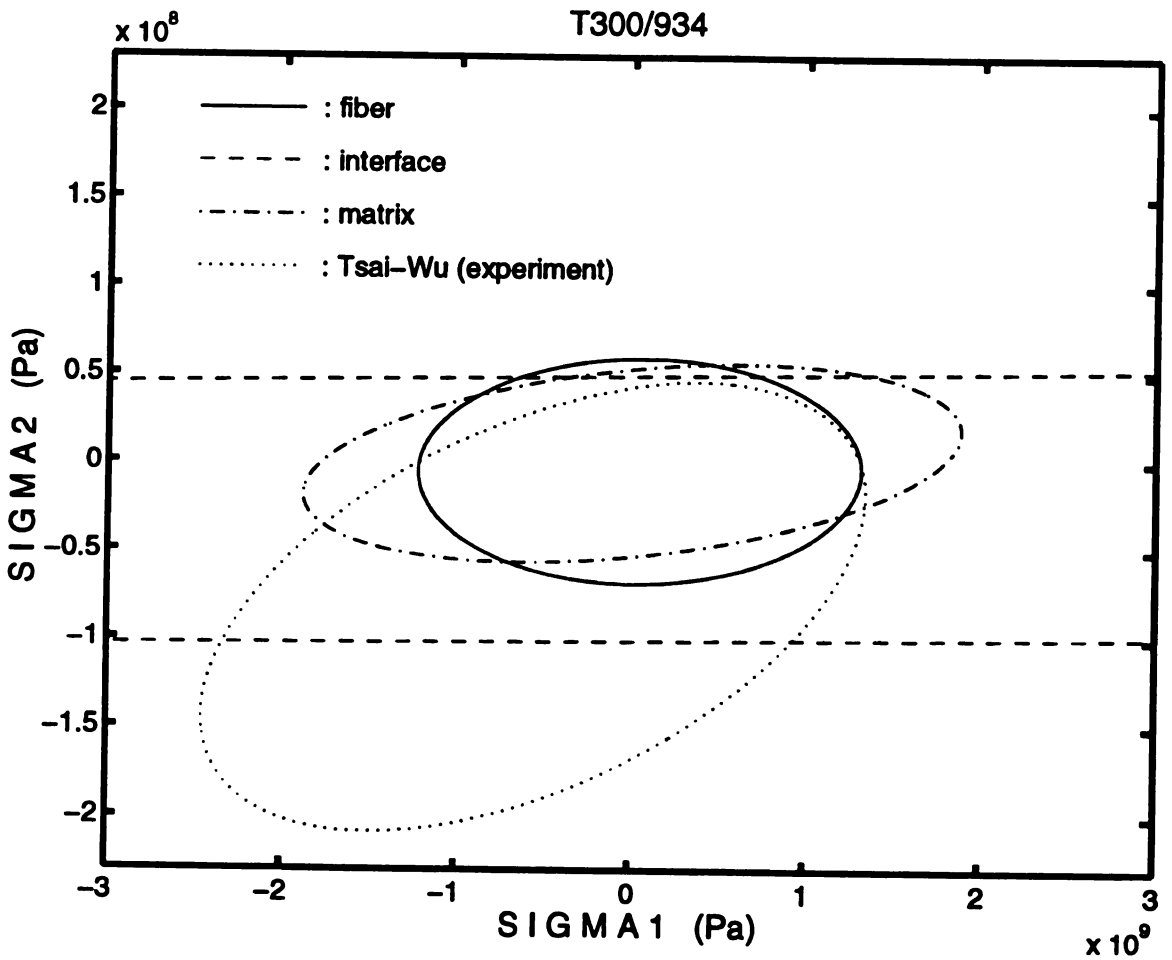

Figure 40. The zoom of curve fitting of independent mode failure envelopes (T300/934)

strength is very close to the Tsai - Wu failure envelope. In Figure 42, the independent mode failure envelopes are shown. In the tension - tension region, the matrix fails at a lower transverse stress as the longitudinal load increases.

TABLE 6. The comparison between bulk- and in-situ strength

	Tension (MPa)		Compression (MPa)	
	Bulk strength	In-situ strength	Bulk strength	In-situ strength
934	58.8	59.8	58.8	233.5
3501-6	83	83.4	207	297.3

Verification of the independent mode failure theory and in-situ strengths

In order to examine the proposed micromechanical approach for the prediction of the strength of composites under combined loading, the unidirectional lamina (AS/3501) under off-axis loading as shown in Figure 43 was simulated. The unavailable properties were determined by backing out "in-situ" properties. As shown in Figure 44, the predicted strengths are in good agreement with the experimental results in both tension and compression loading cases. The composite strength was predicted as follows. First, the failure envelopes and unidirectional strengths were predicted by the micromechanical theory, and the interaction parameters were obtained by fitting to the Tsai-Wu type polynomial failure. Then using the tensor transformation law, the strength parameters were transformed into the off-axis coordinate. The independent mode failure curves were obtained by applying Eqs. 4.3.7 and 4.3.8 to fiber and Eq. (5.3.2) to matrix. As the loading angle varies, it is shown that the failure mode changes from the fiber to the matrix. The used material properties are listed in TABLE 1.

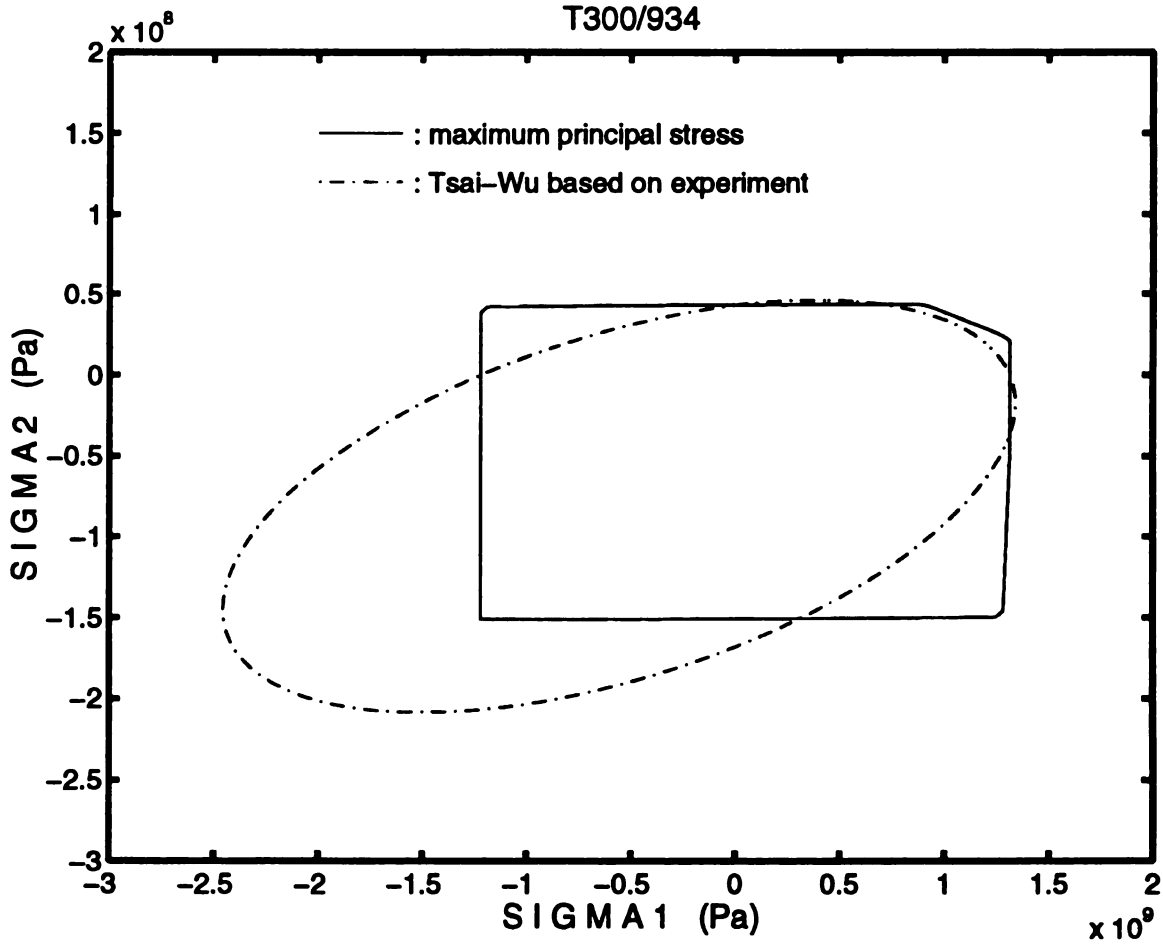

Figure 41. The failure envelope based on in-situ strength

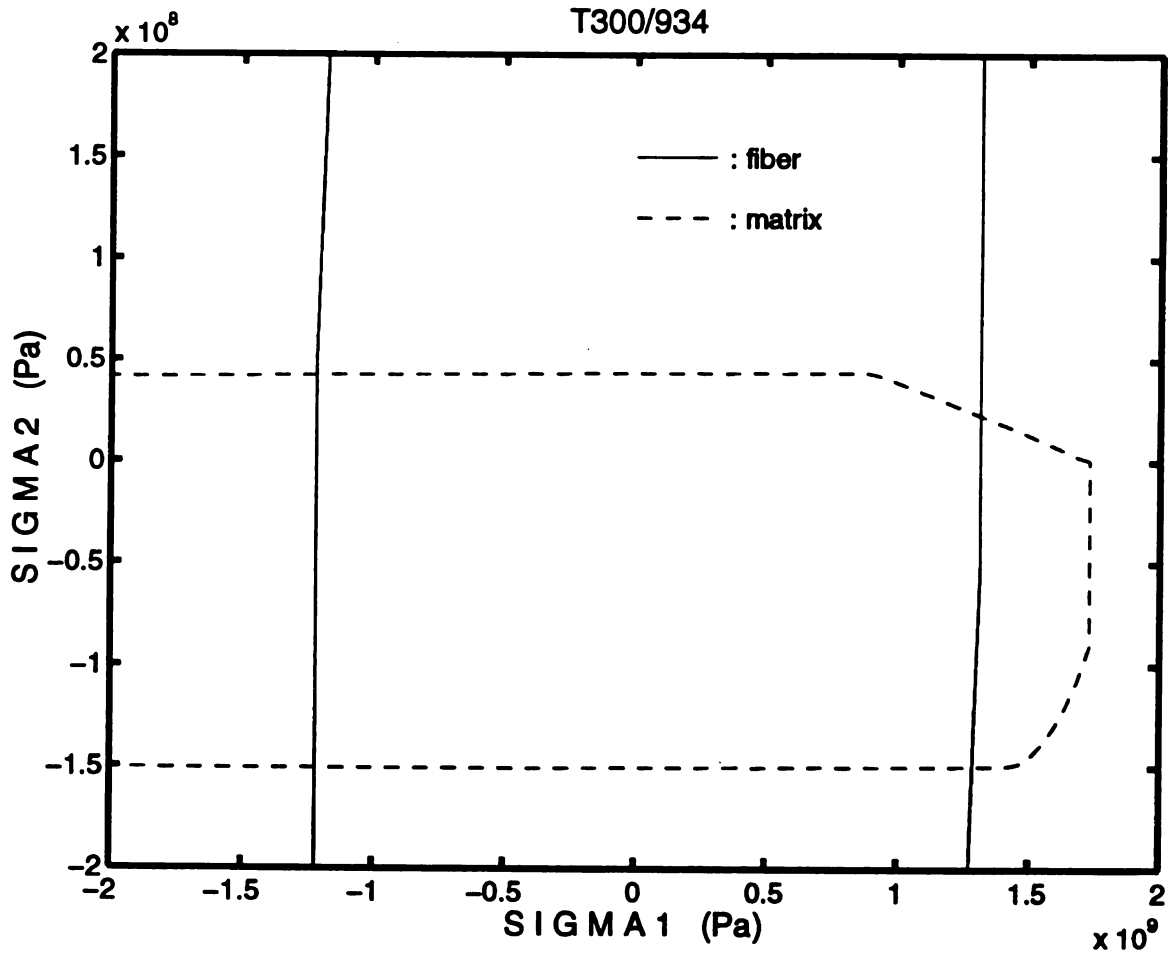

Figure 42. The independent mode failure envelope based on in-situ strength

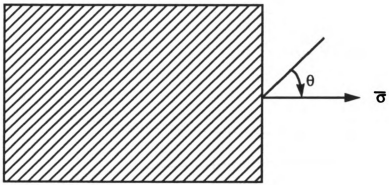

$\overline{\sigma}$: The applied load

θ : The loading direction

Figure 43. The composite under off-axis loading

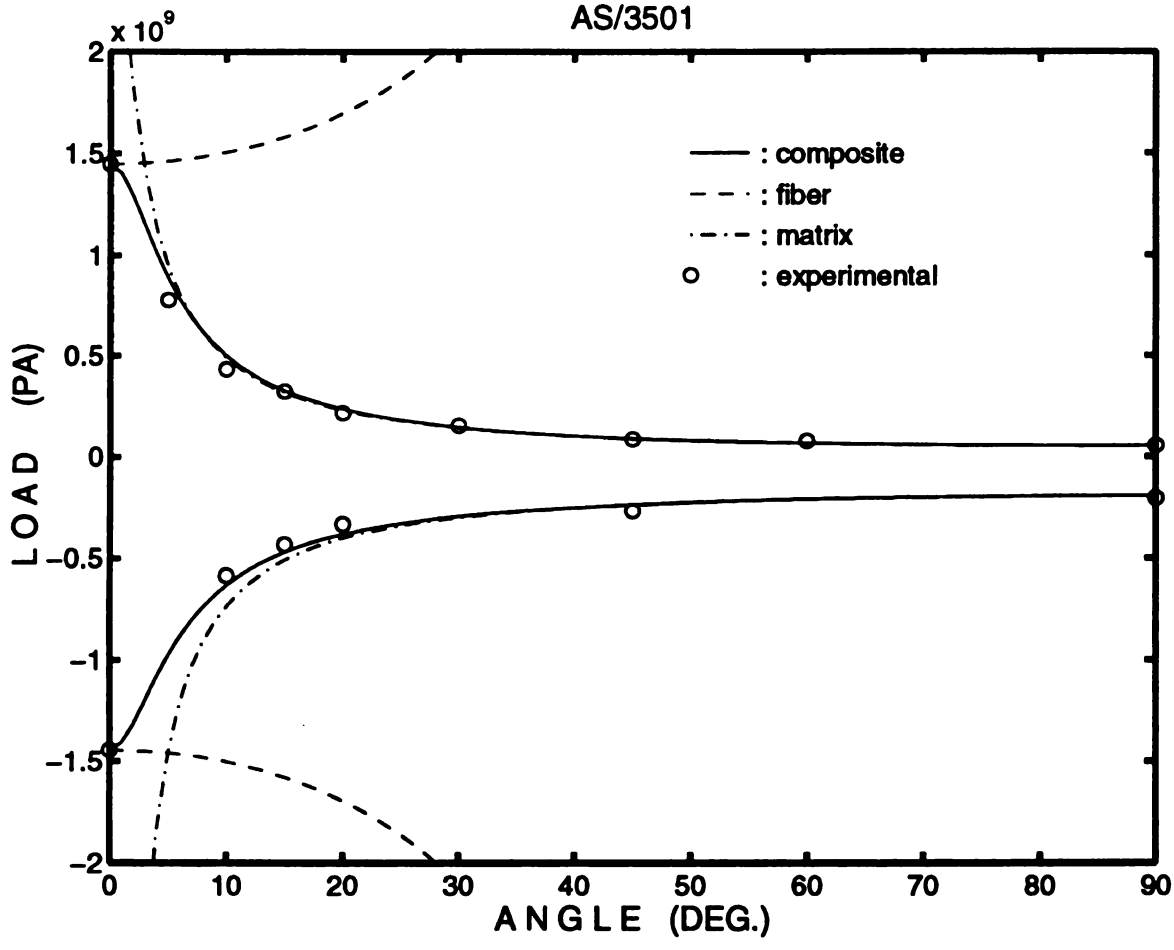

Figure 44. The predicted strengths of AS/3501 under off-axis loading on the basis of in-situ strength

TABLE 7. Material properties used in calculation

	AS	3501
E_1 (GPa)	213.000	3.45000
E_2 (GPa)	13.8000	3.45000
E_3 (GPa)	13.8000	3.45000
nu_{23}	0.2500	0.3500
nu_{13}	0.2000	0.3500
nu_{12}	0.2000	0.3500
G_{23} (GPa)***	5.5200	1.3000
G_{13} (GPa)	13.800	1.3000
G_{12} (GPa)	13.800	1.3000
Tensile Strength (Pa)*	0.01017321**	0.7009612E+08
Compression Strength (Pa)*	-0.01017321**	-0.2792998E+09
	AS/3501	
X1T (MPa)	1447.000	
X1C (MPa)	1447.000	
X2T (MPa)	51.7000	
X2C (MPa)	206.000	

*: The in-situ strengths, **: The maximum allowable strain

***: The assumed property from $G_{23} = \dfrac{E_2}{2(1+\nu_{23})}$

AS, 3501: [31], AS/3501: [20]

CHAPTER VII
CONCLUSIONS

A model for predicting failure in fiber-reinforced composites has been developed and assessed. The following conclusions have been reached:

• On the basis of micromechanics elasticity solutions, the material properties of the lamina can be obtained with good agreement to the experimental results.

• The predicted unidirectional strengths of the lamina based on the micromechanical failure theory are in good agreement with experimental results except the transverse compressive strength.

• To estimate the strength of a lamina for the purpose of designing composite systems, the micromechanical failure theory needing only the fiber volume fraction and the material properties in bulk state as input can be employed.

• The interaction terms in the Tsai-Wu type failure theory can be determined by nonlinear regression and fitting the failure envelope from the current (or other) micromechanics failure theory to a Tsai-Wu type failure criterion.

• When the compressive strength of matrix is different from the tensile strength, the maximum principal stress criterion for matrix gives the best prediction of transverse tensile strength and compressive strength of composites.

• To reflect the difference in tensile and compressive strengths of constituent materials in the micromechanical failure theory, it is better to adopt a failure criterion that can accommodate such a difference in strength.

• For a plane stress state, it was shown that the failure surface is closed and symmetric about the plane where shear load is zero. The longitudinal strength was not affected by a small shear load.

• It is possible to cast the failure model in a simple mathematical form with separate criteria for each mode of failure as a function of lamina load. The strength parameters can be obtained by the micromechanical failure theory.

• The independent mode failure criterion based on "in-situ" constituent strength technique shows excellent promise for inexpensive and efficient characterization of composites under multi-axial loading conditions.

• In the current work, primary attention has been given to the case of plane stress loading. However, the concepts used are sufficiently general to allow extension of the models to fully three-dimensional failure analysis.

• To predict the failure envelope more realistically, it is recommended that the thermal residual stress be considered.

• To verify and develop the suggested theory, more experimental results of multiaxial strength are needed.

• Additional mathematical forms of the independent-mode criteria need be considered.

• Further assessment of the theory is needed. In particular, first-ply and progressive failure analysis of laminates should be performed and the results compared with experimental data.

REFERENCES

1. Chawla, K.K., "Composite Materials Science and Engineering", Springer-Verlag, N.Y. pp 4-5, 1987

2. Ibid, pp. 183

3. Mallick, P.K., "Fiber-Reinforced Composites: Materials, Manufacturing, and Design", Marcel Dekker Inc., N.Y., pp. 6-11, 1988

4. Ibid, pp. 90

5. Zweben, C., "Mechanical Behavior and Properties of Composite Materials" in Delaware Composites Design Encyclopedia, Vol. 1, eds., Zweben, C., Hahn, G.T. and Chou, T.W., Technomic Publishing Co., PA, pp. 3, 1989

6. Swanson, S.R., "Laminates, Static Strength", in International Encyclopedia of Composites, ed., Lee, S.M., Vol. 3 VCH Publisher Inc., NY, pp. 43, 1990

7. Rowlands, R.E., "Strength (failure) theories and their experimental Correlation" in Handbook of Composites, Vol. 3 - Failure Mechanics of Composites, ed. G.C. Sih & A.M. Skudra, Elsevier Science Publisher, North Holland, pp. 71-125, 1985

8. Nahas, M.N., "Survey of Failure and Post-Failure Theories of Laminated Fiber-Reinforced Composites", Journal of Composites Technology & Research, Vol. 8, No. 4, 1986, pp. 138-153

9. Azzi, V.D. and Tsai S.W., "Anisotropic Strength of Composites", Experimental Mechanics, Vol. 5, 1965

10. Hill, R., "The Mathematical Theory of Plasticity, Oxford University Press, London, pp. 317, 1950

11. Hoffman, O., "The brittle Strength of Orthotropic Materials", Journal of Composite Material, Vol. 1 pp. 200-207, 1967

12. Tsai, S.W. and Wu, E.M., "A General Theory of Strength for Anisotropic Materials", Journal of Composite Material, Vol. 5 pp. 58-80, 1971

13. Wu, E.M. and Scheublein, J.K., "Laminated Strength - A Direct Characterization Procedure", Composite Materials: Testing and Design (Third Conference), ASTM STP 546, 1974, pp. 188-206

14. Tennyson, R.C., Macdonald, D. and Nanyaro, A.P., "Evaluation of the Tensor Polynomial Failure Criterion for Composite Materials", Journal of Composite Material, Vol. 12 pp. 63-75, 1978

15. Jiang, Z. and Tennyson, R.C., "Close of the Cubic Tensor Polynomial Failure Surface", Journal of Composite Material, Vol. 23 pp. 208-231, 1989

16. Yeh, H.Y. and Kim, C. H., "The Yeh-Stratton Criterion for Composite Materials", Journal of Composite Material Vol. 28, No. 10, pp. 926-939, 1994

17. Kim, C. H. and Yeh, H.Y., "Development of A New Yielding Criterion: The Yeh-Stratton Criterion", Engineering Fracture Mechanics Vol. 47, No. 4, pp. 569-582, 1994

18. Wu, E.M., "Optimal Experimental Measurements of Anisotropic Failure Tensors", Journal of Composite Material, Vol. 6 pp. 472-489, 1972

19. Tsai, S.W. and Hahn, H.T., "Introduction to Composite Materials", Technomic Publishing Co., CT, pp. 283-286, 1980

20. Ibid. pp. 292

21. Wu, R.Y. and Stachurski, Z., "Evaluation of the Normal Stress Interaction Parameter in the Tensor Polynomial Strength Theory for Anisotropic Materials", Journal of Composite Material, Vol. 18 pp. 456-463, 1984

22. Hashin, Z., "Failure Criteria for Unidirectional Fiber Composites", Journal of Applied Mechanics, Vol. 47 pp. 329-334, 1980

23. Christensen, R.M., "Tensor Transformations and Failure Criteria for the Analysis of Fiber Composite material", Journal of Composite Material, Vol. 22 pp. 874-897, 1989

24. Zhu, Y., Zhou, B., He, G., and Zheng, Z., "A Statistical Theory of Composite Materials Strength", Journal of Composite Material, Vol. 23 pp. 280-287, 1989

25. Neale, K.W. and Labossiere, P., "A General Failure Criterion for the Analysis of Fibre-Reinforced Composite Laminae", in Composite Materials Design and Analysis, de Wilde, W.P. and Blain, W.R., eds., pp.413-427, 1990.

26. Feng, W.W., "A Failure Criterion for Composite Materials", Journal of Composite Material, Vol. 25, pp. 88-100, 1991

27. Wakashima, K., Suzuki, Y. and Umekawa, S., "A Micromechanical Prediction of Initial Yield Surface of Unidirectional Composites", Journal of Composite Material, Vol.

13 pp. 288-302, 1979

28. Ishikawa, T., "Strength and Thermal Residual Stresses of Unidirectional Composites", Journal of Composite Material, Vol. 16, pp. 40 - 52, 1982

29. Dvorak, G.J. and Bahei-El-Din, Y.A., "Plasticity Analysis of Fibrous Composites", Journal of Applied Mechanics, Vol. 49, pp. 327-335, 1982

30. Skudra, A.M., "Micromechanics of Failure of Reinforced Plastics", in Handbook of Composites, Vol. 3 - Failure Mechanics of Composites, eds. G.C. Sih & A.M. Skudra, pp. 1-69, Elsevier Science Publisher, North Holland, 1985

31. Aboudi, J., "Micromechanical Analysis of the Strength of Unidirectional Fiber Composites", Composite Science and Technology, Vol. 33, pp. 79-96, 1988

32. Landriani, G.S., Taliercio, A., "Strength Criteria for Fiber Reinforced Composite Materials", presented at the Twelfth Annual Energy-Sources Technology Conference and Exhibition, Houston, Texas, Composite Material Technology 1989, pp. 49 - 55, 1989

33. Hart-Smith, L.J., "Should Fibrous Composite Failure modes be interacted or Superimposed", Composites, pp. 53-55, Vol., 24, No. 1, 1993

34. Hart-Smith, L.J., "An Inherent Fallacy in Composite Interaction failure Curves", Composites, pp. 523-524, Vol., 24 No. 6, 1993

35. Averill, R.C., and Carman, G.P., "Analytical Modeling of Micromechanical Stress Variations in Continuous Fiber-Reinforced Composites", in proceedings of the IUTAM Symposium on Local Mechanics Concepts for Composite material Systems, pp. 27-61 Blacksburg, VA, October 1991.

36. Leissa, A.W. and Clausen, W.E., "Application of point matching to problems in Micromechanics", in Fundamental Aspects of Fiber Reinforced Plastic Composites (ed. Schwartz, R.T. and Schwartz, H.S.), Interscience Publishers, NY, pp. 29-44, 1968

37. Leissa, A.W., Clausen, W.E. and Agrawal, G.K., "Stress and Deformation Analysis of Fibrous Composite Materials by Point Matching", International Journal for Numerical Methods in Engineering, Vol. 3, pp. 89-101, 1971

38. Kobayashi, S., and Ishikawa, T., "Elastic Properties of Unidirectional Fiber-Reinforced Composites", Composite Material & Structures, Vol. 3, No. 3, pp. 12-20, 1974

39. Mendelson, A., "Plasticity: Theory and Application", Robert E. Krieger Publishing Co., FA, pp. 70 - 77, 1986

40. Whitney, J.M., Daniel, I.M. and Pipes, R.B., "Experimental Mechanics of Fiber Reinforced Composite Material", Prentice-Hall, N.J., pp. 42-43, 1982

41. Rosen, B.W., "Failure of Fiber Composite Laminates", in proceedings of the IUTAM Symposium on Mechanics of Composite Materials, pp. 106-109, Blacksburg, VA, August, 1982

42. Liebowitz, H., ed., "Fracture", Academic Press, N.Y., pp. 651-656

43. Jasiuk, I., and Tong, Y., "The Effect of Interface on the Elastic Stiffness of Composites", in Mechanics of Composite Materials and Structures, eds., Reddy, J.N. and Teply, J.L., pp. 49-54, 1989

44. Tong, Y., and Jasiuk, I., "Transverse Elastic Moduli of Composite Reinforced with Cylindrical Coated Fibers: Successive Iteration Method", in proceedings of the American society for Composites, Technomic, PA, pp. 117-126, 1990

45. Averill, R.C., "Nonlinear Analysis of Laminated Composite Shells Using a Micromechanics-based Progressive Damage Model", Ph.D. Dissertation, Virginia Polytechnic Institute and Sate University, pp. 135-137, June, 1992

46. Ibid, pp. 112 - 113

47. Mase, G. E. and Mase, G. T., "Continuum Mechanics for Engineers", CRC Press, Boca Raton, pp. 47-49, 1992

48. Jones, R.M., "Mechanics of Composite Materials", Scripta Book Company, Washington, D.C., pp. 38, 1975

49. Al-khafaji, A.W. and Tooley, J. R., "Numerical Methods in Engineering Practice", Holt, Rinehart and Winston Inc., pp. 318, 1986.

50. Kominar, V. and Wagner, H.D., "Some Matrix Failure Peculiarities of Unidirectional Fibre-reinforced Plastics and Layers in Laminated Composites", Composites, Vol. 25 No. 1, pp. 5-10, 1994

51. Folias, E.S., "On the Prediction of Failure at a Fiber/Matrix Interface in a Composite Subjected to a Transverse Tensile Load", Journal of Composite Material. Vol. 25, pp. 869-885, 1991

52. Aboudi, J., "Micromechanical Analysis of Composites by the Method of Cells", Applied Mechanics Reviews, Vol. 42 No. 7, pp. 198-202, 1989

53. Lubliner, J., "Plasticity theory", Macmillan Publishing Company, NY, pp. 60, 1990

54. Tsai, S.W., "Composites Design", 4th ed. Think Composites, pp. B-2, 1988

55. Chang, F.K. and Kutlu, Z., "Strength and Response of Cylindrical Composite shells Subjected to Out-of-Plane Loadings", Journal of Composite Material, Vol. 23, pp. 11 - 31, 1989

56. Daniel, I.M., "Testing, Mechanical Characterization", in International Encyclopedia of Composites, ed., Lee, S.M., Vol. 5, VCH Publisher Inc., NY, pp. 438, 1990